Spring 5-15-2018

Negative Regulators of Colonic Peripheral Regulatory T Cell Development

Teresa Lei Ai
Washington University in St. Louis

WASHINGTON UNIVERSITY IN ST. LOUIS

Division of Biology and Biomedical Sciences

Immunology

Dissertation Examination Committee:
Chyi-Song Hsieh, Chair
Paul M. Allen
Kenneth M. Murphy
Gwendalyn J. Randolph
Wayne M. Yokoyama

Negative Regulators of Colonic Peripheral Regulatory T Cell Development

By

Teresa Lei Ai

A dissertation presented to
The Graduate School
of Washington University in
partial fulfillment of the
requirements for the degree
of Doctor of Philosophy

May 2018

St. Louis, Missouri

Table of Contents

List of figures

Page

List of Abbreviations

Citro	*Citrobacter rodentium*
dMLN	Cecum draining lymph node
DSS	Dextran sulfate sodium
DT	Diphtheria toxin
DTR	Diphtheria toxin receptor
FACS	Fluorescence activated cell sorting
FDR	False discovery rate
FoxP3	Forkhead box P3
Gata3	GATA binding protein 3
GF	Germ-free
HFD	High fat diet
IBD	Inflammatory bowel disease
IFN	Interferon
IL	Interleukin
IRES	Internal ribosome entry site
MHC	Major histocompatibility complex
MLN	Mesenteric lymph node
NFAT	Nuclear factor of activated T-cells
OUT	Operational taxonomic unit
pMHC	Peptide MHC
pTreg	Peripheral Treg
RAG	Recombination-activating genes
Rorγt	RAR-related orphan receptor γ t
Tbx21	T-box transcription factor 21
TCR	T cell receptor
Toxo	*Toxoplasma gondii*
Tg	Transgenic
TRAV	T cell receptor alpha variable
Treg	Regulatory T

ACKNOWLEDGEMENTS

I would first like to thank Chyi Hsieh, for acting as my advisor these past few years. Thanks to my experiences in his lab, I was exposed to a diverse array of immunological questions and skills, which helped me learn how to be comfortable with venturing into exciting new areas of immunological research. He taught me the importance of evaluating my own work with the same, if not greater, scientific rigor that I would apply to the work of others—a lesson that I am truly grateful for.

I would also like to acknowledge the tireless members of my thesis committee. I would like to thank Paul Allen for acting as the chair of my committee and for helping me gain the perspective I needed to see the value of my work. I would like to thank Ken Murphy for insistence on scientific clarity during my update meetings, and Wayne Yokoyama for steadfastly suggesting helpful experiments. I would especially like to thank Takeshi Egawa for selflessly assisting me with everything from scientific concepts to protocols to reagents as I established my thesis projects. Last of all, I would like to thank Gwendalyn Randolph for helping me navigate the end of my Ph.D., and for stepping in to serve on my committee last minute.

Thank you to my laboratory, for helping with experiments whenever possible. I would like especially thank Katherine Nutsch and Benjamin Solomon for passing on their knowledge about critical protocols, which made my research possible.

I would also like to thank the Washington University DBBS program staff, especially Melanie Relich, for patiently pursuing students like myself to complete important logistical steps throughout my time in graduate school.

And lastly, I am eternally grateful to the support of my friends and family. You served as my scientific advisors, saved me whenever I ran into car troubles, and made me laugh when I didn't feel like laughing. I would especially like to thank Matthew Gorman, Siddharth Krishnamurthy, and Felipe Romero. Your support gave me the mental and emotional strength I needed to persevere, and your friendship through the years have left me with some of my greatest memories.

Teresa Ai

Washington University in St. Louis
May 2018

ABSTRACT OF THE DISSERTATION

Negative Regulators of Colonic Peripheral Regulatory T Cell Development

By

Teresa Lei Ai

Doctor of Philosophy in Biology and Biomedical Sciences

Immunology

Washington University in St. Louis, 2017

Professor: Chyi-Song Hsieh, Chair

Peripheral Treg cells (pTreg cells) maintain immune homeostasis at mucosal interfaces, where they can develop upon activation of naïve $CD4^+$ T cells by bacteria antigen. However, the cellular and molecular requirements that govern their differentiation in inflamed and homeostatic contexts require further elucidation. To circumvent uncertainties in existing methods of distinguishing pTreg cells from thymic Treg cells (tTreg cells), we analyzed monoclonal cell populations of CT2 and CT6 transgenic (Tg) cells that develop into pTreg cells in response to different species of endogenously presented *Helicobacter* antigen. In our comprehensive assessment of multiple intestinal inflammatory models, including infections and physical injury, we find that pTreg development against *Helicobacter* antigen is largely preserved. In one model, DSS coupled with a high-fat diet (HFD), we observed a TCR-specific defect in Treg cell development with CT6, but not CT2 Tg cells, adopting effector fates. The concurrent development of effector and pTreg cells during inflammation implicate that the cellular and molecular signals that govern pTreg cells and effector T cell development are highly sequestered, protecting the host from the aberrant generation of effector T cells against tolerogenic antigens.

Transcriptional regulators regulate pTreg celll development by promoting FoxP3, antagonizing alternative effector fates, and stabilizing FoxP3 expression. Here, we capture transcriptional snapshots of activated monoclonal CT6 Tg cells pre and post FoxP3 expression to identify relevant transcriptional regulators during different stages of development. Early developing pTreg cells exhibit a burst of transcriptional activity that is not maintained in later stages. Furthermore, early developing pTreg cells transiently express *Eomesodermin* (Eomes) which restrains FoxP3 expression in activated, undivided cells and cells that have undergone one division. Eomes expression correlated with the expression of Nr4a family of transcription factors, which enhance FoxP3 expression. Thus, early developing pTreg cells concurrently express transcriptional regulators that promote or repress Treg cell development early in development.

Chapter 1: Introduction

Introduction

The immune system is designed to mount rapid and functionally specialized defenses against invading pathogens or mutant cells to protect organisms from infectious diseases and cancers. Tolerance mechanisms are in place to firstly, prevent the immune system from mounting effector responses against healthy host cells and secondly, to restrain immune responses after threats have been eliminated. Regulatory T cells (Treg cells), whose development require the FoxP3 transcription factor (1–4), are necessary for the tolerogenic branch of the immune system to function effectively. Defects in FoxP3 lead to death in both human and mice (5–10) , and depletion of $FoxP3^+$ cells from mice result in multi-organ failure (11).

Treg cells are thymically derived, known as thymic Treg cells (tTreg cells), or extrathymically derived in the periphery, known as peripheral Treg cells (pTreg cells). During thymic negative selection, developing T cells with very high affinity to self-antigen are eliminated, preventing the egress of self-reactive T cells into peripheral circulation. Cells with moderate to high affinity to self-antigens are directed to express FoxP3, exiting the thymus into peripheral circulation as tTreg cells. In contrast, pTreg cells originate from naive, pluripotent $CD4^+$ T cells that can differentiate into effector T cells or Treg cells. When naïve $CD4^+$ T cells encounter their antigen, they receive specification signals that allow them to differentiate into functionally appropriate cell fates.

Both thymic and peripheral Treg cells require FoxP3 for their development, but regulate FoxP3 expression through distinct enhancers and may be specialized for distinct functions (12). pTreg cells are emerging to be uniquely critical for immune tolerance at mucosal interfaces. An increasing number of bacteria species and byproducts in mammalian microbiota are being found

to induce pTreg cells and/or promote pTreg function (13–21). Their selective deletion by ablating the CNS1$^{-/-}$ enhancer, critical for FoxP3 upregulation in pTreg cells, (12) leads to spontaneous type 2 inflammation at mucosal interfaces (22).

The appropriate selection and development of pTreg cells is thus, an important area of study. Perturbing this process may compromise tolerance at mucosal interfaces, which are constitutively encountering bacteria, food, and self-antigens. Aberrant immune reactivity to such antigens may contribute towards the manifestation and/or amplification of intestinal diseases, including inflammatory bowel disease (IBD) and celiac disease. My research aimed to understand what factors inhibit appropriate pTreg differentiation and development against commensal bacteria. I evaluated both cell-extrinsic conditions, specifically intestinal inflammation, and cell-intrinsic factors, specifically genes transcribed prior to FoxP3 in pTreg cells developing *in vivo*.

My thesis work found that pTreg development by *Helicobacter*-reactive TCR Tg cells are largely able to differentiate in multiple models of intestinal inflammation. Their development into pTreg cells is negatively affected in one model, the DSS model of colitis coupled with high fat diet (HFD), which uniquely induces a dramatic expansion of *Enterobacter* species in the microbiota. Additionally, early stages of pTreg development are more transcriptionally active than later stages. *Eomesodermin* (Eomes), which can inhibit Treg cell development, is expressed early in developing T cells upon TCR engagement, restricting the rate of FoxP3 expression in undivided or recently divided cells.

Microbiota and T cells

Mammalian microbiota is composed of trillions of bacteria species that promote host health by aiding with digestion, nutrient extraction, and protection from gastrointestinal pathogens (23–25). Hosts and bacterial communities have evolved to co-exist in a state of symbiosis. Thus, mechanisms are in place to prevent the uncontrolled outgrowth of commensal bacteria, without eradicating them from the host. The mucus and epithelial layers provide a passive layer of protection, serving as a barrier that protects the microbiota and host by largely sequestering bacteria from the host immune system. However, the immune response also plays an active role in regulating commensal bacteria by adopting effector or Treg fates when encountering bacteria antigens (25, 26).

Numerous human and mouse species of bacteria stimulate T cell responses and direct either effector or tolerogenic cell fates. Notably, segmented filamentous bacteria (SFB), which adhere to intestinal epithelial cells, elevate the number of Th17 cells in the small intestine (27–29). Th17 responses exacerbate inflammation and tissue damage by recruiting neutrophils and activating epithelial cells (30). SFB antigen is directly presented to T cells and is able to specifically instruct Th17 development due to the environment in which it is presented (31). Interestingly, bacteria prevalent in oral bacterial communities can induce robust Th1 responses in the gut (32). Antibiotic resistant strains of *Klebsiella pneumoniae* trigger Th1 proliferation in the gut of germ-free (GF) —a phenotype recapitulated in GF mice colonized with saliva samples from human ulcerative colitis patients (32). These saliva samples also contained strains of *Klebsiella*, supporting the plausibility that oral bacteria that colonizes the gut, which likely lacks tolerogenic mechanisms required for their control, may promote disease through Th1 generation (32).

Clusters IV and XIVa of *Clostridium* species on the other hand, are sequestered from the epithelial layer and induce Treg responses in the large intestine (13, 14). The Treg cells induced are primarily Helios$^-$(*Ikzf2*), a transcription factor that marks Treg cells that are thymically derived, produce anti-inflammatory IL-10, and are sufficient to reduce the severity of TNBS-mediated colitis (13). However, whether the pTreg cell enrichment is the result of antigen-specific processes, or the non-specific expansion of pre-existing Treg cells present in the colon, remains a point of debate. Treg TCRs isolated from the tTreg cell population are reactive to antigen from numerous *Clostridium* species *in vitro* (33), but studies from our laboratory identified that the CT6 TCR, which reacts to *Clostridium* antigen, can instruct naïve CD4$^+$ T cells to differentiate into pTreg cells. The tTreg TCRs have never been verified to react to *Clostridium in vivo*, and the CT6 TCR has since been found to react more potently to *Helicobacter* antigens *in vivo* (18). pTreg and tTreg cells both contribute towards intestinal tolerance, evidenced by the delayed inflammation in CNS1$^{-/-}$ mice (12). However, whether *Clostridium* is predominantly inducing the expansion of pre-existing pTreg cells or generation of new pTreg cells specific to *Clostridium* antigen remains a point of debate.

Interestingly, commensals that can act as pathobionts also induce Treg responses (18, 34). Treg cells generated by *Helicobacter hepaticus* antigen more effectively suppress colitis driven by effector T cells specific to *Helicobacter hepaticus* antigen in lymphodeficient mice than Treg cells not specific to *Helicobacter hepaticus* (34). Our laboratory further found that two TCRs which instruct naïve CD4$^+$ T cells to differentiate into pTreg cells (35–37) react to *Helicobacter* antigen *in vitro* and develop in mice colonized with *Helicobacter spp.* (18). Naïve CT2 and CT6 TCRs Tg cells, which recognize *Helicobacter typhlonius* and *Helicobacter apodemus*, respectively, differentiate predominantly into Treg cells in the lymph node that drains

the cecum (dMLN)–the primary site of *Helicobacter* colonization. However, both species of *Helicobacter* exacerbate intestinal disease despite their robust induction of IL-10 producing Treg cells. This contrasts starkly with the protection conferred by *Clostridium* colonization. A prevalent school of thought with regards to the function of commensal-specific Treg cells, is that Treg induction balances Th17-mediated inflammation caused by commensals or pathogens (29, 38). A second proposal is that Treg cells promote colonization of certain species given that Treg depleted mice and CNS1$^{-/-}$ mice have microbiota distinct from healthy counterparts (22, 39). Although it is possible that *Helicobacter* induces a greater number of effector T cells than pTreg cells to drive disease, the insufficiency of Treg induction by *Helicobacter* to protect hosts from intestinal disease highlights that the functional significance of Treg cells specific to commensal bacteria has not been rigorously studied.

Although the functional significance of bacteria-specific pTreg cell responses remains a future area of study, the body of literature demonstrates that intestinal bacteria play an active role in shaping mucosal adaptive immune responses. These processes occur in homeostatic contexts, supporting that the bi-directional dynamic of immune-commensal interactions promotes a balanced environment suitable for both the promotion and restraint of commensal bacteria.

TCR T cell repertoires

T cell receptor repertoires need to acquire a level of diversity that maximizes the probability that immune responses will be launched against foreign antigens and tolerance enforced against self-antigens. Mechanisms that ensure this diversity include somatic rearrangements of the V, D, and J chains via VDJ recombination, non-germline encoded coded point mutations at the juncture of these gene segments, and combinatorial pairing of TCR alpha

and beta chains. In mice, $2x10^{15}$ different TCRs are generated during T cell development in the thymus, a number reduced to approximately $2x10^{6}$ TCRs based on *in silico* estimation (40) after thymic negative selection and death by neglect in the periphery.

The development of appropriate TCR repertoires is critical for effective immune responses against pathogens and tolerance. Mice with restricted repertoires due to the insertion of a TCR-β transgene ($4x10^{5}$ TCRs) are less able to reject bone marrow transplants, or clear viral infections (40). Presumably, fewer T cells recognize diverse epitopes presented by pathogens, which have adapted to escape immune responses by producing highly various epitopes and/or mutations. Interestingly, mice with limited TCR diversities, including TCRβ $TCR\alpha^{-/-}$ and TCR Tg mice develop spontaneous colitis, suggesting that Treg populations in these mice are not sufficient to restrain what are likely, limited effector responses (41–44). Spontaneous colitis caused by limited TCR diversity enriches for Th2 cytokines (42, 44). This observation is abrogated in TCRβ $TCR\alpha^{-/-}$ mice in germ-free conditions, suggesting that limited Treg diversity leads to Th2 responses against commensal bacteria (42).

Disruptions of TCR repertoire diversity or composition alter the antigen specificities of Treg cell populations, and potentially its function. Treg cells have been shown to be more effective at suppressing effector T cells when they are antigen specific in the context of colitis, and autoimmune disease like diabetes (34, 45, 46). The relevance of these studies to tolerance against commensals is unclear. However, the intestinal Treg cell population has characteristics that implicate the importance of antigen specificity in its maintenance of gut homeostasis. Treg TCR repertoires are more diverse than effector T cells, and are relatively similar between mice to mice (35, 37). In contrast, effector TCR repertoires are less diverse, with Th17 cells exhibiting the least diversity. Effector TCR repertoires also show more variation from mouse to mouse,

suggesting that effector TCR repertoires in the periphery are selected through a process that is stochastic relative to the selection of the intestinal Treg TCR repertoires. Thus, the maintenance of Treg cell populations in the intestine during homeostasis may be highly shaped by a conserved pool of homeostatically accessible antigens, whereas effector TCR repertoires are relatively shaped by stochasticity. Disruptions in the homeostatic processes that shape Treg TCR repertoires are likely to impair peripheral tolerance.

Inflammation and Treg cells

Intestinal inflammation elevates inflammatory cytokines, some of which can impair Treg cell development. Th1 and Th2 cytokines block FoxP3 induction *in vitro* through transcriptional targets of Tbet and GATA3 (47, 48). IFNγ signaling, which increases Tbet expression and can interfere with Smad3-mediated transcription (49, 50), is also sufficient to inhibit FoxP3 expression (50). However, IFNγ is not necessary for Tbet blockade, given that IL-12 treatment of IFNγ $^{-/-}$ T cells continues to block FoxP3 expression *in vitro* (47).Furthermore, IL-6 addition to Tgfβ in cultures induces Th17 differentiation programs by amplifying IL-21, IL-23, and subsequently, Rorγt (51). Cumulatively, effector cytokines can overwhelm Tgfβ signals, block Treg differentiation programs, and divert cells to effector fates.

The impact of inflammation on Treg cells at a population level has resulted in different, although not necessarily conflicting, results. One study, generating a FoxP3 lineage-tracing FoxP3-GFP-Cre x Rosa26-YFP transgenic mouse found that a significant population of cells that once expressed FoxP3, lose their FoxP3 expression and became effector T cells in the context of EAE, a mouse model for multiple sclerosis (52, 53). Alternative studies have reported that Treg cells are long-lasting and stable. Instead of becoming destabilized, Treg cells process

inflammatory signals and undergo transcriptional changes that enhance their tolerogenic function (54, 55). Another study has argued that priming naïve $CD4^+$ T cells with type 1 interferon signals can enhance Treg numbers, with increased Treg number correlating with delayed tumor rejection (56). It is important to note that these studies evaluate Treg cells at a population level, and do not characterize Treg cells at the resolution of an individual T cell clone.

It is possible that Treg stability at a population level depends on the model being evaluated, given that the signals that drive pathology in different tissues and organs vary significantly. Furthermore, seeming contradictions may also be related to the different ratios of pTreg cells, which are enriched in tissues at mucosal interfaces relative to lymphoid tissues, to tTreg cells (57). Mucosal and non-mucosal tissues contain different proportions of early developing vs. mature tTreg cells. pTreg cells in intestinal tissue, but not lymphoid organs, increase with age, suggesting that pTreg cells are constitutively being generated against intestinal antigen (36). Thus, populations of pTreg cells in the intestine will include a significant population of cells at early stages of development, mixed with mature pTreg and tTreg cells. Deciphering the impact of inflammation at early and late developmental stages can be approached with monoclonal cells by controlling the timepoint at which disease is induced, either prior or after Tg cell transfer. Our laboratory has investigated the development of naïve CT2 and CT6 Tg cells in the context of strong intestinal insult, induced by a combination of DSS and α-IL10R treatment (18). The naïve Tg cells develop into Th17 cells, and not pTreg cells, demonstrating that in extreme models of inflammation, pTreg development from naïve cells can be blocked (18). However, it was not determined how inflammation affected mature, $FoxP3^+$ populations of monoclonal Tg cells.

Inflammatory models

Infection models

Citrobacter rodentium is a murine model pathogen used to study host responses to enteropathogenic *Escherichia coli* (58–60). It colonizes along epithelial cells and belongs to a class of pathogens that utilize a type III secretion system to penetrate cell membranes and inject effector molecules into infected cells (58, 61). Thus, *Citrobacter* has served as an effective organism for the study of bacterial virulence factors, the pathogenesis of enteropathogenic (EPEC) and enterohemorrhagic (EHEC) diseases, and the immunological requirements for its clearance (59–61).

Citrobacter infection stimulates different effector cytokines at early and late timepoints after infection. IL-22, IL-6, IL-23, and IL-12 peak early after infection on day 4 (62). However, IL-17 cytokines are elevated later on at day 12 post infection (62). Innate mechanisms of defense are mediated by cytokines like IL-22, which maintains epithelial integrity. $IL22^{-/-}$ mice exhibit exacerbated colitis and increased morbidity in response to *Citrobacter* infection (59). Cytokines, including IL-23, IL-12, and IL-6, produced by innate cells, direct the development of adaptive responses. Effector T cells activate innate responses and generate antigen-specific IgG and IgM antibodies to clear the pathogen. (63). However, Th1 cytokines directly produced by $CD4^+$ T cells specific to *Citrobacter* antigen are also important for host defenses (60, 63–65) , given that deficiencies in $CD4^+$ T cell sources of IFNγ led to higher bacteria burden upon *Citrobacter* infection (60).

Toxoplasma gondii is an intracellular coccidian parasite that infects the gut epithelial cells of many different mammalian hosts (66). Failure to control *T. gondii* infection virtually always leads to host death (66). Lymphodeficient mice that lack T cells are extremely susceptible

to *T. gondii* infection, demonstrating that T cell responses are critically important for its control. Furthermore, *T.gondii* specifically induces a strong Th1 response, characterized by high levels of IFNγ, TNFα, IL-18, and IL-12, which likely activate macrophages to control intracellular parasite replication (66–68). The sustaining of IFNγ levels during *T. gondii* infection requires IL-12 signaling, given that IL-12 p40 deficient mice experience increased brain cyst burdens before eventual morbidity (69).

DSS and DSS and HFD

The dextran sulfate sodium (DSS) is a chemically induced model for acute and chronic colitis. It is a sulfated polysaccharide composed of approximately 17% sulfur, with on average, 3 sulfur groups per glucose molecule (70, 71). DSS most potently affects gut epithelial cells by compromising the mucus layer and damaging the basal crypts, which results in apoptosis of colonic epithelium cells (71, 72). Mice administered DSS in their drinking water between 1-10% will develop inflammation of varying severity primarily limited to the colon, accompanied by cellular infiltration of mucosa and submucosa with innate immune cells and relatively few number of lymphocytes (70). DSS-mediated colitis is characterized by elevated Th1 and Th2 responses (73), but does not require these T cell responses for disease, given that $Rag^{-/-}$ mice develop disease that is more severe than in lymphoreplete hosts (72). Thus, DSS is widely considered to be a suitable model for assessing innate responses in acute and chronic colitis.

High fat diet (HFD) coupled with DSS exacerbates the severity of intestinal diseases. Dietary fats, independently of DSS, can elevate the circulation of inflammatory cytokines like IL-6 and TNF-α and accelerate or exacerbate spontaneous colitis and colon tumorigenesis (74–76). HFD weakens tight junctions, increasing intestinal permeability and susceptibility to barrier

breach (77, 78). HFD can additionally enrich the gut microbiota for pathobionts, including *Helicobacter* species and *Bilophila wadsworthia,* which is sufficient to increase numbers of Th1 cells in GF conditions. Microbiota shaped by HFD is sufficient to transmit increased disease susceptibility, showing that microbiota changes, independently of stromal damaged caused by HFD, is sufficient to increase disease risk (79). Thus, DSS and HFD worsens disease due to a combination of factors, that include compromised barrier function, enrichment of pathobionts that can further damage the epithelial layers, and elevated effector T cell responses.

FoxP3 and Treg development

FoxP3 is the hallmark transcription factor required for both tTreg and pTreg development. Evidence of a T-cell mediated tolerogenic function first arose with a spontaneous 2 bp insertion that shortens FoxP3 into a non-functional protein, resulting in the Scurfy mouse model (7–9) . Scurfy mice lack $CD4^+CD25^+$ cells, have enlarged organs, and undergo premature death within 3 weeks of birth (7, 8, 80). This phenotype parallels that of IPEX patients (immune-mediated polyendocrinopathy X-linked syndrome), who have naturally occurring mutations in FoxP3, undergo multi-organ failure, and have shortened life expectancies (9). The failure of $FoxP3^-$ bone marrow cells, transplanted into wild-type hosts, to acquire $CD4^+CD25^+$ regulatory phenotypes, provided additional early evidence that FoxP3 is the central transcriptional regulator for $CD4^+CD25^+$ regulatory T cells (1).

FoxP3 is also necessary for the suppressive function of Treg cells. Ectopic overexpression of FoxP3 into human naive $CD4^+$ T cells is sufficient to confer suppressive function and cells with non-functional FoxP3 protein are deficient in their ability to suppress effector T cells (1, 3, 81, 82). In the absence of FoxP3, these cells produce inflammatory

cytokines and IL-2, which are hallmark characteristics of $CD4^+$ effector T cells (6). However, the level of inflammatory cytokine production remains less than that of effector T cells, suggesting that the failure to develop into FoxP3 is not the result of a complete diversion of cells to effector cell fates.(83)

Tgfβ, which exists in 3 isoforoms (TGFB1, TGFB2, TGFB3), is a critical signal for FoxP3 induction in $CD4^+$ naïve T cells (84). Tgfβ is secreted in a latent form as a complex with the latent Tgfβ binding protein (LTBP) and the latency associated peptide (LAP). When Tgfβ reaches a cell surface, it is cleaved by proteinases, dimerizes, and activates the Tgfβ receptor and subsequently, FoxP3 transcription in $CD4^+$ T cells (84, 85).

An important signaling pathway downstream of Tgfβ is through the Smad family of transcription factors. Smad transcription factors can bind to activated Tgfβ receptors, and are subsequently phosphorylated by the kinase domains on the cytoplasmic region of the Tgfβ receptors (86). Smad3 and Smad2 dimerize, and then bind to Smad4 for nuclear translocation to initiate transcription. Subsequently, they interact with the FoxP3 promoter and the CNS1 enhancer region to regulate FoxP3 expression (12).

However, Tgfβ can also signal through Smad independent mechanisms. Including MAP kinase (MAPK) pathways, Rho-like GTPase signaling pathways, and phosphatidylinositol-3-kinase (PI3K)/AKT pathways (84). Notably, Smad3 deletion does not result in loss of FoxP3 expression in T cells activated with Tgfβ *in vitro*, nor were Smad proteins critical for Th17 or Treg cells *in vivo* (87, 88). This is in part explained by redundancy in Smad2 and Smad3 function for FoxP3 induction (89). However, selective targeting of non-Smad pathways, including ERK and JNK pathways, resulted in defects in Tgfβ-mediated FoxP3 induction and Th17 development despite the presence of Smad3 (90, 91). These studies, however, did not

validate that Smad3 was being properly phosphorylated, leaving open the possibility that deficiencies in these alternative pathways indirectly affect Smad-mediated FoxP3 expression. Nonetheless, evidence is supportive that Smad proteins, although important, may not be required for Treg development.

Co-regulators of Tgfβ signaling in Treg cells

FoxP3 induction by Tgfβ can be amplified by co-factors. Notably, retinoic acid and Ahr ligands amplify FoxP3 expression by *in vitro* cultured $CD4^+$ T cells. Retinoic acid induces FoxP3 independently of IL-2 and concurrently antagonizes the expansion of contaminating effector cells or memory cells in cultures (92–96). Specifically, retinoic acid contributes towards the suppression of Th17 differentiation profiles by inhibiting IL-6 and IL-23 receptor upregulation (94–96). Additionally, Ahr ligands promote Treg or Th17 differentiation depending on the type of ligand, with TCDD promoting Treg development and FICZ promoting Th17 development (97, 98). This differential outcome may be dependent on the affinity of the ligand for Ahr, which can further regulate retinoic acid receptors (99). However, it should be noted endogenously found Ahr ligands are processed from food antigens, whereas the tested Ahr ligands are synthetic ligands (97).

Short chain fatty acids (SCFAs), produced by certain species of commensal bacteria, have emerged as an additional contributor to FoxP3 induction in the intestine (15, 17, 100). SCFA's are sufficient to increase the numbers of $FoxP3^+$ cells in GF mice and *in vitro* activated naïve $CD4^+$ T cells (15, 16). SCFA's may promote FoxP3 expression by signaling through GPR43 to inhibit histone deacetylases (HDACs), which can also increase Treg gene expression

and suppressive function (101). Thus, FoxP3 induction is initiated by Tgfβ and can be further enhanced by a variety of co-regulators prevalent in the intestine.

Regulation of FoxP3 induction

In addition to its promoter, FoxP3 expression in tTegs and pTreg cells is regulated by a series of conserved, non-coding sequences found downstream of the FoxP3 promoter (12). These regions are highly conserved in the FoxP3 locus across different species, hinting at their functional importance in regulating FoxP3 transcription, and are bound to permissive H3 modifications (H3K4me3, H3K9/14Ac) (12). CNS3 promotes FoxP3 expression in tTreg cells, potentially through interactions with c-Rel induced by co-stimulatory molecules (12). CNS1, downstream of CNS3, contains a Tgfβ-NFAT response elements and is critical for pTreg cell development but dispensable for tTreg cell development (12). CNS2 maintains FoxP3 expression in Treg cells that originate from dividing Treg cells, supporting that its molecular partners stabilize FoxP3 (12). Deletion of the CNS1 region ablates pTreg cells, but this deficiency is compensated for by an increased number of tTreg cells and FoxP3$^-$ IL-10 producing cells, known as Tr1 regulatory T cells (12).

The Nr4a family of transcription factors (Nr4a1, Nr4a2, Nr4a3) interacts with the CNS regions and FoxP3 promoters to regulate FoxP3 expression in both pTreg cells and tTreg cells (102–104). Nr4a1 expression is directly proportional to the strength of TCR signaling, and has transcriptional targets that are characteristic of Treg cells, including *Ikzf2* (103, 105). Nr4a2 directly induces FoxP3 transcription by binding to the FoxP3 promoter and incorporating permissive histone modifications (102). All 3 Nr4a proteins can induce FoxP3, with Nr4a2 induction being the most potent, Nr4a3 inducing intermediate levels, and Nr4a1 having the

mildest effect (102). Deficiency in one of the Nr4a proteins does not result in Treg deficiency, but deletion of all three has a deleterious effect on Treg cells, and similarly to Scurfy mice, results in morbidity in approximately 30 days (104, 106).

Nr4a response elements were identified in both the FoxP3 promoter and in the CNS regions. However, the response elements in the CNS1, but not CNS2 region, most potently enhanced FoxP3 promoter activity (102). Binding of Nr4a proteins to the CNS1 region was supported with ChIP data, which further verified that Nr4a proteins do not bind to the CNS3 regions (102). Thus, Nr4a proteins, most effectively Nr4a2, promote FoxP3 expression in both tTergs and pTreg cells, but may also enhance pTreg cell induction by incorporating permissive histone modifications at H3 regions that interact with the CNS1 enhancer.

Antagonism of effector phenotypes to promote Treg development

Treg development is orchestrated by the concurrent induction of FoxP3 and the antagonism of alternative fates. Transcriptional regulators not required for the development of Th1 and Th2 cells, can antagonize Th1 and Th2 fates and promote Treg cells. Musculin2 ($Msc^{-/-}$), which antagonizes Th2 differentiation, is expressed within 10 hours of Tgfβ signaling via the Smad3 signaling pathway in $CD4^+$ T cells activated *in vitro* (107). Musculin2 deficient mice exhibit autoimmune pathology, including increased cellular infiltration in tissues, most significantly at mucosal interfaces like the small intestine and lungs. This correlates with reduced numbers of $FoxP3^+$ cells. This is a cell-intrinsic phenomenon, evidenced by reduced efficiency of Tgfβ induced FoxP3 expression by musculin2 deficient cells *in vitro.* Populations of musculin2 deficient $CD4^+$ T cells more effectively adopt Th2 profiles, with increased numbers producing IL-4, IL-5, and IL-13 *in vitro* and *in vivo*. Enhanced Th2 responses at mucosal

interfaces in CNS1$^{-/-}$ mice (22), further supports that Th2 and Treg differentiation programs antagonize one another.

The PHD family of transcription factors, which serve as oxygen sensors in T cells, promote Treg responses by antagonizing Th1 profiles (108). Mice with T-cell specific deletions of PHD1, PHD2, and PHD3 proteins had increased serum antibodies and spontaneous pathology in the lung. Numbers of IFNγ producing CD4^{+} T cells increased in the lungs and colon lamina propia, which correlated with a 2-fold reduction of Nrp1^{lo} FoxP3^{+} cells, a population that is predominantly pTreg cells. Enhanced IFNγ production was argued to be cell-intrinsic, given that PHD deficient cells show increased Th1 and reduced Treg responses *in vitro*. An unaddressed caveat here however, is that the decreased Treg responses may be the result of enhanced IFNγ levels in cell cultures, which can block Treg induction independently of PHD protein activity.

Although transcriptional regulators can antagonize alternative fates at a population level, the extent of their physiological relevance at a monoclonal level remains uncertain. Our laboratory assessed differentiation by CNS1$^{-/-}$ CT6 Tg cells, which as expected, exhibit dramatically reduced FoxP3 expression after 1 week of development in wild-type hosts (36). The activated, FoxP3^{-} cells mildly expressed IFNγ, suggesting that the absence of Treg induction can lead to the spontaneous adoption of effector cells despite the absence of effector inducing signals. However, the fraction of IFNγ producing cells was insignificant, at only 1-2% (36). In contrast, 40-60% of Tg cells become FoxP3^{+} cells 1 week after transfer (36). Thus it remains unclear if mechanisms that antagonize effector differentiation are relevant *in vivo*, or if these mechanisms are not activated in the absence of effector cytokines in the environment of CT6:pMHC engagement.

FoxP3-independent factors in Treg development

Cells deficient for the FoxP3 protein are still able to adopt Treg signature genes, implicating that genes independent of FoxP3 contribute to the transcriptional profiles of mature Treg cells (109). Treg signatures were defined by evaluating the transcriptional profiles of cells retrovirally overexpressed with FoxP3, *ex vivo* isolated Treg cells, as well conventional T effector cells. Treg signature genes include factors unique to Treg cells including *CTLA4, IL2rb, Socs2*, and *Ikzf2* (109). A significant portion of Treg signature genes are however, activated by FoxP3 independent signals, including TCR signaling, co-stimulation, and/or Tgfβ signaling (109). A number of genes differentially expressed in response to Tgfβ signaling were blunted in $CD4^+$ T cells isolated from Scurfy mice, supporting that FoxP3 promotes Treg development in part by amplifying gene networks triggered independently of FoxP3 (109). A more recent study verified that FoxP3 independent gene targets, which are potentially amplified by FoxP3, are sufficient to downregulate effector responses in the context of diabetes (110). This study observed that conditional deletion of Tgf-β receptor II (TβRII) in genetic mouse models for diabetes resulted in disease that was more severe than in FoxP3 deficient mice. The implication here is that Tgfβ targets, independently of FoxP3, are sufficient to confer a level of tolerance. Thus, Foxp3 can likely promote tolerance by amplifying FoxP3 independent targets in conjunction with activating and repressing its own target genes (111).

Eomesodermin and $CD4^+$ T cells

Eomesodermin (Eomes) is a member of the Tbx family of transcription factors, which serve critical functions in embryogenesis (112, 113). Eomes is regulated by Tgfβ and can interact with Smad2/3 targets (114). In addition to their developmental functions, Tbx transcription

factors, Eomes and Tbet, serve critical functions in the development and differentiation of immune cells. Tbet is the hallmark transcription factor for Th1 differentiation (115), and is also expressed in subsets of NK cells (116). Eomes and Tbet share numerous transcriptional targets, and serve complementary functions in $CD8^+$ T cell development, with their co-expression increasing production of effector molecules like IFNγ, granzyme, and perforin relative to mice with single deletions of Tbet or Eomes (117).

In $CD4^+$ T cells, Eomes has emerged to be promiscuously expressed in multiple lineages and can both antagonize and promote effector cell functions. Eomes is suppressed by Tgfβ signaling in $Smad2^{-/-}Smad3^{-/-}$ mice through the c-Jun N-terminal kinase (JNK)-c-Jun signaling pathway, promoting Th17 cell development (91). Eomes overexpression blocks Th17 development by potentially recapitulating the effects of strong Tgfβ signaling, which would skew cells towards a Treg fate (118, 119). Eomes also regulates effector $CD4^+$ T cell responses by negatively regulating IL-5 production by memory Th2 cells (120). Eomes is specifically expressed in memory Th2 cells, defined by $CD62L^{lo}CXCR3^{lo}$ Th2 cells, and prevents GATA3 from binding to the IL-5 locus (120).

In addition to antagonize effector phenotypes, Eomes expression actively promotes tolerogenic phenotypes. Eomes deficiency increases FoxP3 expression, with Treg cells numbers increasing in older mice relative to Eomes sufficient littermate controls (121). Eomes mediated enhancement was sufficient to alleviate EAE severity, which authors attribute towards elevated Treg numbers in the mice (121). However, a more recent study finds that Tbet and Eomes cooperate to induce IL-10 production by $FoxP3^-CD4^+$ Tr1 cells (122). In this study, Eomes deficiency increased the severity of GVHD, which authors attribute to deficiencies in Tr1 cells (122). One possibility for these different results is the usage of different conditional knockouts.

In the study with alleviated EAE symptoms, *Eomes* $^{fl/fl}$ mice (123) were crossed to Lck-Cre^{+} mice, whereas the study with exacerbated GVHD utilized mice crossed to the CD4 Cre. It is additionally possible that enhanced Treg cells are more effective at protecting against Th17 mediated disease in the context of EAE (124), and Tr1 responses are more critical for antagonizing Th1 responses, which are critical for GVHD (125).

However, Eomes can also amplify effector responses by increasing IFNγ production by Th1 cells independently of Tbet (126–128). Eomes deficiency also increases Th1 cell plasticity, promoting Th1 destabilization towards IL-6 mediated Th17 differentiation (126). This is consistent with the aforementioned study, which reported Eomes suppression promotes Th17 differentiation. It is possible that this increased Th17 differentiation in response to Eomes suppression is through the destabilization of Th1 cells *in vivo.* Cumulatively, the literature shows that Eomes can facilitate both effector and tolerogenic responses, and thus, serves a multi-faceted function in CD4^{+} T cell differentiation and development.

Chapter 2: The impact of inflammation on colonic peripheral Treg cell development

Abstract

Peripheral regulatory T (pTreg) cell differentiation in response to intestinal commensal bacteria is important for gut homeostasis. However, it remains unclear if environmental factors that trigger intestinal inflammation, such as dietary fats, physical insults, and enteric infections, interrupt this process universally or only under select conditions. In this study, we found that pTreg cell differentiation to *Helicobacter* is generally preserved in multiple models of intestinal inflammation or infection. However, colitis caused by DSS coupled with high fat diet (HFD) led to a selective blockage of pTreg cell generation of TCR transgenic cells that respond to *Helicobacter apodemus* (CT6), but not *Helicobacter typhlonius* (CT2). This phenomenon was also observed with analysis of polyclonal Treg TCR repertoires, in which distinct subsets of TCRs either expand or contract in clonal frequency during DSS and HFD. DSS and HFD promoted a marked expansion of *Enterobacter* species. A possible explanation for these results is suggested by the fact that CT6, but not CT2, is weakly cross-reactive to *Enterobacter* species *in vitro*, which could result in TCR stimulation of CT6 in an environment favoring effector, and not pTreg, cell development. Thus, these data show that TCR specificity can determine regulatory vs effector T cell fates in the same host, and imply the existence of multiple microenvironments that direct distinct T cell differentiation pathways during intestinal inflammation.

Introduction

The gastrointestinal tract is a complex environment that constitutively exposes the host to bacteria, food, and self-antigen. FoxP3^{+} regulatory T (Treg) cells play a critical role in inhibiting unwanted immune responses to these intestinal antigens, which can lead to afflictions such as inflammatory bowel disease (9, 22, 129, 130). The gut Treg cell population appears to be shaped by intestinal antigens, as the colonic Treg TCR repertoire is more conserved from mouse to mouse relative to effector T cell TCR repertoires (18, 35). Moreover, TCR transgenic (Tg) studies have suggested that antigens from gut commensal bacteria can directly facilitate colonic Treg cell selection (18, 21, 36, 37). Thus, intestinal antigens appear to play a critical role in inducing Treg cell selection important for maintaining gut homeostasis (13, 14, 21, 28, 131, 132).

Specific species of commensal bacteria shape gut TCR repertoires by selecting for T cell clones which adopt either effector or tolerogenic fates (21, 31, 33, 133). Colonization with segmented filamentous bacteria (SFB), which induce Th17 responses (27, 28), is sufficient to exacerbate colitis, whereas colonization with *Clostridium,* which induce Treg responses (13, 14, 21, 33) is sufficient to ameliorate colitis. Although these species also affect the innate immune response (29, 134), these data suggests that commensal-driven shaping of the intestinal TCR repertoire of effector and Treg populations may contribute to disease susceptibility.

Intestinal inflammation has been reported to influence the differentiation of T cells selected on bacterial antigen. For example, CBir Tg cells, which react to *Clostridium* antigen upon barrier breach with *Toxoplasma gondii* infection, differentiate into a long-lasting population of Th1 cells (133). In addition, we have found that intestinal inflammation can affect the differentiation of T cells from two TCR Tg lines, CT2 and CT6, which react to *Helicobacter*

typhlonius and *Helicobacter apodemus*, respectively (18). When naïve CT2/6 TCR Tg cells are adoptively transferred into hosts colonized with *Helicobacter*, they rapidly differentiate into peripheral Tregs (pTregs) (36). However, the Tg cells aberrantly differentiate into Th17 cells instead of Treg cells in mice with blocked IL-10 signaling and DSS mediated mucosal injury (18). Together, these data suggest that T cell responses against bacterial antigen can be influenced by an inflammatory environment.

Early life incidences of intestinal inflammation from environmental sources, including infections, physical insults, and dietary fats, have been correlated with increased risk for intestinal disorders (135). Although current data suggest that intestinal inflammation can direct effector responses against commensal bacteria, it remains unclear whether this is a general outcome of all triggers of intestinal inflammation. Here, we investigated the differentiation of CT2 and CT6 cells in multiple infectious and non-infectious models of intestinal inflammation. Unexpectedly, these studies found that pTreg cell selection is generally preserved in multiple models of intestinal inflammation, suggesting an important role for T cell developmental microenvironments in protecting immune responses from environmental perturbations.

Materials and Methods

Mice

CT2 (36) and CT6 Tg (21) mice were generated as described (136) and bred to *Rag1*$^{-/-}$ [the Jackson Laboratory (JAX) #002216] and *FoxP3*$^{\text{IRES-GFP}}$ (JAX #006772) or *FoxP3*$^{\text{IRES-Thy1.1}}$ (137), *IL-17A*$^{\text{IRES-GFP}}$ (JAX #18472), and *IFNγ*$^{\text{IRES-YFP}}$(GREAT) (138). TCli TCRβ *Tcra*$^{+/-}$ mice (139) were bred to *FoxP3*$^{\text{IRES-Thy1.1}}$ *IL-17A*$^{\text{IRES-GFP}}$ and *IFNγ*$^{\text{IRES-YFP}}$. CT6 Tg mice were also bred to *Tbx21*$^{-/-}$ (JAX #004648) or *Rorc*$^{\text{GFP}}$ mice (JAX #007572). FoxP3-DTR mice (11) were bred onto a CD45.1 background. *IFNγ*$^{\text{IRES-YFP}}$ mice were a gift from R. Locksley (University of California, San Francisco); *FoxP3*$^{\text{IRES-Thy1.1}}$ and FoxP3-DTR mice were gifts from A. Rudensky (Memorial Sloan Kettering Cancer Center). *FoxP3*$^{\text{IRES-GFP}}$ CD45.1 (JAX #006772) host mice used for adoptive transfer experiments were interbred in our colony to maintain their microbiota. Animal experiments were performed in a specific pathogen-free facility in accordance with the guidelines of the Institutional Animal Care and Use Committee at Washington University.

Adoptive transfer experiments

Naive (CD4^{+}FoxP3^{-}CD25^{-}CD44^{lo}CD62L^{hi}) T cells were FACS purified from the draining lymph nodes and spleens from CD45.2 or CD45.1/2 Tg mice bred to *FoxP3*$^{\text{IRES-GFP}}$ *Rag1*$^{-/-}$ or *FoxP3*$^{\text{IRES-Thy1.1}}$ *IL-17A*$^{\text{IRES-GFP}}$ *IFNγ*$^{\text{IRES-YFP}}$ *Rag1*$^{-/-}$. Cells were labeled with Cell-Trace Violet (ThermoFisher) to assess proliferation and 10^5 cells were retro-orbitally injected into 3-4 weeks old wild-type CD45.1 *FoxP3*$^{\text{IRES-GFP}}$ hosts unless otherwise indicated. All experiments were conducted with littermate controls. For experiments evaluating the impact of CD4 effector polarizing cytokines on Tg cells, naïve cells were sorted as described above and plated in α-CD3

(Bio X Cell #BE0001-1; 10 μg/ml) coated 24 well tissue culture plates at $1x10^6$ cells/well in 1ml. Additives to the culture included soluble α-CD28 (Bio X Cell #BE0015-1; 1 μg/ml), anti-cytokine antibodies [all Bio X Cell; α–transforming growth factor–β (20 μg/ml; #BE0057), α-IFNγ (5 μg/ml; #BE0054), α–IL-4 (5 μg/ml; #BE0045), and α–IL-12 (5 μg/ml; #BE0052)] and/or cytokines [Peprotech; IL12 (10 ng/ml, #210-12), IFNγ (50 ng/ml, #500-M90), IL-4 (10 ng/ml, #214-14), muTNF-α (50 ng/ml, #310-12)]. After 48 hours in culture, $1x10^5$ cells were retro-orbitally injected into 3-4 week old congenic CD45.1 *FoxP3*$^{IRES\text{-}GFP}$ mice. For all transfer experiments, the distal mesenteric lymph node (dMLN), which drains the cecum, and/or colon lamina propria were harvested at various time points after transfer and Tg cells (CD45.2 or CD45.1/2, $CD4^+V\alpha2^+$) were analyzed on a BD FACSAria IIu (BD Biosciences).

Lamina propria cell isolation

Colon lamina propria tissue was flushed with PBS to remove fecal content. To remove intraepithelial lymphocytes, lamina propria tissue was incubated in RPMI 1640 media containing 3% FBS, 20 mM HEPES, 1 mM DTT, and 50 mM EDTA for 20 min at 37˚C, and washed with RPMI 1640 plus 22.5 mM EDTA. Lymphocytes were isolated from remaining stromal tissue by mincing and digesting in 28.3 μg/ml Liberase TL (Roche) and 200 μg/ml RNase 1 (Roche) for 30 min at 37˚C. Suspended cells were filtered through a 40 μm filter prior to use.

Infections and inflammatory models

For *Citrobacter* infections, 3-4 week old congenic CD45.1 FoxP3$^{IRES\text{-}GFP}$ mice were infected with $2x10^9$ CFU *C. rodentium* or OVA-*C. rodentium* (60) via oral gavage. For *Toxoplasma gondii* infections, 3-4 week old congenic CD45.1 FoxP3$^{IRES\text{-}GFP}$ mice were orally gavaged with 1

tissue cyst per mouse. Tissue cysts were obtained from the brain of mice harboring chronic infection with of the type II ME49 strain. For DSS and high fat diet (HFD), mice were maintained on HFD from Harlan-Tekland (TD.88137) (140). Mice fed HFD were either maintained on water or switched onto 2% DSS water on day 7.

TCR sequencing

Naïve ($CD44^{lo}CD62L^{hi}$), $CD44^{hi}$ ($FoxP3^{-}CD44^{hi}$), $CXCR3^{+}$ ($FoxP3^{-}CD44^{hi}IL17A^{-}CXCR3^{+}$) and IL-$17^{+}$ ($FoxP3^{-}CD44^{hi}IL\text{-}17A^{+}CXCR3^{-}$) cells were sorted from the MLN of wild type, HFD treated, or DSS and HFD treated TCli TCRβ *FoxP3*$^{\text{IRES-Thy1.1}}$ *IL-17A*$^{\text{IRES-GFP}}$ *IFNγ*$^{\text{IRES-YFP}}$ *Tcra*$^{+/-}$ mice using BD FACSAria IIu. TCR amplicons were sequenced as described (18), and unique TCRα sequences identified via unique TRAV and CDR3 sequences. TCR sequences were rarefied to 10,000 reads to normalize for experimental variation and analysis of reproducible TCRs limited to TRAV_CDR3 species found in 50% or more of mice per condition. Primer bias was corrected by multiplying TCR frequencies with a correction factor as described (18).

T cell hybridoma stimulation assay

NFAT-GFP T cell hybridomas cells (141) transduced with CT6 or CT2 TCRα (21) chains. $1.5x10^{4}$ cells were cultured with *in vivo* flt3 ligand-expanded $CD11c^{+}$ DCs ($5x10^{4}$) in 96 well flat bottom tissue culture plates. 20 μg of antigens generated by autoclaving bacteria isolates were added. TCR stimulation by $CD4^{+}$ $V\beta6^{+}$ cells was assessed by GFP expression after 72 hours in culture.

16S rRNA sequencing

Colon and cecum were cut longitudinally with sterile scissors and fecal content from lumen was harvested with sterile forceps. To harvest mucosal-associated bacteria, lumen content was washed 3x with sterile PBS from colon and cecum tissues. Mucosal-associated bacteria was obtained by washing the tissue vigorously 2x for 20 minutes with PBS + DTT (1 μM/ml) +EDTA (5 μM/ml) at 37°C, filtering through 40 μm filter, and removing epithelial cells via centrifugation at 1500 rpm for 10 minutes. The supernatant, which includes bacteria in suspension, was harvested and pelleted at 2500 rpm for 15 minutes. Pellets were washed with PBS and resuspended in 30% glycerol for storage. Bacteria DNA was isolated from mucosal-associated and luminal bacteria using the ISOLATE Fecal DNA Kit (Bioline). The V4 region of 16S rRNA gene was PCR-amplified and sequenced on the Illumina MiSeq Platform (2x250–bp paired-end reads). Operational taxonomic units (OTU) picking was performed as described (18, 36).

Statistical analysis

GraphPad Prism v6 was used for statistical and graphical analysis. Statistical significance was calculated using the Student T test, *$*P<0.05$, ** $P<0.005$, ***$P\leq0.001$, **** $P\leq0.0001$*; ns = not significant. Error bars = ± SEM. PCoA analysis of 16S sequencing data was done using Bray-curtis distance using Phyloseq (BioConductor). Hierarchical clustering of TCR sequences was conducted using Euclidean distance with R.

Results

Peripheral induction of FoxP3 by Helicobacter-reactive T cells is not markedly impaired by gastrointestinal infections.

Intestinal infections facilitate the development of effector T cells reactive to commensal bacteria that are presented to the immune system for the first time after mucosal injury (133). However, the effect of infection on the development of pTreg cells that react to commensal antigens constitutively presented during homeostasis, such as *Helicobacter* (21, 36), remains unknown. We hypothesized, based on the aforementioned study (133), that infection would favor effector differentiation of T cells that would normally become pTreg cells, which would allow us to study the physiologic signals that determine effector vs pTreg cell differentiation in the gut.

We tested this by studying the development of adoptively transferred naïve CT2/6 TCR Tg cells in hosts infected with *Citrobacter rodentium*, a murine model for human infection with enteropathogenic *E. coli*, or *Toxoplasma gondii*, a parasite that infects the gut and induces a strong Th1 response (61). Contrary to our hypothesis, we saw no reduction in the frequencies of $FoxP3^+$ cells of TCR Tg cells. FoxP3 frequencies were not decreased in Tg cells transferred at early stages of *Citrobacter* infection (day 4) and increased in $FoxP3^+$ CT2 cells transferred at peak infection (day 9) **(Fig. 2.1A, 2.1B)** (60, 62). Similarly, in *Toxoplasma* infected hosts, CT2 cells showed a modest decrease in pTreg cell generation, whereas CT6 cells increased **(Fig. 2.1A).** We confirmed that *Citrobacter* infection elicited effector cell responses by showing that OTII cells became $FoxP3^-CD25^+$ in response to OVA-expressing *Citrobacter* (60) **(Fig 2.1B),** whereas CT6 cells co-transferred into the same mouse underwent pTreg cell generation. Thus, this data demonstrates that *Citrobacter* elicits effector T cell responses without generating a

global environment that impairs pTreg cell generation to commensal antigens.

We did observe some changes in TCR Tg responses during *Citrobacter* infection, including decreased cell numbers, lower CD25 level in FoxP3^{+} Treg cells, and decreased T cell proliferation based on Cell Trace Violet dilution (**Fig. 2.1C-F; 2.8C, 2.8D).** Like *Citrobacte*r infection, Tg cell numbers decreased in *Toxoplasma* infected mice **(Fig. 2.8A).** One interpretation is that there is a relative decrease in the presentation of *Helicobacter* antigens during *Citrobacter* and *Toxoplasma* infection, but the proportion of cells that become FoxP3^{+} in response to *Helicobacter* is not altered. Thus, although *Toxoplasma* infection has been reported to drive T cells selected on commensal antigen towards effector lineages (133), our data shows that the intestinal environment during infections can still be permissive to pTreg cell selection by commensal antigen.

We next verified that *Helicobacter*-reactive T cells can respond to inflammatory cytokines by stimulating naïve CT2/6 TCR Tg cells *in vitro* in the presence of Th1 and Th2 polarizing cytokines. Cytokine-exposed Tg cells were transferred into wild-type hosts where the cells encounter *in vivo* pTreg differentiation signals. Exposure to Th1 or Th2-promoting cytokines *in vitro* inhibited pTreg cell differentiation *in vivo*, with Th1 conditions being more stable in their blockade **(Fig. 2.1G; Fig 2.8E).** As the infection models are not known to induce Th2 responses (59, 142), we assessed individual Th1-promoting cytokines and found that IFNγ is a primary factor that blocks *in vivo* pTreg cell selection **(Fig. 2.1G; Fig 2.8F).** We further validated that polarized CT6 cells can adopt a Th1 phenotype based on IFNγ$^{\text{IRES-YFP}}$ (GREAT) (138) expression **(Fig. 2.1H).** Thus, these data suggest that pTreg cell generation to *Helicobacter* during infection is not due to the inability of Tg cells to differentiate into and maintain effector cell phenotypes.

Selective effect of high-fat diet and DSS on CT6, but not CT2, pTreg cell differentiation.

We next examined if non-infectious models of intestinal inflammation affect pTreg cell differentiation. Given that Th1 signals can block FoxP3 induction in naïve T cells, we focused on models that favor a Th1 environment, characterized by cytokines such as IL-12 and IFNγ (47, 143, 144). As acute Treg cell depletion has been reported to increase the numbers and frequencies of IFNγ producing cells (11, 145), we treated FoxP3-DTR mice with 1 dose of DT followed by adoptive transfer of naïve CT2 TCR Tg cells 24 hours later. TCR Tg cells exhibited a moderate decrease in FoxP3 frequency, and showed a marked increase in the expression of the Tbet regulated gene, CXCR3 (146, 147), in both the $FoxP3^+$ and $FoxP3^-$ fractions of Tg cells **(Fig 2.9A).** Thus, acute Treg cell depletion induces an environment in the gut that is antagonistic to normal pTreg cell selection.

Another model associated with enhanced colonic Th1 responses is DSS in the context of high fat diet (HFD) (11, 140). As we previously reported (18), DSS by itself is not sufficient to inhibit Treg cell development of CT2/CT6 cells **(Fig. 2.2A).** However, CT6 Tg cells transferred into 2% DSS treated hosts proliferated more relative to Tg cells in untreated controls, indicating that the inflammatory environment does not block pTreg cell development by *Helicobacter*-reactive T cells despite potential changes in cytokine levels or antigen presentation **(Fig. 2.2B).** To assess the effect of diet, we added HFD for only 1 week prior to DSS to limit secondary effects such as changes in food intake or obesity that occurs around 3 and 19 weeks, respectively (148). Notably, DSS and HFD inhibited FoxP3 upregulation by naïve CT6, but not CT2 cells **(Fig. 2.2C).** In addition, $FoxP3^+$ CT2, but not CT6, cells showed increased CD25 expression

with DSS and HFD **(Fig. 2.2D).** Thus, DSS colitis in the context of HFD can selectively impair antigen-specific pTreg cell differentiation to commensal bacteria.

Loss of antigen presentation is unlikely to explain the defect in pTreg cell generation by CT6 cells because we observed robust cell division and expansion in both FoxP3^{-} and FoxP3^{+} fractions **(Fig. 2.2D, Fig 2.9B).** Another possibility is that transferred CT2 or CT6 cells are affecting the global inflammatory response to DSS and HFD in different ways. To exclude this possibility, the aforementioned DSS and HFD experiments were performed using co-transfer of both CT2 and CT6 naive cells into the same mouse. This also rules out the possibility that the defect seen with CT6 is due to mouse to mouse variation in DSS water consumption or global inflammatory state. Together with the infection results, these data demonstrate that in a population of CD4^{+} T cells, effector and pTreg cells can concurrently develop during colonic inflammation. This suggests that the phenotypic outcome of T cell selection against intestinal antigen during DSS and HFD is dictated by whether the T cell is encountering its antigen in a Treg or effector-selecting microenvironment.

Effector cell phenotypes of CT6 cells in DSS and HFD

Given our findings that CT2/6 Tg cells can differentiate into effector cells under conditions such as Treg cell depletion **(Fig 2.9A),** DSS + α-IL-10R, and lymphopenia (18, 21), we asked whether CT6 FoxP3^{-} cells were differentiating into Th1 or Th17 cells during DSS and HFD treatment. We addressed this by using the IFNγ$^{\text{IRES-YFP}}$ (138) and IL-17A$^{\text{IRES-GFP}}$ reporters and found that ~4% of FoxP3^{-} CT6 cells were IL-17A$^{\text{IRES-GFP+}}$ in the dMLN, increasing to 15% in the colon lamina propria **(Fig. 2.3A).** Since the Tg cells are first activated in the dMLN (36), this is consistent with the notion that Th17 development is a multi-step process involving signals

from both the lymph node and intestinal tissues. Unexpectedly, FoxP3$^-$ IL-17A$^-$ CT6 cells did not adopt Th1 properties, with no expression of IFNγ by reporter **(Fig. 2.9C),** even though there was a trend towards increased Th1 frequencies in the polyclonal colonic T cell population in DSS and HFD treated mice **(Fig 2.9D).** Moreover, Tbet deficiency in CT6 cells did not abrogate the effect of DSS and HFD on FoxP3 expression, suggesting that the inhibition of FoxP3 induction was not due to Th1 differentiation **(Fig. 2.3B).** FoxP3$^-$IL-17A$^-$ cells were highly proliferative and upregulated CD44 **(Fig. 2.3C, 2.3D),** indicating that they were antigen experienced. In addition, *Rorc*-deficiency led to a modest increase in CT6 conversion, but largely did not rescue the defect in FoxP3-induction **(Fig. 2.3E).** Thus, this result, in addition to the lack of FoxP3 rescue by *Tbet*-deficiency **(Fig. 2.3B),** suggests that canonical Th1 or Th17 differentiation is not solely responsible for the inhibition of FoxP3 induction.

Population stability of pre-existing FoxP3$^+$ and FoxP3$^-$ TCR Tg cells during inflammation.

Given the lack of evidence supporting blockade of naïve CT6 development by canonical effector differentiation, we considered whether the Treg cell subset (52, 149) of CT6 cells can be maintained during DSS and HFD. To investigate the impact of DSS and HFD on antigen experienced FoxP3$^+$ CT6 cells, naïve CT2/6 transgenic cells were co-transferred into wild-type hosts at weaning and allowed to develop normally over 2 weeks. At this timepoint, they are comprised mostly of FoxP3$^+$ cells (36). In contrast to our observations of naïve TCR Tg cells, exposure of antigen experienced cells to DSS and HFD did not affect the proportion of FoxP3$^+$ CT2 or CT6 cells **(Fig. 2.4A, 2.4B).** We then tested the DSS and αIL-10R model of colitis, which impairs pTreg cell selection of both CT2 and CT6 naïve T cells (18). As with DSS and HFD treatment, Tg cells did not exhibit a decrease in FoxP3 frequencies relative to controls **(Fig.**

2.4C). Thus, in two models of intestinal inflammation known to impair naïve CT2 or CT6 development, Tg Treg cells maintained a stable population of FoxP3^{+} cells, implying that the effects of inflammation are on T cell selection at the time of initial T cell activation.

Properties of polyclonal Treg TCR selection in DSS and HFD conditions.

Although we observed a marked reduction in the efficiency of CT6 Treg differentiation during DSS and HFD, the frequency of polyclonal Treg cells in the colon undergo a moderate increase relative to wild-type controls **(Fig 2.9D),** which could reflect expansion of existing Tg Treg cells **(Fig. 2.4A).** Together with the CT2 TCR Tg data, the polyclonal data are consistent with the notion that DSS and HFD treatment does not globally block Treg generation. Thus, we asked whether the different behavior of CT6 and CT2 are reflective of DSS and HFD induced changes in polyclonal Treg cell selection, which could represent alterations in development, expansion, and survival.

To better understand how T cell selection is affected by DSS and HFD, we analyzed the TCR repertoires in control, HFD, and DSS and HFD conditions. As before (18, 35), we utilized a fixed TCRβ model to overcome the limitations of TCR diversity and alpha-beta pairing inherent to analyzing the fully polyclonal TCR repertoire, with the caveat that the polyclonal repertoire in this model has reduced diversity. TCli-β TCR Tg mice were weaned onto HFD and administered DSS as described above. T cells from the mesenteric LN were sorted into FoxP3^{+}and FoxP3^{-} (**naïve:** CD44^{lo}CD62L^{hi}; **CD44^{hi}:** FoxP3^{-}CD44^{hi}; **CXCR3^{+}:** FoxP3^{-}CD44^{hi}IL17A$^{IRES\text{-}GFP-}$CXCR3^{+}; **IL-17^{+}:** FoxP3^{-}CD44^{hi}IL-17$^{IRES\text{-}GFP+}$CXCR3^{-}) subpopulations. We analyzed "intra-population" similarities, i.e. between mice of the same T cell subset and experimental condition, using the Morisita-Horn similarity index (1 = completely similar, 0 = completely dissimilar).

Consistent with prior reports (18, 35), Treg TCR repertoires were more similar than effector TCR repertoires when analyzed between control mice **(Fig. 2.5A, 2.5B).**

Interestingly, the intra-population similarity in DSS and HFD mice exhibited a decrease for Treg, but not FoxP3^{-}, TCR repertoires, relative to control mice **(Fig. 2.5A, 2.5B).** One possibility for the increased mouse-to-mouse variability in the Treg TCR repertoire is that DSS and HFD treatment stochastically induces the appearance of TCRs in only a fraction of the mice, i.e. private TCRs. Consistent with this hypothesis, we observed a 50% reduction in the number of TCR sequences that could be reproducibly found, arbitrarily defined as ≥50% of mice, in DSS and HFD vs control Treg TCR repertoires **(Fig. 2.5C),** without a decrease in the total number of detected TCR sequences or alpha diversity **(Fig. 2.5C; Fig. 2.10A).** Furthermore, we found that over a quarter of reproducibly detected control Treg TCRs were undetectable in DSS and HFD conditions **(Fig. 2.5D),** suggesting that Treg cell selection to those homeostatic antigens are reduced. Collectively, this data verifies that the Treg cell population is not globally affected by DSS and HFD treatment, but does stochastically result in the loss and gain of TCR specificities in the Treg cell population.

We further characterized the reproducibly detected Treg TCRs in control and DSS and HFD conditions. Notably, 14% of reproducibly found Treg TCRs in control mice behaved like CT2 **(Fig. 2.5E),** with Treg clonal frequencies that were maintained or expanded in DSS and HFD. ~5% of control Treg TCRs behaved like CT6, which showed reduced Treg and increased CD44^{hi} clonal frequencies with DSS and HFD **(Fig. 2.5E).** CT2-like TCRs and the cluster of new Treg TCRs found in DSS and HFD conditions were enriched in the TRAV12 subset **(Fig. 2.5E; Fig. 2.10D, 2.10E).** CT6-like TCRs and the control Treg TCRs lost in DSS and HFD were preferentially TRAV6 **(Fig. 2.5E; Fig 2.10D, 2.10E).** Thus, these data support the notion that

different subsets of TCRs are subject to unique selective or developmental microenvironments, which are represented in part by CT2 and CT6.

Treg and FoxP3^{-} TCR repertoires remain distinct during DSS and HFD.

Given that HFD worsens the severity of intestinal disease (140, 150, 151), and that a subset of TCRs are like CT6, which are Treg under homeostasis but become effector with DSS and HFD, we asked whether effector cells utilize the same TCRs as Treg cells during colitis. In contrast with our prior study (18), Morisita-Horn analysis did not reveal increased similarity between Treg and FoxP3^{-} populations in DSS and HFD conditions **(Fig. 2.5F).** This was supported by principal components analysis, which further showed that Treg TCR repertoires were most distinct from CXCR3^{+} and Th17^{+} TCR repertoires, and distinct, but more closely related to CD44^{hi} cells **(Fig. 2.10F).** Additionally, DSS and HFD treatment did not increase the proportion of TCRs that overlap in Treg and FoxP3^{-} TCR repertoires **(Fig. 2.5G; Fig 2.10G, 2.10H).** Cumulatively, the data supports our monoclonal observations: DSS and HFD treatment alters Treg TCR selection without abrogating the distinction in TCR usage between pTreg and effector T cells. However, as noted above, DSS and HFD treatment does induce a subset of TCRs that are Treg during homeostasis to adopt a CD44^{hi} phenotype. In conjunction with the TCR Tg data, these TCR repertoire analyses suggest that blending of the Treg and effector TCR repertoire is not a general feature of DSS and HFD colitis.

Increased bacterial frequency does not explain lack of pTreg cell selection by CT6.

We next hypothesized that alterations in Treg TCR repertoire with DSS and HFD are driven by changes in the microbiota, and therefore performed 16S rRNA profiling of the mucosal

and luminal bacteria as before (18). We first focused on *Helicobacter spp.* to determine whether an increase in frequency might predict the loss of pTreg cell selection in CT6 but not CT2 with DSS and HFD, based on previous studies showing that increased antigen presentation could limit the frequency of $Foxp3^+$ cells generated from naïve TCR Tg cells at a non-mucosal site (152). Contrary to this hypothesis, the bacteria recognized by CT6, *H. apodemus*, actually decreased in frequency with DSS and HFD, whereas the *H. typhlonius* recognized by CT2 increased **(Fig. 2.6A).** We then asked whether there were changes in the biogeography of these two *Helicobacter spp*. The frequency of these *Helicobacter spp.* in the cecum vs distal 1/3 of the colon were similarly affected by DSS and HFD, although *H. apodemus* appeared to preferentially shift towards becoming more abundant distally **(Fig. 2.6B).** Whether this is relevant for pTreg cell selection is uncertain, as the dMLN still remains the primary site of CT6 **(Fig. 2.6C)** accumulation as previously reported (36). While we cannot exclude other changes with DSS and HFD that can affect the expression of the TCR Tg epitopes or their acquisition and presentation by antigen presenting cells, these data suggest that changes in *Helicobacter* abundance do not provide a ready explanation for the differential pTreg cell development of CT2 and CT6 with DSS and HFD.

HFD induces Enterobacter expansion during DSS-mediated colitis.

One hypothesis for the expansion of CT6 cells in the cecum draining lymph node despite reduction in *H.apodemus* abundance is that the TCR is being stimulated by non-*Helicobacter* antigens. Analysis of the mucosal and luminal 16S rRNA profiles revealed that DSS and HFD induced marked changes in both the mucosal-associated and luminal bacterial communities **(Fig. 2.7A; Fig. 2.11A).** Contrary to published reports, we did not observe a significant decrease in *Clostridium* species in DSS and HFD relative to control mice **(Fig. 2.11B)** (140). Rather, we observed a dramatic bloom of *Enterobacter* species in the mucosal-associated and luminal bacteria of DSS and HFD treated mice **(Fig. 2.7B, 2.7C).** The 16S sequences were confirmed by culture of the mucosal-associated bacteria (~1.8 x 10^4 CFUs/ml) **(Fig. 2.7D).** Thus, the loss of *H. apodemus* with DSS and HFD colitis is associated with a strong expansion of *Enterobacter spp*.

Interestingly, the bloom of *Enterobacter* was not nearly as marked with DSS alone, although we did observe some increase **(Fig. 2.7D, 2.7E)** consistent with previous studies (153). In addition, we did not observe *Enterobacter* in mucosal-associated bacteria from Treg cell depleted hosts by 16S rRNA sequencing **(Fig 2.11C).** The magnitude of *Enterobacter* expansion is therefore driven by the combination of DSS and HFD and not by inflammation alone. Notably, DSS and HFD colitis also leads to a blurring of the mucosa-associated and luminal community **(Fig. 2.7A),** and suggests that the *Enterobacter* bloom may have direct access to adaptive immune cells during DSS and HFD colitis.

Our prior studies found that CT6 is weakly cross-reactive to *Clostridium* (21). Since the abundance of *Clostridium* species was not increased, we tested the reactivity of CT6 TCR expressed on NFAT-GFP hybridoma cells to *Enterobacter* species presented by dendritic cells *in*

vitro (141) **(Fig. 2.7F).** CT6, in contrast with CT2, showed cross-reactivity to *E. coli***.** Thus, these data raise the possibility that a subset of commensal-reactive TCRs such as CT6 encounters dysbiotic microbes such as *Enterobacter* during DSS and HFD in a microenvironment that is not conducive for Foxp3 induction.

Discussion

In this study, we found that pTreg cell development to commensal bacterial antigens was remarkably preserved in the context of multiple models of intestinal inflammation, including infections and experimental colitis. However, in one colitis model using DSS and HFD, we found that development of pTreg cells was selectively lost with CT6, but not CT2, TCR Tg cells. Our analysis of polyclonal T cell repertoires supported these monoclonal findings, revealing that the Treg and FoxP3$^-$ TCR repertoires did not become overall more similar upon DSS and HFD treatment. Thus, these data predict the existence of microenvironments that preserve pTreg cell development to homeostatic commensal antigens even in the face of infection or other intestinal inflammation.

Our monoclonal TCR Tg data are consistent with previous reports showing that Th17 differentiation against antigen from SFB is highly preserved in Th1 skewing environments caused by *Listeria* infections (31). One common feature is that both SFB and *Helicobacter* derived antigens induce T cell responses during homeostasis in the absence of disease (18, 31, 36). In contrast, *Clostridium* flagellin antigen is presented in adults only upon mucosal injury (133). In this prior study, infection with Toxoplasma led to activation of Th1 effector cells that responded to commensal-specific flagellin epitopes, although such responses are normally not present in the absence of infection. In contrast, we observed that Treg cells that recognize *Helicobacter* antigens remain intact, and T effector cells that recognize *Helicobacter* do not emerge following *Toxoplasma* infection. Therefore, it is possible that the resilience of T cell differentiation in the context of environmental inflammation is dependent on the homeostatic accessibility of the antigen. We speculate that homeostatic vs "inflammation-associated"

antigens may be delivered and presented to the immune system through distinct mechanisms, leading to different microenvironments that facilitate pTreg vs effector cell development.

However, DSS and HFD did lead to a loss of pTreg cell development of CT6, but not CT2, cells, both of which react to homeostatic commensal antigen. As this occurred within the same animal, this finding demonstrates that TCR specificity, and therefore, properties associated with the antigen or the mechanism of antigen uptake, can determine the outcome of T cell development in inflammatory environments. The differential effect of CT2 and CT6 was mirrored in the polyclonal population, which had clusters of TCRs that were both lost and expanded during DSS and HFD. Although the specific mechanisms behind Treg induction by intestinal bacteria remain elusive, we believe that T cell differentiation is dictated by the environment in which the antigen is being presented, and not intrinsic to the antigen or TCR. The lack of FoxP3-induction of CT6 cells is unlikely due to antigen loss, as CT6 cells proliferate more during DSS and HFD. One hypothesis is that CT6, which has previously shown weak reactivity to a *Clostridium* spp. (21), may react with non-*Helicobacter* derived antigens in different microenvironments. In support of this hypothesis, CT6, but not CT2 Tg cells, were weakly cross-reactive *in vitro* with *Enterobacter spp.* that bloom during DSS and HFD. This may reflect antigen presentation in an effector microenvironment context similar to that seen for CBir discussed above (133). Although future studies are required to test this hypothesis, there appears to be a subset of T cells that may see their homeostatic antigens or "inflammation-associated" antigens in the context of an inflammatory microenvironment that can suppress FoxP3 or lack FoxP3 inducing signals, potentially leading to effector T cell development.

In summary, our study demonstrates that 1) homeostatic Treg differentiation against bacteria antigen is maintained in multiple models of intestinal inflammation 2) TCR specificity

can determine the outcome of T cell differentiation during intestinal inflammation, and 3) HFD can selectively alter T cell development and Treg TCR repertoires. Our data suggests that there are robust mechanisms to preserve microenvironments to protect the host from aberrant immune responses to homeostatic antigens. Understanding the cellular and molecular features of these microenvironments may be useful for therapy of inflammatory bowel disease.

Figures

Figure 2.1

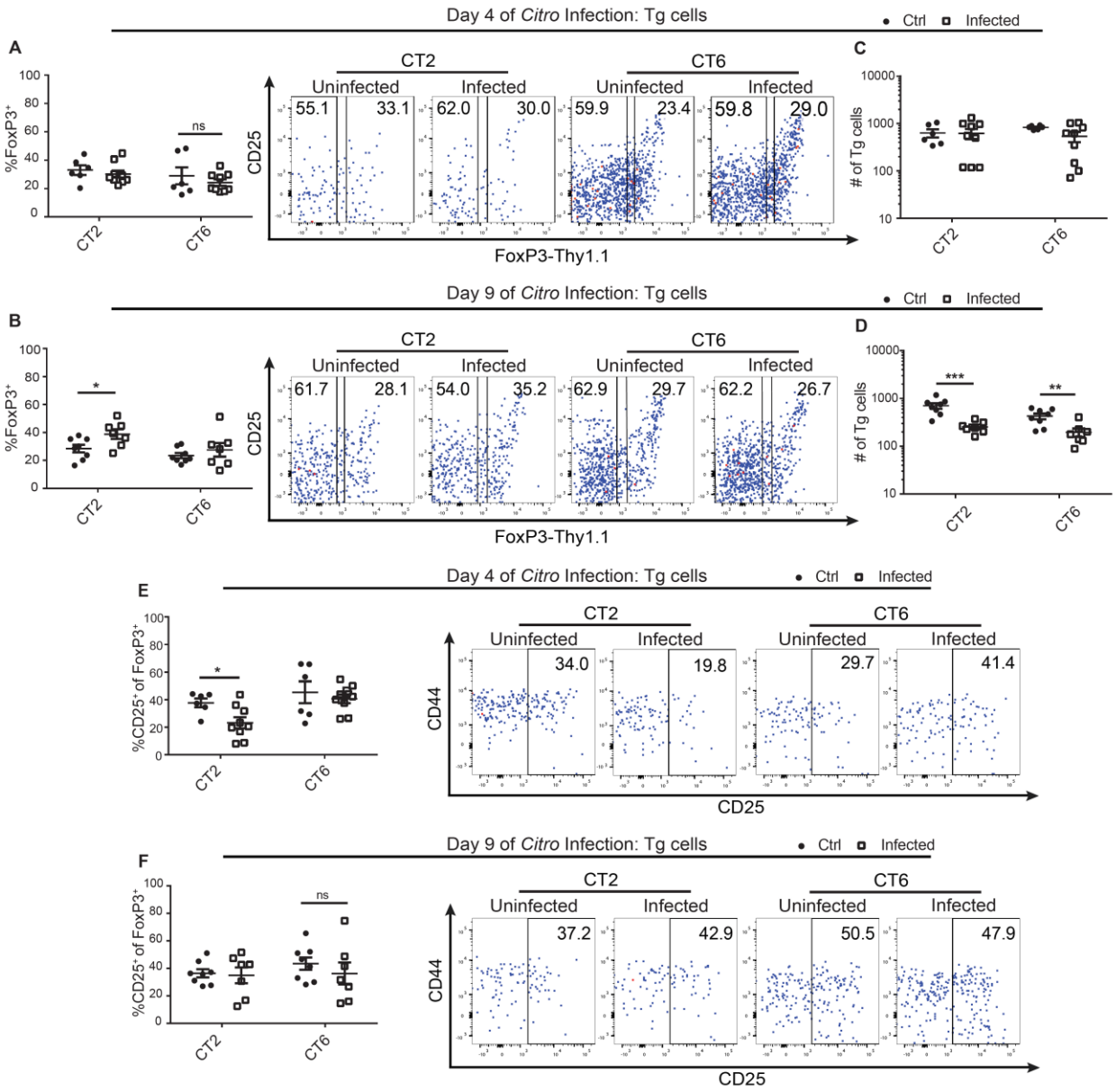

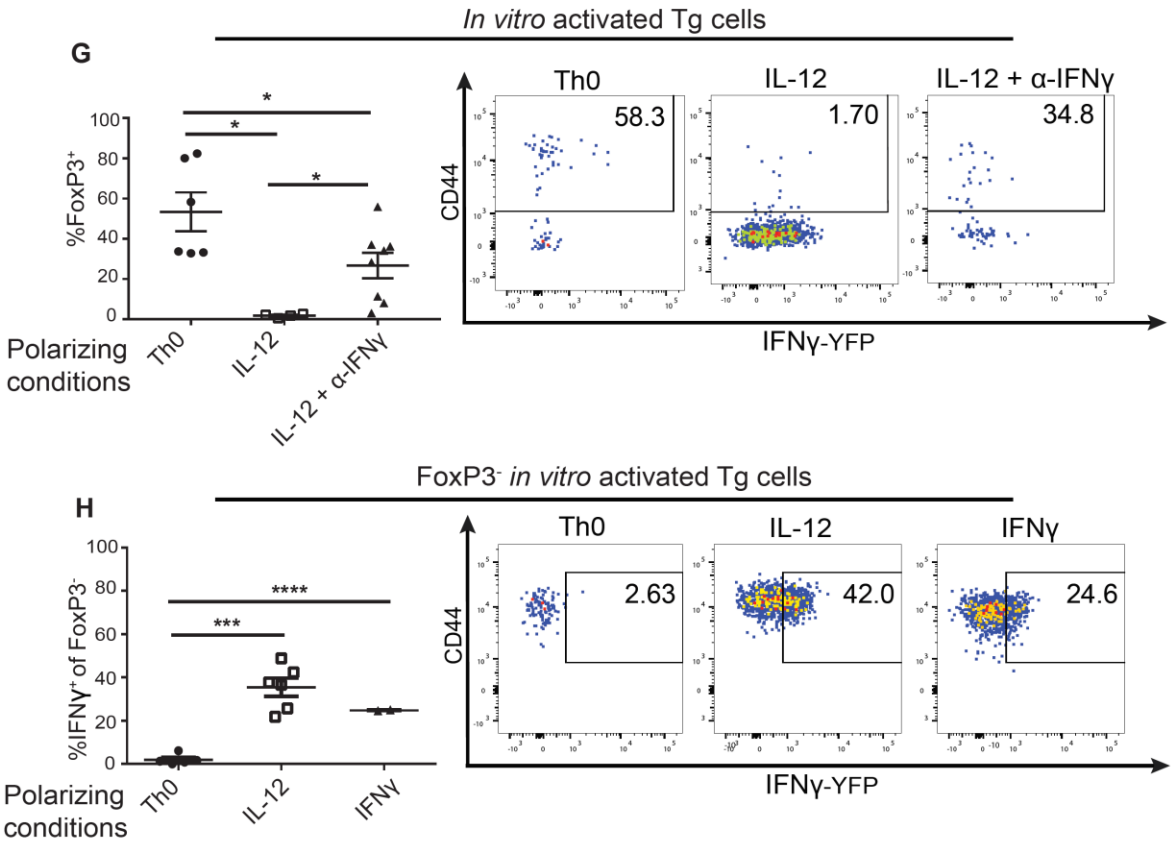

Figure 2.1: *Helicobacter* reactive TCR transgenic cells develop into pTreg cells during *Citrobacter rodentium* infection. (A-F) CD45.1 wild-type mice were infected with $2x10^9$ CFU of *Citrobacter rodentium.* $1x10^5$ Congenically marked CT2 (CD45.1/2) and CT6 (CD45.2) naïve cells ($CD44^{lo}CD62L^{hi}$) were stained with Cell-Trace Violet, mixed 1:1, and retro-orbitally injected into wild-type and experimental mice on day 4 or 9 of infection**.** Shown are summary plots and representative FACS plots of $FoxP3^{IRES\text{-}Thy1.1}$ expression and CD25 expression of Tg cells isolated from cecum draining mesenteric lymph (dMLN) node 1 week after transfer. Cells were gated on congenically marked $CD4^+V\alpha2^+$ TCR Tg cells. Graphs are percentages of all Tg cells, $FoxP3^{IRES\text{-}Thy1.1+}$ or $FoxP3^{IRES\text{-}Thy1.1-}$ fractions of Tg cells (replicates = 2 for each infection timepoint, *n* = 4-6). (**G, H**) Congenically marked CT2 *FoxP3*$^{IRES\text{-}GFP}$ or CT2 *IFNγ*$^{IRES\text{-}YFP}$

FoxP3$^{\text{IRES-Thy1.1}}$ naïve cells were sorted as described above and activated in polarizing conditions (see methods) for 48 hours before retro-orbital transfer (1.5 x 10^5 into wild-type CD45.1 hosts). Tg cells were analyzed via flow cytometry from the dMLN 1 week post transfer. Representative FACS plots of FoxP3$^{\text{IRES-GFP+}}$ percentages were gated on congenically marked CD4^{+}Vα2^{+}. CT2 IFNγ$^{\text{IRES-YFP+}}$ percentages were gated on CD4^{+}Vα2^{+}FoxP3$^{\text{IRES-Thy1.1-}}$ (replicates = 2, *n* = 1-3 for all). Statistical significance was calculated using Student T test, *$P<0.05$, ** $P<0.005$, *** $P \leq 0.001$, **** $P \leq 0.0001$; ns = not significant. Error bars = ±SEM.

Figure 2.2

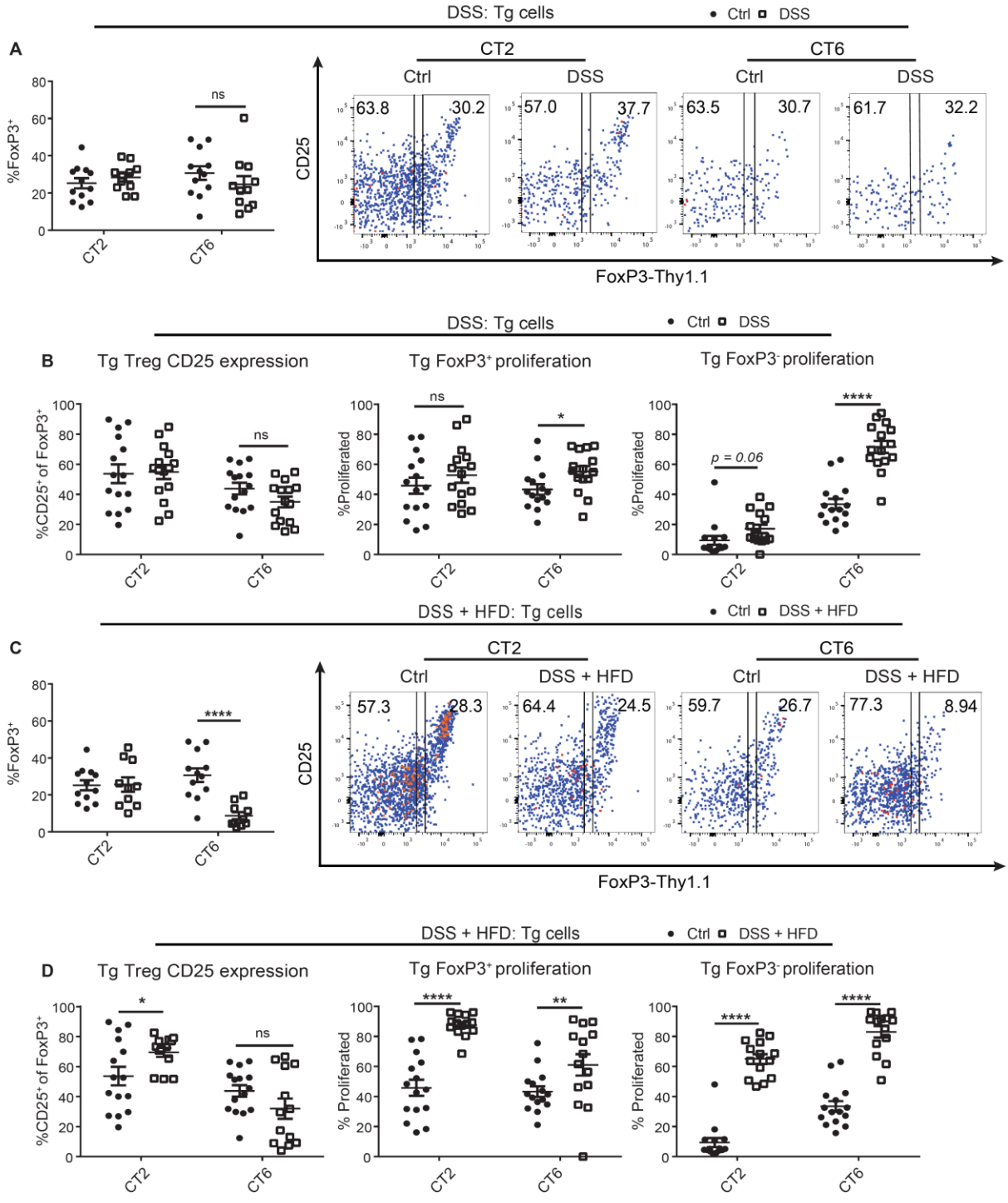
DSS: Tg cells
Ctrl DSS
A
CT2
CT6
Ctrl
DSS
%FoxP3+
ns
63.8
30.2
57.0
37.7
63.5
30.7
61.7
32.2
CD25
FoxP3-Thy1.1
B
Tg Treg CD25 expression
Tg FoxP3+ proliferation
Tg FoxP3- proliferation
%CD25+ of FoxP3+
%Proliferated
p = 0.06
*
****
DSS + HFD: Tg cells
Ctrl DSS + HFD
C
DSS + HFD
57.3
28.3
64.4
24.5
59.7
26.7
77.3
8.94
D
% Proliferated
**
CT2
CT6

Figure 2.2: DSS coupled with high fat diet (HFD) inhibits pTreg cell development by *Helicobacter apodemus* (CT6), but not *Helicobacter typhlonius* (CT2) reactive TCR transgenic cells. (A-D) CD45.1 wild-type mice were weaned onto control or high fat diet (HFD) chow. Experimental mice were treated with 2% DSS via drinking water 7 days after weaning (replicates = 5, *n* = 2-5). Naïve CT2 (CD45.1/2) and CT6 (CD45.2) Tg cells were prepared as described in Figure 2.1 and transferred on day 4 of DSS treatment. Flow cytometric analysis was done as described in Figure 2.1 from dMLN 7 days after Tg cell transfer— the equivalent of d18 after weaning. Two or more divisions were considered to be proliferated cells based on Cell-Trace-Violet dilution. Statistical significance was calculated using Student T test, *$P<0.05$, ** $P<0.005$, *** $P \leq 0.001$, **** = $P \leq 0.0001$; ns = not significant. Error bars = ±SEM.

Figure 2.3

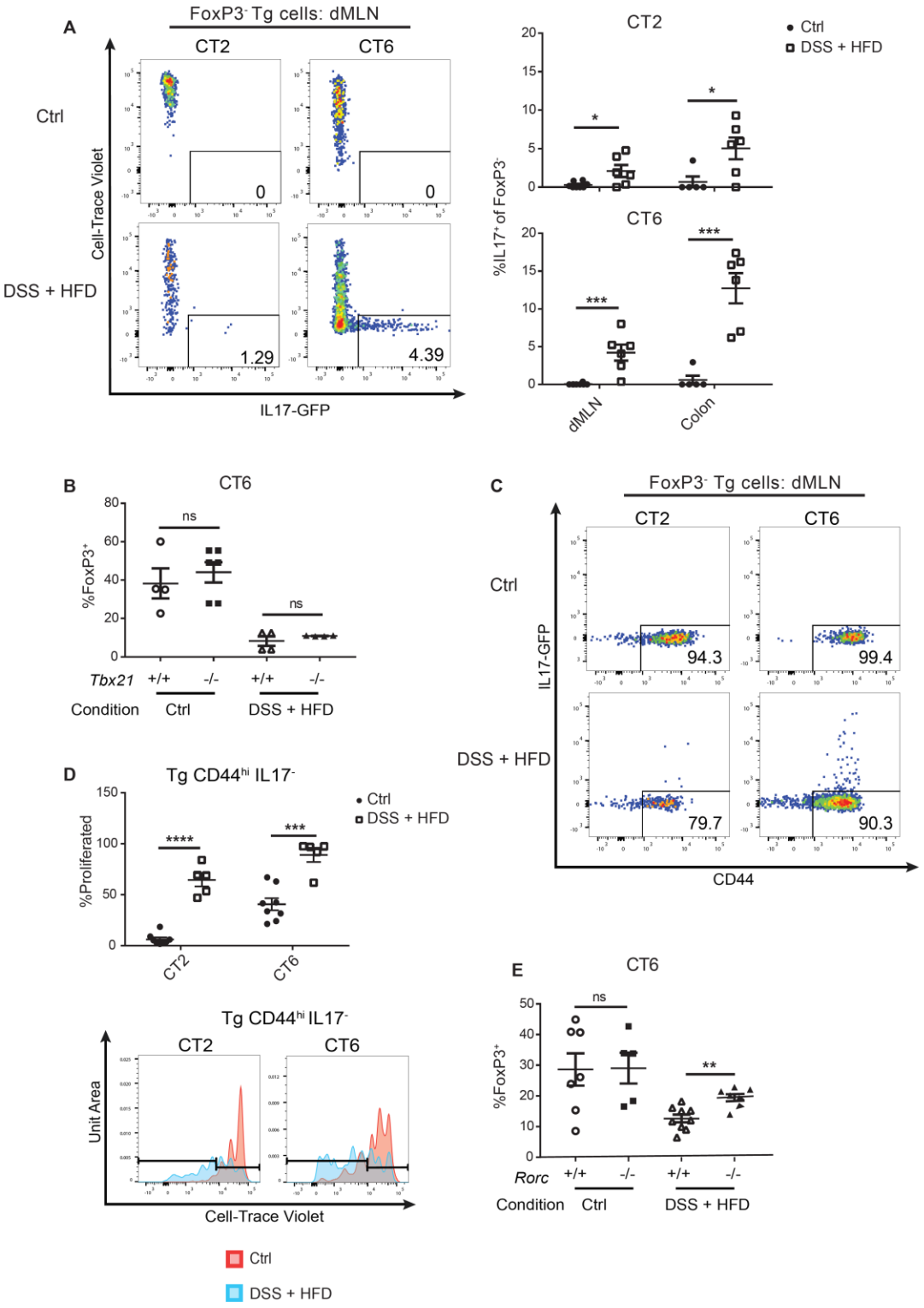

Figure 2.3: FoxP3⁻ CT6 cells adopt effector phenotypes in DSS and HFD treated hosts. (A, C, D)

Naive CT2 *FoxP3*$^{\text{IRES-Thy1.1}}$ *IL-17A*$^{\text{IRES-GFP}}$ *IFNγ*$^{\text{IRES-YFP}}$ and CT6 *FoxP3*$^{\text{IRES-Thy1.1}}$ *IL-17A*$^{\text{IRES-GFP}}$ *IFNγ*$^{\text{IRES-YFP}}$ Tg cells were sorted and transferred into DSS and HFD treated mice as described in Figure 2 (replicates = 3; *n* = 2). **(A)** Flow cytometric analysis and representative FACS plots of IL-17A production by CD4^{+}Vα2^{+} FoxP3$^{\text{IRES-Thy1.1}-}$ Tg cells. Graphs are percentages of IL-17A^{+} of Foxp3$^{\text{IRES-Thy1.1}-}$ Tg cells. **(B)** 1x10^{5} naïve CT6 *Tbx21*$^{-/-}$ *FoxP3*$^{\text{IRES-GFP}}$ and CT6 *Tbx21*$^{+/+}$ *FoxP3*$^{\text{IRES-GFP}}$ Tg cells were sorted and retro-orbitally injected into DSS and HFD treated mice as described in Figure 2.2. Shown is flow cytometric analysis of congenically marked CD4^{+}Vα2^{+} Tg cells from dMLN 7 days after Tg cell transfer (replicates = 2; *n* = 2-3). **(C)** Representative FACS plots of CD44 expression by CD4^{+}Vα2^{+} FoxP3$^{\text{IRES-Thy1.1}-}$IL17A$^{\text{IRES-GFP}-}$ Tg cells. **(D)** Flow cytometric analysis and representative FACS plots of proliferation by CD4^{+} Vα2^{+} FoxP3$^{\text{IRES-Thy1.1}-}$ IL17A$^{\text{GFP}-}$ Tg cells. Cells undergoing 2 or more divisions based on Cell-Trace-Violet dilutions were considered to be proliferated. **(E)** Naïve CT6 *Rorc*$^{-/-}$ *FoxP3*$^{\text{IRES-GFP}}$ and CT6 *Rorc*$^{+/+}$ *FoxP3*$^{\text{IRES-GFP}}$ Tg cells were sorted and injected into DSS and HFD treated mice as described above. Flow cytometric analysis of CD4^{+}Vα2^{+} Tg cells from dMLN 7 days after Tg cell transfer (replicates = 2; *n* = 2-4). Statistical significance was calculated using Student T test, **P<0.05*, ** *P<0.005*. ****P ≤0.001*, *****P ≤0.0001*; ns = not significant. Error bars = ± SEM.

Figure 2.4

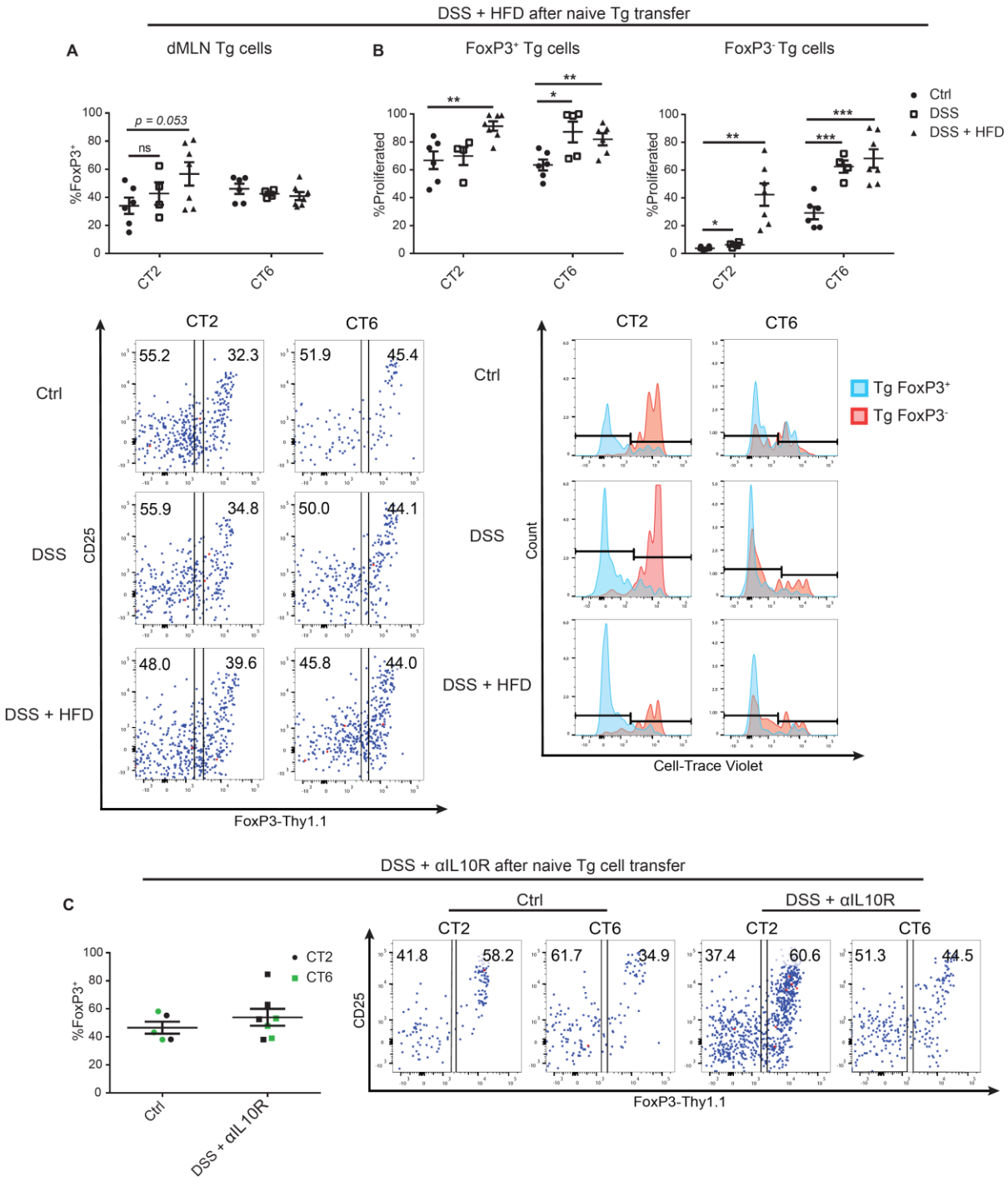
DSS + HFD after naive Tg transfer
A
dMLN Tg cells
B
FoxP3+ Tg cells
FoxP3- Tg cells
%FoxP3+
%Proliferated
p = 0.053
ns
CT2
CT6
Ctrl
DSS
DSS + HFD
55.2
32.3
51.9
45.4
55.9
34.8
50.0
44.1
48.0
39.6
45.8
44.0
CD25
FoxP3-Thy1.1
Count
Cell-Trace Violet
Tg FoxP3+
Tg FoxP3-
DSS + αIL10R after naive Tg cell transfer
C
Ctrl
DSS + αIL10R
41.8
58.2
61.7
34.9
37.4
60.6
51.3
44.5

Figure 2.4: Defects in transgenic pTreg development is not due to reduced transgenic Treg population stability (A, B) Naïve CT2 *FoxP3*$^{\text{IRES-Thy1.1}}$ and CT6 *FoxP3*$^{\text{IRES-Thy1.1}}$ cells were sorted and injected into mice on control or HFD chow as described in Figure 2.1. Two weeks after transfer, experimental mice were administered 2% DSS in drinking water. Tg cells from dMLN analyzed for FoxP3$^{\text{IRES-Thy1.1}}$ expression 11 days after DSS treatment. Flow cytometric analysis and representative facs plots were of congenically marked Tg cells from dMLN 11 days after DSS treatment (replicates = 2; *n* = 2-4). **(C)** Naïve CT2 *FoxP3*$^{\text{IRES-Thy1.1}}$ and CT6 *FoxP3*$^{\text{IRES-Thy1.1}}$ cells were sorted as described above and transferred into mice weaned onto control chow. 2 weeks after transfer, mice were administered 1.5% DSS in drinking water and 1mg α-IL10R injected intraperitoneally. Controls were injected with 1 mg of IgG isotype controls (replicates = 2; *n* = 2-4). Flow cytometric analysis and representative FACS plots of Tg cells from dMLN 7 days after antibody injection. Statistical significance was calculated using Student T test, $*P<0.05,\ **P<0.005,\ ***P\leq0.001$; ns = not significant. Error bars = ± SEM.

Figure 2.5

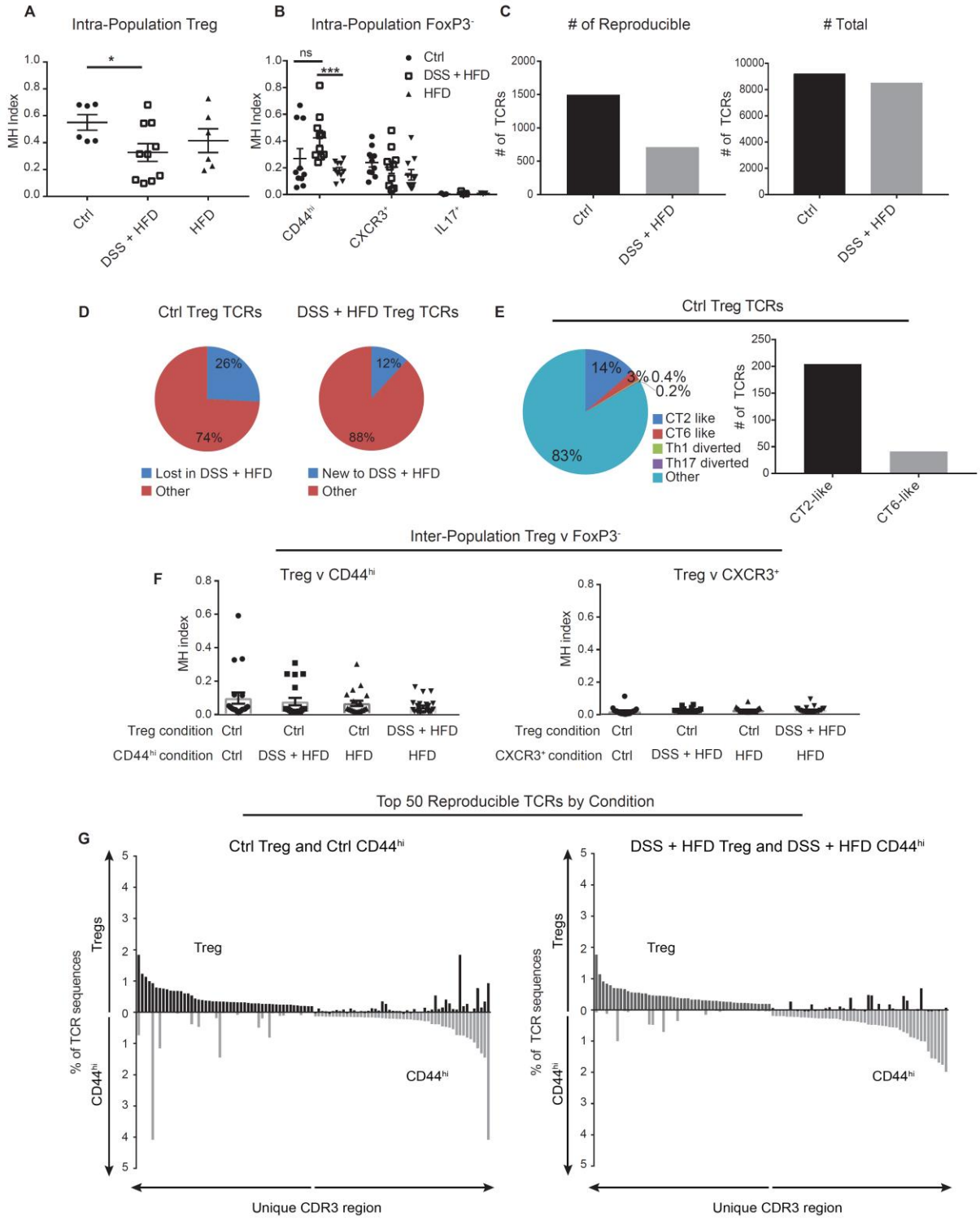
A
Intra-Population Treg
MH Index
Ctrl
DSS + HFD
HFD
B
Intra-Population FoxP3-
ns
***
Ctrl
DSS + HFD
HFD
CD44hi
CXCR3+
IL17+
C
# of Reproducible
Total
of TCRs
D
Ctrl Treg TCRs
DSS + HFD Treg TCRs
26%
74%
12%
88%
Lost in DSS + HFD
Other
New to DSS + HFD
Other
E
Ctrl Treg TCRs
14%
3%
0.4%
0.2%
83%
CT2 like
CT6 like
Th1 diverted
Th17 diverted
Other
CT2-like
CT6-like
Inter-Population Treg v FoxP3-
F
Treg v CD44hi
Treg v CXCR3+
MH index
Treg condition
CD44hi condition
CXCR3+ condition
Top 50 Reproducible TCRs by Condition
G
Ctrl Treg and Ctrl CD44hi
DSS + HFD Treg and DSS + HFD CD44hi
% of TCR sequences
Tregs
Treg
CD44hi
Unique CDR3 region

Figure 2.5: Polyclonal Treg TCR repertoires are altered by DSS and HFD treatment, but remain distinct from effector TCR repertoires. (**A-G**) $CD4^+$ T cells were sorted into $FoxP3^{IRES\text{-}Thy1.1+}$ (Treg), $FoxP3^{IRES\text{-}Thy1.1-}$ $CD44^{hi}$ $IL\text{-}17A^{IRES\text{-}GFP-}$ $CXCR3^+$ ($CXCR3^+$), $FoxP3^{IRES\text{-}Thy1.1-}$ $CD44^{hi}$ $IL\text{-}17A^+$ ($IL\text{-}17^+$), and $FoxP3^{IRES\text{-}Thy1.1-}$ $CD44^{hi}$ $IL\text{-}17A^{IRES\text{-}GFP-}CXCR3^-$ ($CD44^{hi}$) subsets from mesenteric lymph nodes of 3-4 weeks old TCli TCRβ $Tcra^{+/-}$ mice on control chow, HFD, or 2% DSS and HFD at the same timepoint as Tg cell analysis for adoptive transfer experiments (replicates = 4, *n* = 1-2 mice). **(A, B, F)** Intra-population (between same T cell population, same condition) Morisita-Horn (MH) similarity index (0 = complete dissimilarity, 1 = identical) of rarefied TCR sequences (10,000 reads) between $FoxP3^{IRES\text{-}Thy1.1+}$ and $FoxP3^{IRES\text{-}Thy1.1-}$ TCR populations for each condition. **(C)** Total number of TCRs determined from sum of unique TCRs found in each mouse. Reproducible TCRs were defined as those found in ≥ 50% mice in each control and/or experimental condition. (**D**) Reproducible TCRs were analyzed for responsiveness to DSS and HFD conditions. TCRs lost in DSS and HFD were reproducibly found in control Treg TCR repertoires, but undetectable in any mice in DSS and HFD conditions. TCRs new to DSS and HFD were reproducibly found in DSS and HFD Treg TCR repertoires, but undetectable in control Treg TCR repertoires. "Other" TCRs in Ctrl Treg TCR diagram are TCRs not lost in DSS and HFD. For DSS and HFD diagram, "Other TCRs" include TCRs not new to Control conditions, **(E)** Proportion and number of reproducibly found Treg TCRs that are CT2 and CT6-like. CT2-like TCRs were defined as TCRs with clonal frequencies that fall within the union of the following parameters: Ctrl Treg < DSS and HFD Treg, Ctrl Treg > Ctrl $CD44^{hi}$, and DSS and HFD Treg > DSS and HFD $CD44^{hi}$. CT6-like TCRs were defined as TCRs with clonal frequencies that fall within the union of the following parameters: Ctrl Treg >

DSS and HFD Treg, Ctrl Treg > Ctrl CD44^{hi}, DSS and HFD Treg < DSS and HFD CD44^{hi}, Ctrl CD44^{hi} < DSS and HFD CD44^{hi}. **(F)** Inter-population (between different T cell populations and conditions) MH index of rarefied TCR sequences (10,000 reads) between FoxP3$^{IRES\text{-}Thy1.1+}$ and FoxP3$^{IRES\text{-}Thy1.1-}$ TCR populations for each condition. Statistical significance was calculated using Student T test, **P<0.05, ** P<0.005*; ns = not significant. Error bars = ±SEM. **(G)** Top 50 reproducibly found TCRs in Treg or CD44^{hi} repertoires ranked on average clonal frequencies (adjusted for TRAV primer bias) were identified. Plots display the clonal frequencies of top ranked TCRs, ordered by decreasing frequency towards the center of the graph, and their clonal frequencies in the alternate T cell population. Statistical significance was calculated using Student T test, **P<0.05, *** P≤0.001*; ns = not significant. Error bars = ±SEM.

Figure 2.6

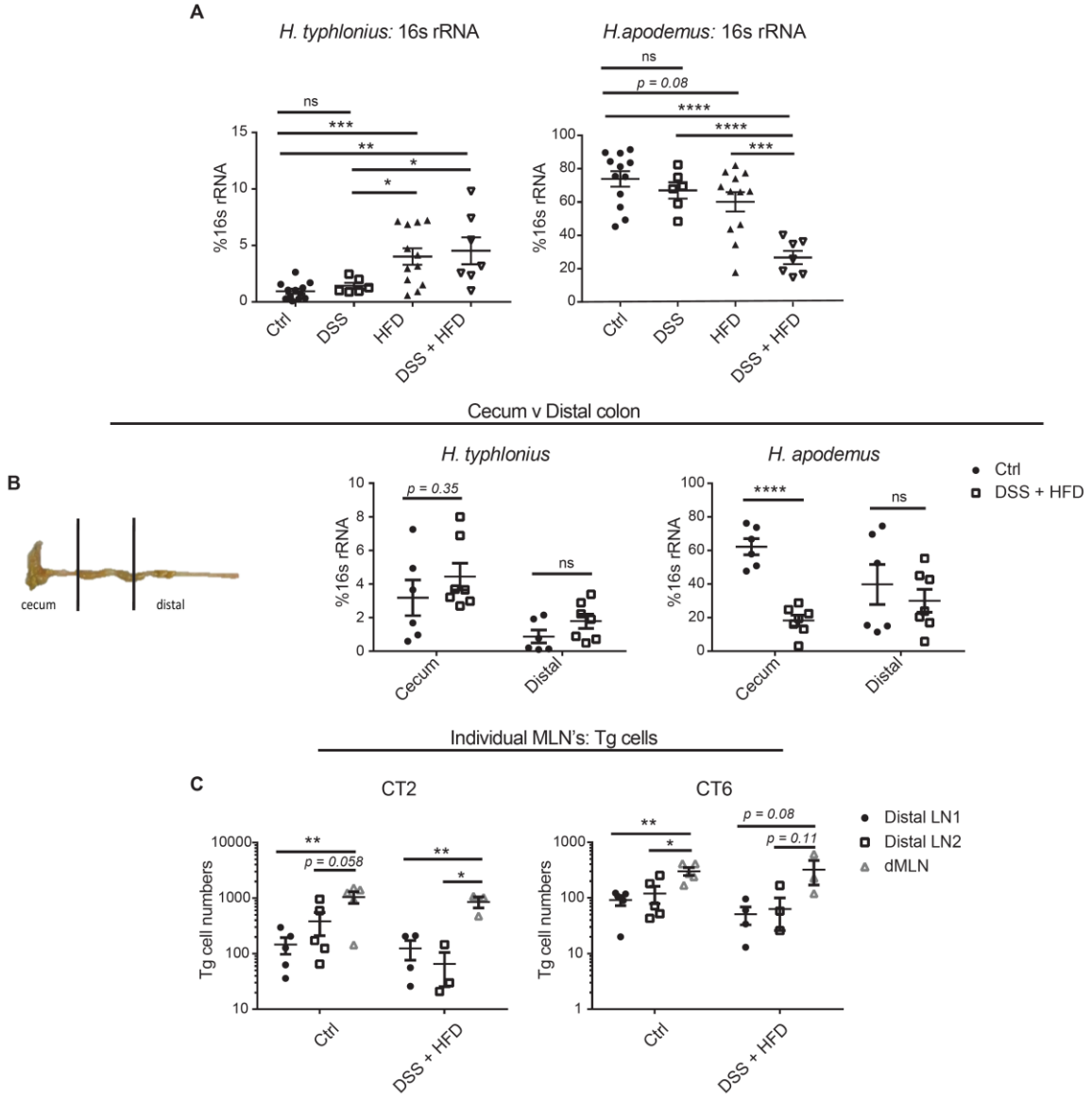

Figure 2.6: *Helicobacter apodemus* and *Helicobacter typhlonius* are differentially affected by DSS and HFD. (A) 16S rRNA percentages of *Helicobacter* operational taxonomic units *(*OTUs) that stimulate CT2 and CT6 Tg cells as a percentage of total 16S rRNA sequences derived from the mucosal-associated preparation of the entire large intestine. Bacteria were harvested at same timepoint as Tg cell analysis (replicates = 3; *n* = 2-4). **(B)** 16S rRNA percentages of

Helicobacter OTUs from mucosal-associated preparations cecum or distal sections of the large intestine, which were segmented as indicated. **(C)** Naïve CT2 and CT6 Tg cells were sorted and transferred into DSS and HFD treated mice as described in Figure 2. Tg cell numbers were counted from lymph nodes that drain antigen from either the distal colon (LN1 = lymph node more proximal to rectum along descending colon, LN2 = adjacent to small intestine draining lymph nodes) (154) or cecum (dMLN) of the large intestine (n = 2). Statistical significance was calculated using Student T test, *$P<0.05$, ** $P<0.005$. ***$P \leq 0.001$, ****$P \leq 0.0001$; ns = not significant. Error bars = ± SEM.

Figure 2.7

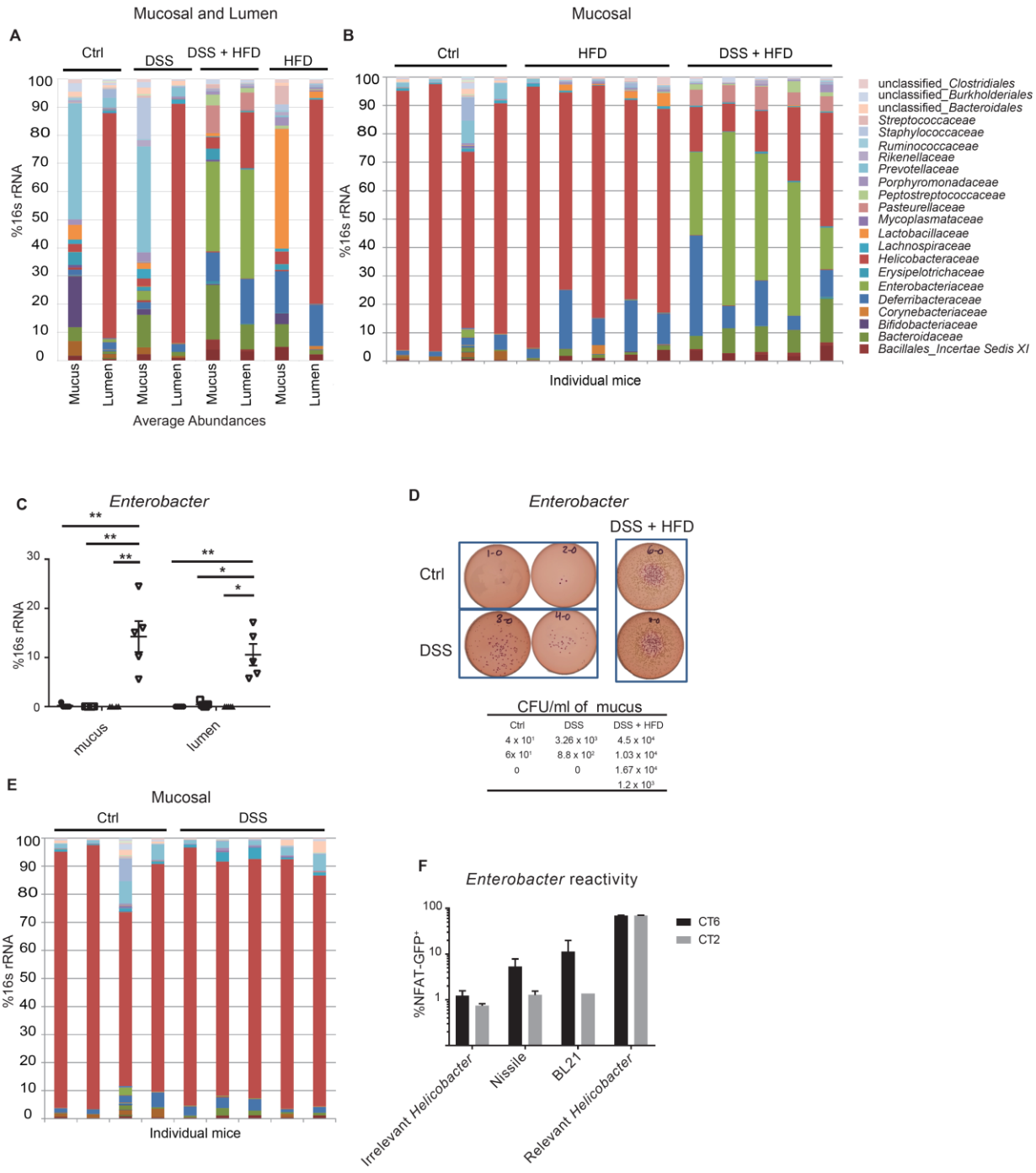
A
Mucosal and Lumen
Ctrl
DSS
DSS + HFD
HFD
%16s rRNA
Mucus
Lumen
Average Abundances
B
Mucosal
Ctrl
HFD
DSS + HFD
%16s rRNA
Individual mice
unclassified_Clostridiales
unclassified_Burkholderiales
unclassified_Bacteroidales
Streptococcaceae
Staphylococcaceae
Ruminococcaceae
Rikenellaceae
Prevotellaceae
Porphyromonadaceae
Peptostreptococcaceae
Pasteurellaceae
Mycoplasmataceae
Lactobacillaceae
Lachnospiraceae
Helicobacteraceae
Erysipelotrichaceae
Enterobacteriaceae
Deferribacteraceae
Corynebacteriaceae
Bifidobacteriaceae
Bacteroidaceae
Bacillales_Incertae Sedis XI
C
Enterobacter
%16s rRNA
mucus
lumen
D
Enterobacter
DSS + HFD
Ctrl
DSS
CFU/ml of mucus
Ctrl
DSS
DSS + HFD
4 x 10¹
3.26 x 10³
4.5 x 10⁴
6x 10¹
8.8 x 10²
1.03 x 10⁴
0
0
1.67 x 10⁴
1.2 x 10³
E
Mucosal
Ctrl
DSS
%16s rRNA
Individual mice
F
Enterobacter reactivity
%NFAT-GFP⁺
CT6
CT2
Irrelevant Helicobacter
Nissile
BL21
Relevant Helicobacter

Figure 2.7: Microbiota of mice treated with DSS and HFD are characterized by a large expansion of *Enterobacter*. (A, B) 16S rRNA sequences of bacteria families were derived from the lumen and mucosal-associated preparation of DSS and HFD treated mice. Bacteria were harvested at the same timepoint as Tg cell analysis from adoptive transfer experiments. 16S rRNA percentages of bacterial families analyzed (replicates = 3; *n* = 2-4). **(C)** Single dominant *Enterobacter* OTU percentage displayed as a proportion of total 16S rRNA sequences. Statistical significance was calculated using Student T test, *$P<0.05$, ** $P<0.005$; ns = not significant. Error bars = ± SEM. **(D)** CFU counts and representative images for mucosal-associated bacteria from control and experimental mice plated onto *Enterobacter*-selecting MacConkey agar plates. CFUs were counted after 18 hours of incubation at 37ºC. **(E)** 16S rRNA sequences of mucosal-associated bacteria families from mice on control chow treated with 2% DSS. Bacteria collected at same timepoint as Tg cell from adoptive transfer experiments. **(F)** Hybrids transduced with CT2 and CT6 TCRα chains were co-cultured with *ex vivo* isolated flt3L expanded dendritic cells and autoclaved antigen generated from known *Enterobacter* strains. TCR stimulation was determined by NFAT-GFP expression (replicates = 3).

Figure 2.8

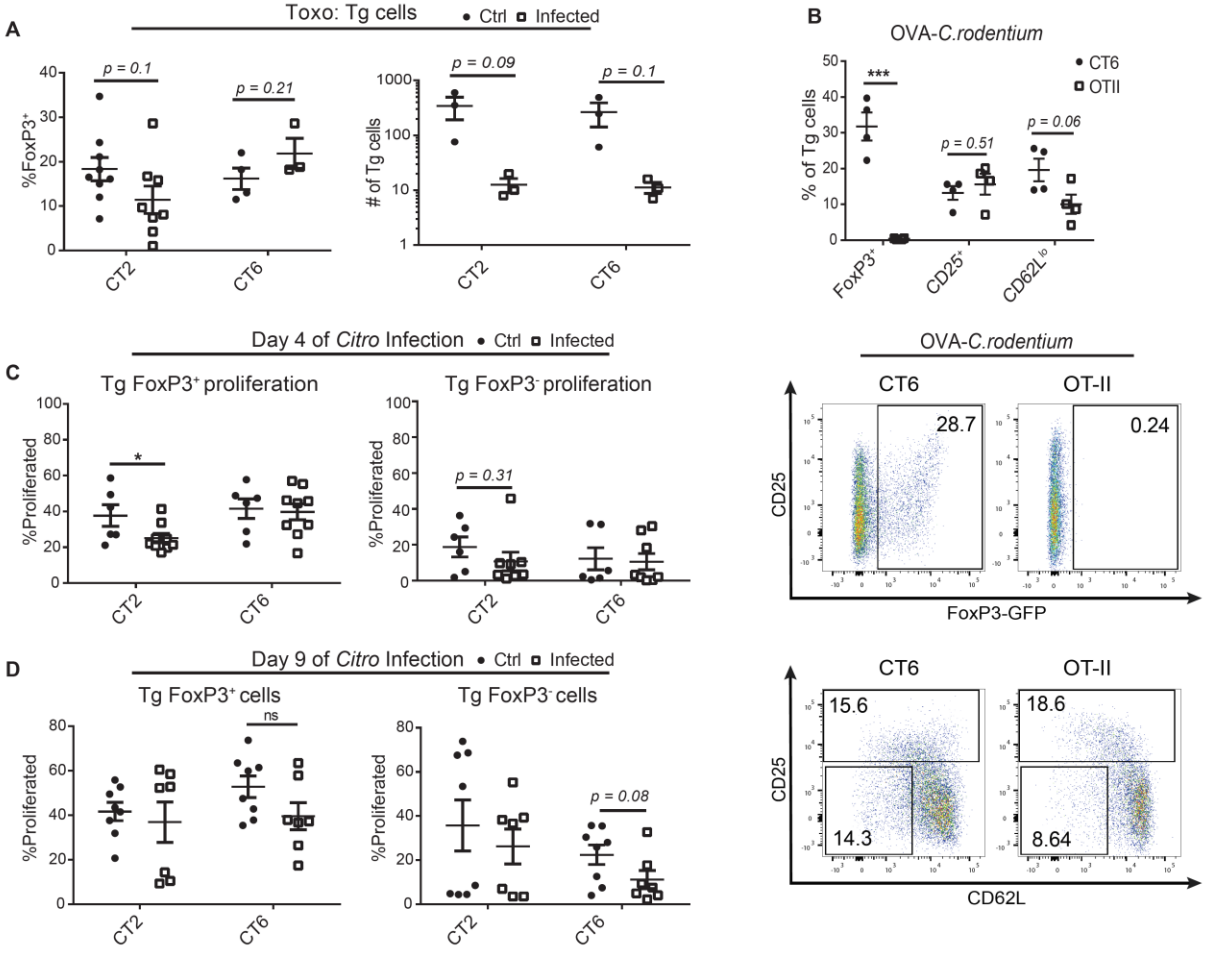
A
Toxo: Tg cells
Ctrl
Infected
%FoxP3+
p = 0.1
p = 0.21
# of Tg cells
p = 0.09
p = 0.1
CT2
CT6
B
OVA-C.rodentium
CT6
OTII
% of Tg cells
***
p = 0.51
p = 0.06
FoxP3+
CD25+
CD62L lo
C
Day 4 of Citro Infection
Ctrl
Infected
Tg FoxP3+ proliferation
Tg FoxP3- proliferation
%Proliferated
*
p = 0.31
OVA-C.rodentium
CT6
OT-II
28.7
0.24
CD25
FoxP3-GFP
D
Day 9 of Citro Infection
Ctrl
Infected
Tg FoxP3+ cells
Tg FoxP3- cells
ns
p = 0.08
15.6
18.6
14.3
8.64
CD62L

Figure 2.8

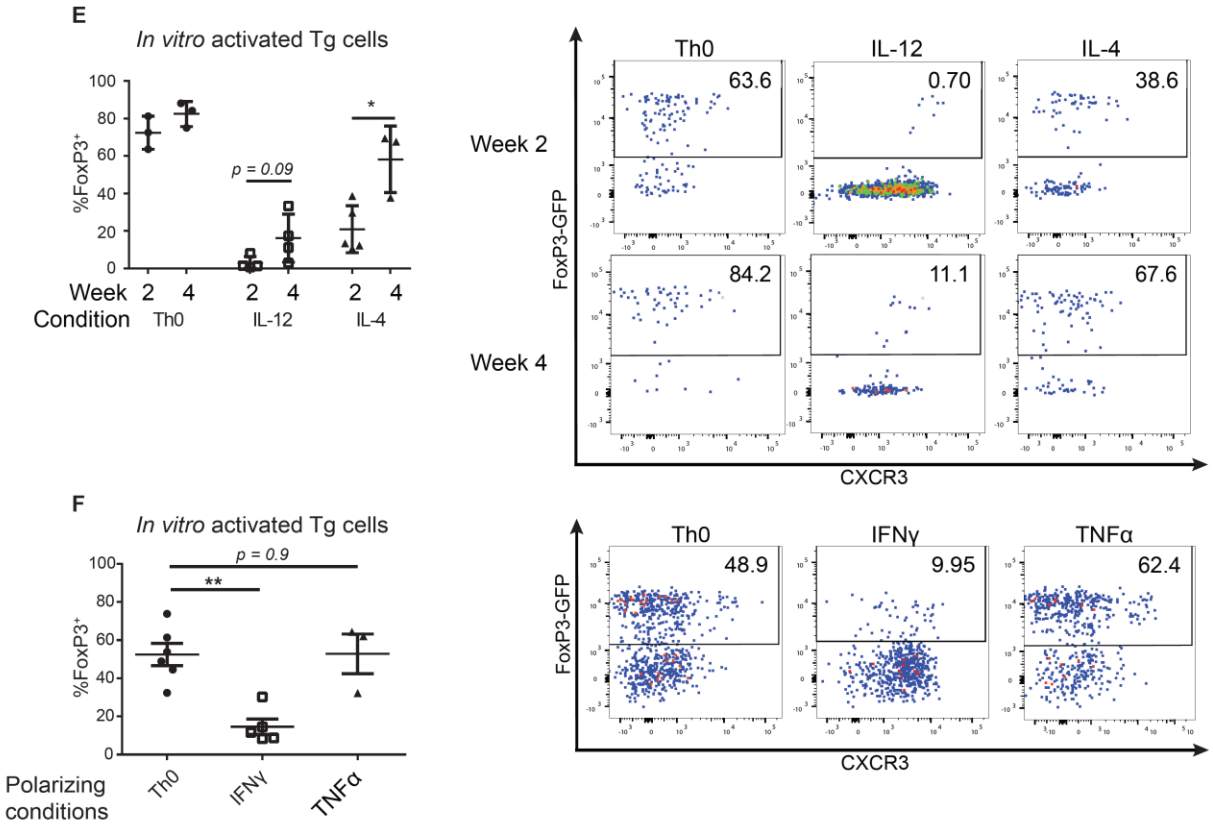

Figure 2.8: Expansion of CT2 and CT6 cells, but not FoxP3 induction, is reduced during *Citrobacter rodentium* and *Toxoplasma gondii* infection. (A) CD45.1 wild-type mice were infected with *Toxoplasma gondii* by oral gavage of 1 brain cyst per recipient mouse. $1x10^5$ congenically marked CT2 *FoxP3*$^{IRES\text{-}GFP}$ (CD45.1/2) and CT6 *FoxP3*$^{IRES\text{-}GFP}$ (CD45.2) naïve cells were prepared and transferred as described in Figure 2.1 into control and experimental mice on day 4 of *Toxoplasma gondii* infection. Tg cells were analyzed from the MLN 6-7 days after transfer. Flow cytometric analysis performed on congenically marked $CD4^+V\alpha2^+$ Tg cells (replicates = 2; *n* = 1-3). **(B)** CD45.1 wild-type mice were infected with $2x10^9$ CFU of OVA-expressing *Citrobacter rodentium.* Naïve CT6 *FoxP3*$^{IRES\text{-}GFP}$ and OT-II *FoxP3*$^{IRES\text{-}GFP}$ cells were mixed 1:1, and retro-orbitally injected into wild-type and experimental mice on d4 of infection.

Flow cytometric analysis and representative FACS plots of FoxP3, CD25, and CD62L expression are displayed as a percentage of all congenically marked Tg cells (replicates = 4, *n* = 6-8 mice pooled for one datapoint). **(C, D)** CD45.1 wild-type mice were infected with $2x10^9$ CFU of *Citrobacter rodentium*. Naive CT2 *FoxP3*$^{\text{IRES-Thy1.1}}$ *IL-17A*$^{\text{IRES-GFP}}$ *IFNγ*$^{\text{IRES-YFP}}$ and CT6 *FoxP3*$^{\text{IRES-Thy1.1}}$ *IL-17A*$^{\text{IRES-GFP}}$ *IFNγ*$^{\text{IRES-YFP}}$ Tg cells were sorted and transferred as described in Figure 1 in control and experimental mice on day 4 or day 9 of infection. Tg cells were analyzed in dMLN 7 days after transfer. Graphs are percentages of all Tg cells, FoxP3$^{\text{IRES-Thy1.1+}}$ or FoxP3$^{\text{IRES-Thy1.1–}}$ fractions of Tg cells (replicates = 2; *n* = 4-6). **(E)** Congenically marked CT2 *FoxP3*$^{\text{IRES-GFP}}$ or CT2 *IFNγ*$^{\text{IRES-YFP}}$ *FoxP3*$^{\text{IRES-Thy1.1}}$ naïve cells were sorted as described above and activated in polarizing conditions (see methods) before retro-orbital transfer (1.5×10^5 into wild-type CD45.1 hosts). Tg cells were analyzed via flow cytometry from the dMLN 2 or 4 weeks post transfer (replicates = 2; *n* = 1-2) **(F)** Tg cells were sorted, polarized, and transferred as described in (E) and analyzed in the dMLN 1 week post transfer (replicates = 2, *n* = 1-2 for all). Representative FACS plots of FoxP3$^{\text{GFP+}}$ percentages gated on congenically marked $CD4^+V\alpha2^+$ Tg cells. Statistical significance was calculated using Student T test, **P<0.05,* ** *P<0.005,* *** *P < 0.001*; ns = not significant. Error bars = ± SEM.

Figure 2.9

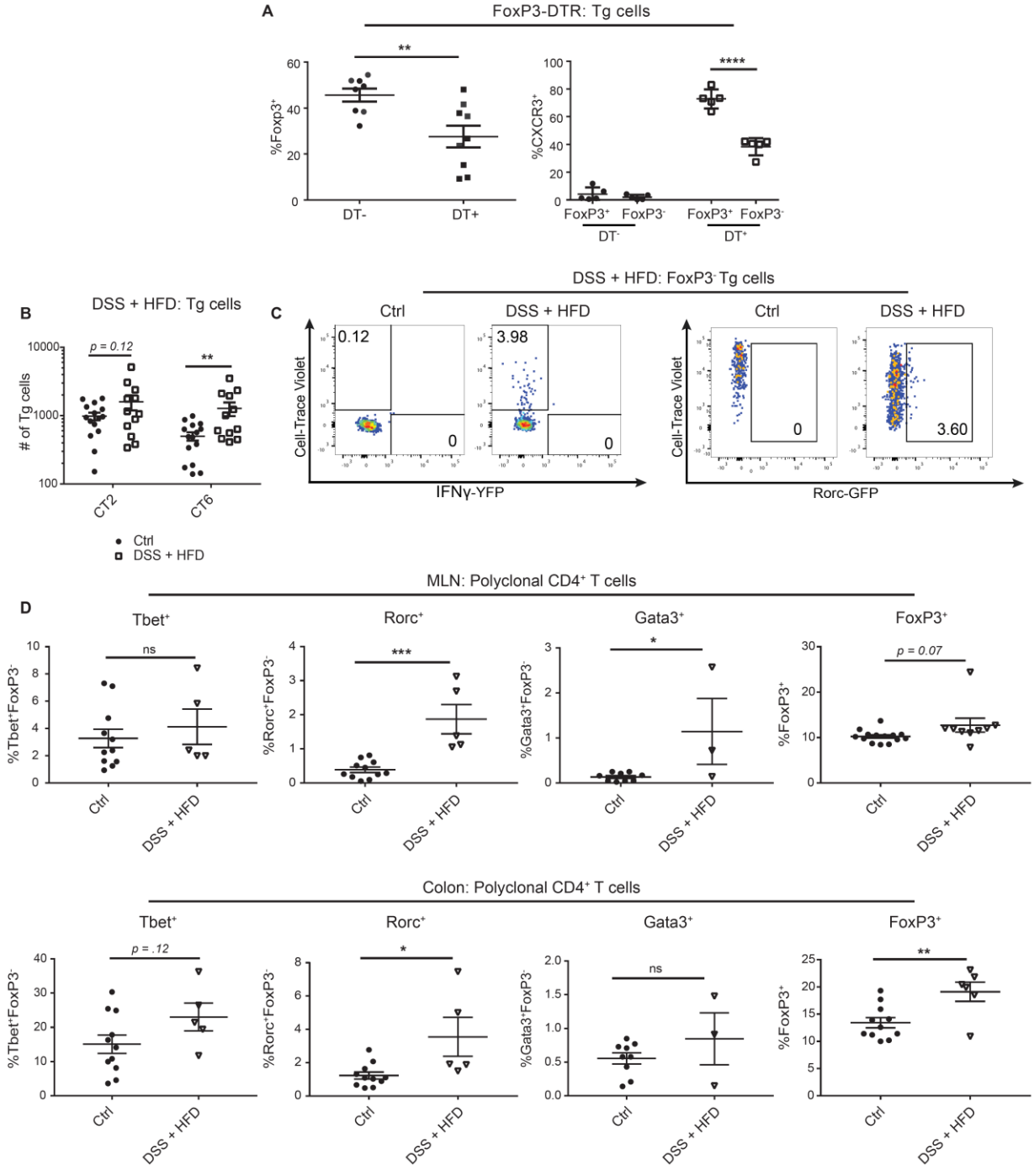
A
FoxP3-DTR: Tg cells
%Foxp3+
DT-
DT+
%CXCR3+
FoxP3+ FoxP3-
DT-
DT+
B
DSS + HFD: Tg cells
# of Tg cells
p = 0.12
CT2
CT6
Ctrl
DSS + HFD
C
DSS + HFD: FoxP3- Tg cells
Ctrl
DSS + HFD
Cell-Trace Violet
IFNγ-YFP
Rorc-GFP
0.12
3.98
3.60
D
MLN: Polyclonal CD4+ T cells
Tbet+
Rorc+
Gata3+
FoxP3+
%Tbet+FoxP3-
%Rorc+FoxP3-
%Gata3+FoxP3-
%FoxP3+
ns
p = 0.07
Colon: Polyclonal CD4+ T cells
p = .12

Figure 2.9: Additional analyses of polyclonal and Tg cells during intestinal inflammation. **(A)** CD45.1 FoxP3-DTR mice were injected with one dose of DT (40 ng/g mouse). 24 hours later, naïve CT2 *FoxP3*$^{\text{IRES-GFP}}$ cells were transferred as described in Figure 1 (replicates = 3; *n* = 2-4). (**B, C**) Mice were treated with DSS and HFD and naïve CT2 *FoxP3*$^{\text{IRES-Thy1.1}}$ *IL-17A*$^{\text{IRES-GFP}}$ *IFNγ*$^{\text{IRES-YFP}}$ and CT6 *FoxP3*$^{\text{IRES-Thy1.1}}$ *IL-17A*$^{\text{IRES-GFP}}$ *IFNγ*$^{\text{IRES-YFP}}$ or CT6 *Rorc*$^{\text{GFP}}$ cells co-transferred as described in Figure 2.1. GFP (replicates = 2, *n* = 2-3) and YFP (replicates = 3; n = 2-3) expression was assessed in the dMLN one week after transfer. **(D)** CD45.1 wild-type mice were treated with HFD as described before and analyzed on day 5 after 2% DSS treatment. T cells from the MLN and colon lamina propria were isolated and analyzed for FoxP3, Tbet, Rorc, and GATA3 expression via transcription factor staining (replicates = 2; *n* = 2-3). Statistical significance was calculated using Student T test, *$P<0.05$, ** $P<0.005$, *** = $P \leq 0.001$, **** = $P \leq 0.0001$; ns = not significant. Error bars = ± SEM.

Figure 2.10

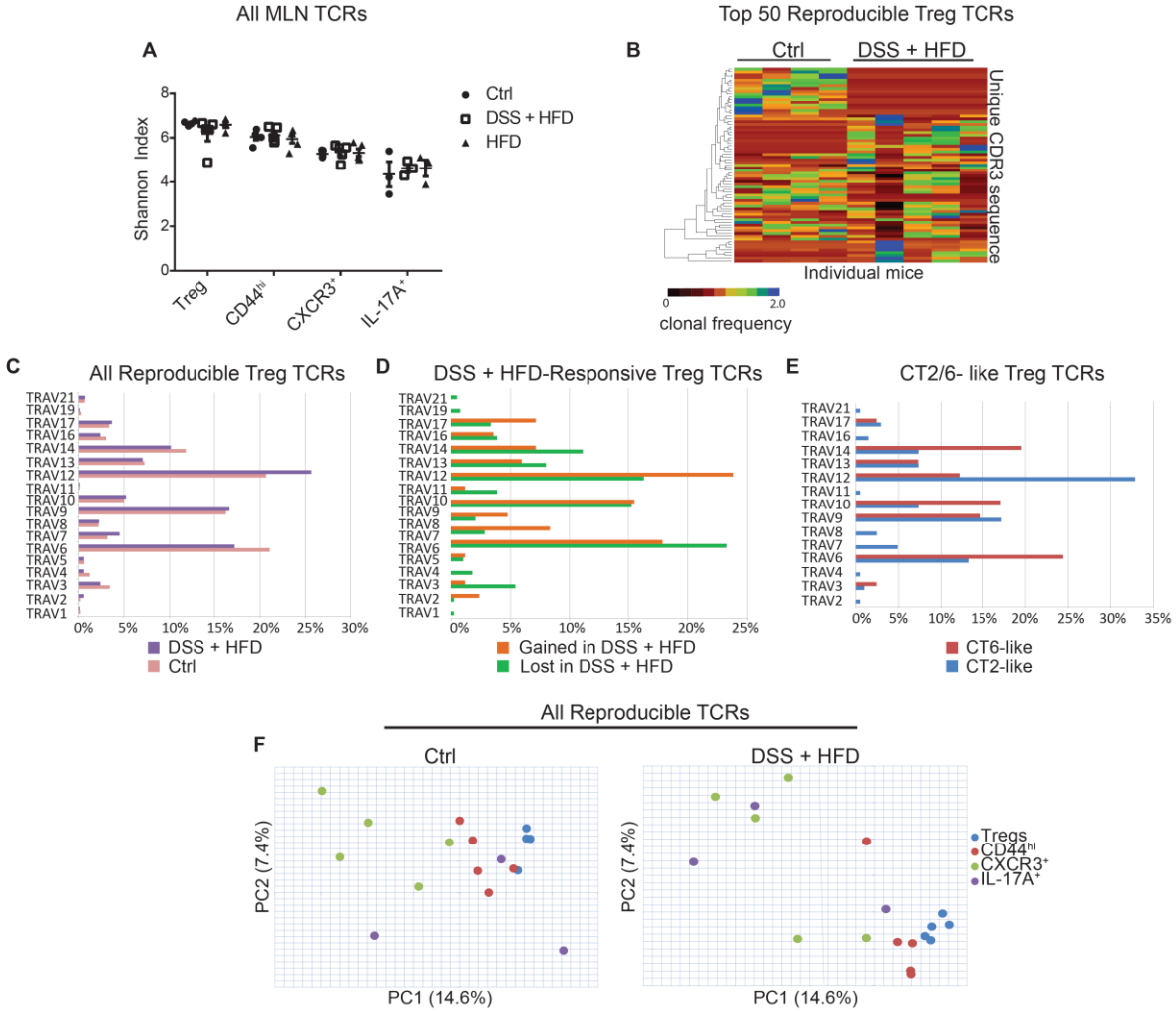
All MLN TCRs
A
Shannon Index
Ctrl
DSS + HFD
HFD
Treg
CD44hi
CXCR3+
IL-17A+
Top 50 Reproducible Treg TCRs
B
Ctrl
DSS + HFD
Unique CDR3 sequence
Individual mice
clonal frequency
C
All Reproducible Treg TCRs
DSS + HFD
Ctrl
D
DSS + HFD-Responsive Treg TCRs
Gained in DSS + HFD
Lost in DSS + HFD
E
CT2/6- like Treg TCRs
CT6-like
CT2-like
All Reproducible TCRs
F
Ctrl
DSS + HFD
PC2 (7.4%)
PC1 (14.6%)
Tregs
CD44hi
CXCR3+
IL-17A+

Figure 2.10

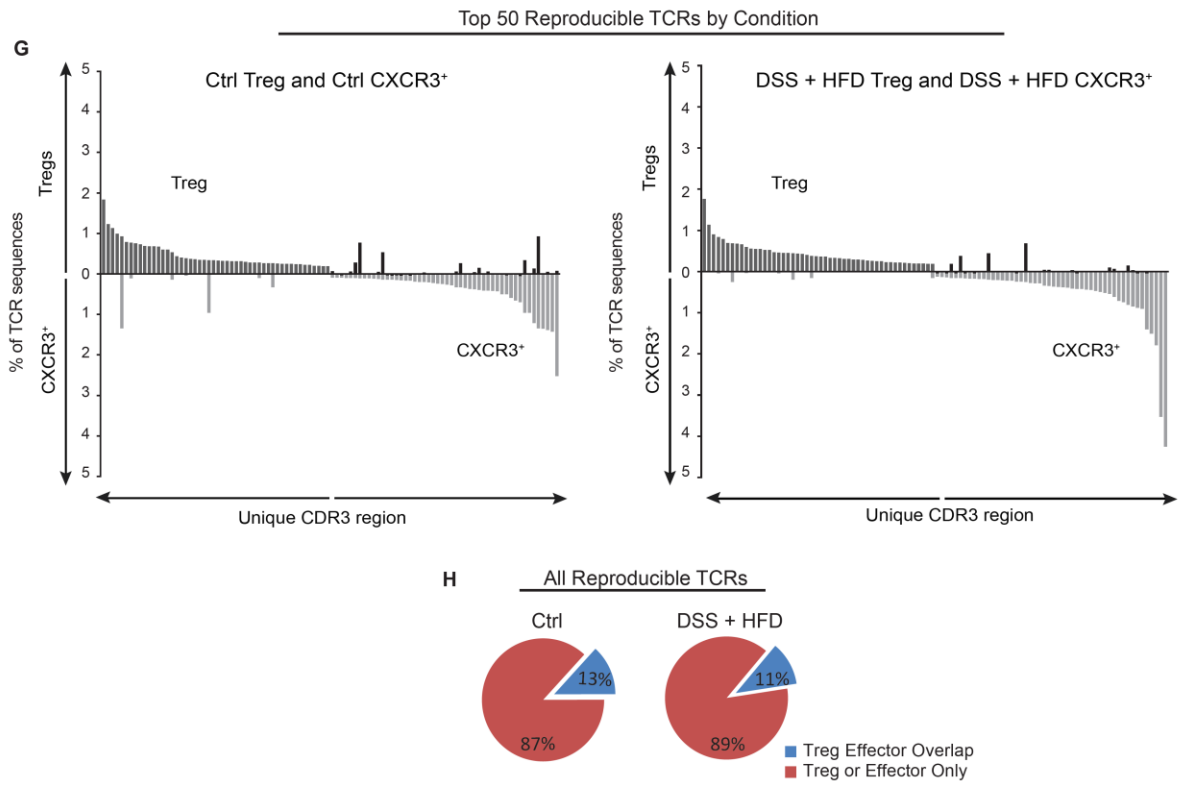

Figure 2.10: Characteristics of TCR repertoires in DSS and HFD. (**A-G**) TCR sequences acquired and data rarefied to 10,000 reads as described in Figure 2.5 (replicates = 4, *n* = 1-2 mice). **(A)** Shannon diversity calculated for respective populations per condition. **(B)** Hierarchical clustering (distance = Euclidean) by clonal frequency of top 50 reproducible TCRs (≥ 50% of mice) (**C-E**) TRAV distribution of respective TCR categories, described in Figure 5. **(F)** PCA analysis of reproducibly found TCRs from rarefied dataset. **(G)** Top 50 reproducibly found TCRs in Treg or CXCR3^{+} TCR repertoires ranked on average clonal frequencies (adjusted for TRAV primer bias) were identified. Plots display the clonal frequencies of top ranked TCRs, ordered in decreasing rank towards the center, and their clonal frequencies in the other T cell

population. **(H)** Frequency of reproducibly found control Treg TCRs that are also reproducibly found in control FoxP3^{-} repertoires. The same analysis was done for reproducibly found DSS and HFD Treg TCRs.

Figure 2.11

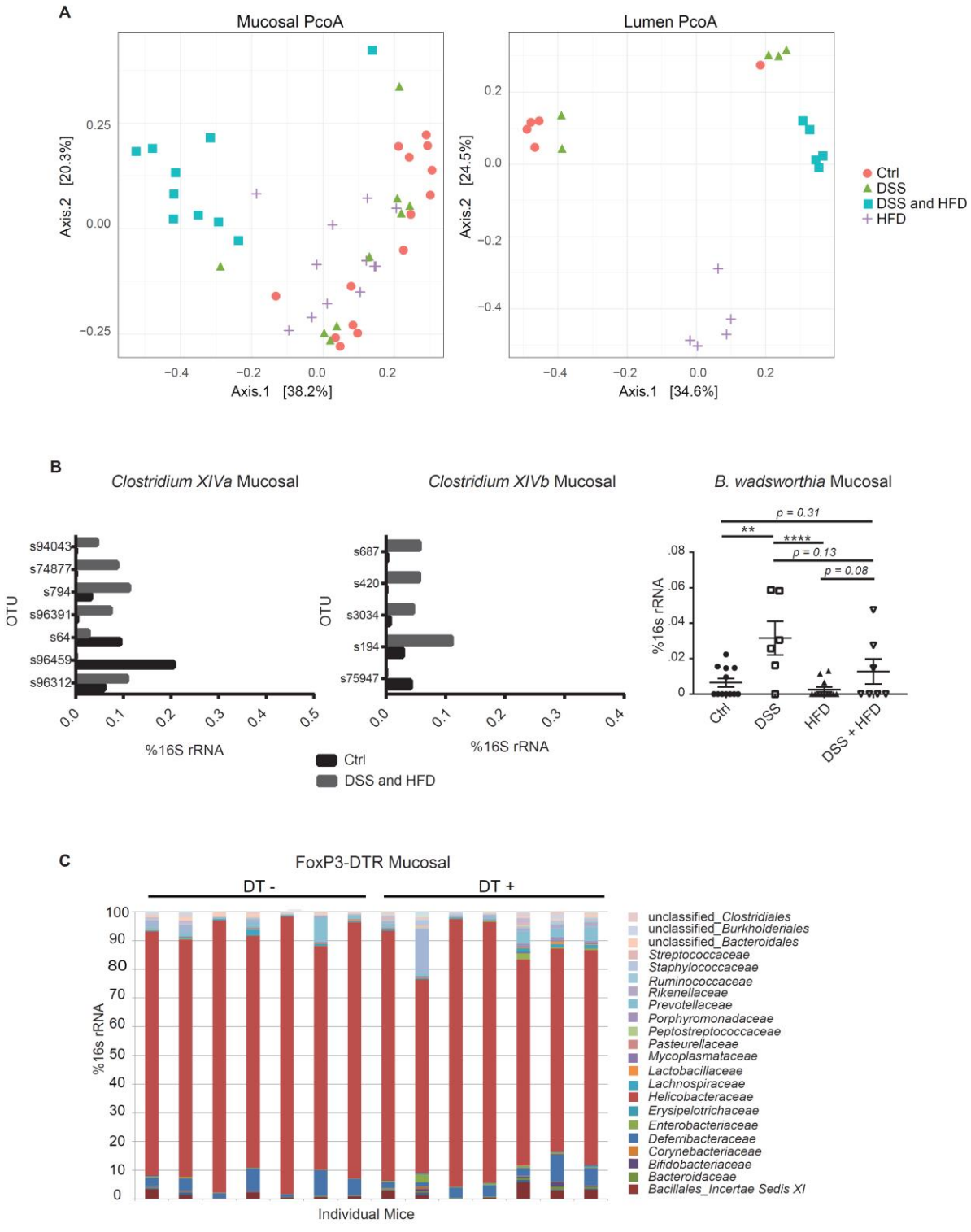
A
Mucosal PcoA
Lumen PcoA
Axis.2 [20.3%]
Axis.1 [38.2%]
Axis.2 [24.5%]
Axis.1 [34.6%]
Ctrl
DSS
DSS and HFD
HFD
B
Clostridium XIVa Mucosal
Clostridium XIVb Mucosal
B. wadsworthia Mucosal
OTU
%16S rRNA
p = 0.31
p = 0.13
p = 0.08
Ctrl
DSS
HFD
DSS + HFD
C
FoxP3-DTR Mucosal
DT -
DT +
%16s rRNA
Individual Mice
unclassified_Clostridiales
unclassified_Burkholderiales
unclassified_Bacteroidales
Streptococcaceae
Staphylococcaceae
Ruminococcaceae
Rikenellaceae
Prevotellaceae
Porphyromonadaceae
Peptostreptococcaceae
Pasteurellaceae
Mycoplasmataceae
Lactobacillaceae
Lachnospiraceae
Helicobacteraceae
Erysipelotrichaceae
Enterobacteriaceae
Deferribacteraceae
Corynebacteriaceae
Bifidobacteriaceae
Bacteroidaceae
Bacillales_Incertae Sedis XI

Figure 2.11: DSS and HFD treatment alters mucosal-associated and luminal bacteria communities. (A) PCoA analysis (distance = Bray) for 16S rRNA sequences from mucosal-associated bacteria (replicates = 3; *n* = 2-4) and lumen bacteria (replicates = 2; *n* = 2-3 mice) isolated from control and DSS and HFD treated mice. Bacteria DNA was isolated at the same timepoint as Tg cell from adoptive transfer experiments. **(B)** Select *Clostridium* OTUs detectable in the mucosal-associated preparation in ≥ 50% of mice treated with DSS and HFD. The OTU percentage of total 16S rRNA sequences are shown. **(C)** 3-4 weeks old FoxP3-DTR mice were intraperitoneally injected with 20ng DT/g mouse every other day for a week. A total of 5 treatments were administered before mucosal-associated bacteria were harvested for 16S rRNA sequence analysis. Controls were injected with equal volumes of PBS (replicates = 3; *n* = 2-3). Statistical significance was calculated using Student T test, ** $P<0.005$, **** $P \leq 0.0001$; ns = not significant. Error bars = ± SEM.

Chapter 3: Transcriptional regulators of peripheral Treg cells *in vivo*

ABSTRACT

Peripheral T regulatory (pTreg cells) develop from pluripotent naïve $CD4^+$ T cells, which can differentiate into either tolerogenic or effector lineages. pTreg development is a process that involves the concerted induction of the FoxP3 program and suppression of effector T cell lineages. However, the transcriptional profiles of early and late developmental stages of *in vivo* derived pTreg cells have never been characterized. Therefore, the *in vivo* relevance of known transcriptional regulators, their expression patterns throughout pTreg development, and identity of correlating gene networks are molecular details that remain unclear. In this study, we capture the transcriptional profiles of activated $FoxP3^-$ and $FoxP3^+$ CT6 TCR transgenic (Tg) cells which differentiate into pTreg cells in wild-type hosts against constitutively presented antigen. We find that early activated ($FoxP3^-$) and mature ($FoxP3^+$) pTreg cells show marked differences in enriched functional pathways, although Treg signature genes were enriched in both fractions. Interestingly, we did not observe the differential expression of known transcription factors reported to antagonize Th1 and Th2 responses, but verified that Nr4a family of transcription factors, which promote FoxP3 transcription, are enriched in early developmental stages prior to FoxP3 expression. Lastly, Eomes restriction of FoxP3 correlates with its expression in early $FoxP3^-CD25^{lo}$ Tg cells, with its deficiency predominantly increasing FoxP3 percentages in cells that have undergone 0 or 1 divisions. Thus, early stages of pTreg development are characterized by the enrichment of both Treg promoting and antagonizing transcription factors, but not regulators known to antagonize canonical effector T cell lineages.

Introduction

T cells undergo extensive proliferation and clonal expansion upon activation while acquiring the transcriptional profiles that commit them to effector or tolerogenic fates (155–157). Gene networks that coordinate activation, proliferation, and differentiation are differentially regulated in early and late developmental stages. Transcriptional networks that modulate differentiation decisions need to be initiated early, whereas genes that stabilize lineage decisions are likely to become more prevalent at later stages of development.

FoxP3 is necessary for Treg development and function (1, 81, 82, 158), but additional genes expressed early during development, independently of FoxP3 upregulation, also serve critical roles. Cells that express a functionally null version of FoxP3 are unable to effectively suppress effector responses, but still express hallmark Treg signature genes (3). Furthermore, numerous transcription factors have been identified to regulate FoxP3 expression by blocking effector fates, or by inducing FoxP3's expression through the promoter and/or CNS1 enhancer (12, 103, 104, 106). Identifying additional genes that co-regulate or initiate the transcription of critical genes in early developing Treg cells can further contribute to elucidating the molecular networks prevalent during early stages of pTreg development.

These gaps in knowledge persist, in part, because of limitations of *in vitro* and *ex vivo* polyclonal studies. *In vitro* studies are limited to Tgfβ derived signals, which may not capture transcriptional changes that result from *in vivo* signals that can vary from tissue to tissue. This is particularly relevant for Treg cells, which have tissue-specific transcriptional profiles which may drive tissue specific suppressive or repair functions (159–161). Polyclonal studies isolating Treg cells *ex vivo* depend on FoxP3 reporters (3), which limit analysis to cells in more mature stages,

or surface markers that are enriched for Treg precursors (162), but likely include contaminating cells processing non-Treg signals.

To circumvent these limitations, our study examines developing monoclonal TCR transgenic cells that differentiate into pTreg cells against commensal antigen *in vivo* under homeostatic conditions. We defined early and late developmental populations, captured their transcriptional profiles, and identified highly expressed transcription factors in different developmental stages. With this approach, we were able to clarify that *Eomesodermin* is induced early in developing T cells, reducing Treg frequencies by reducing the rate of FoxP3 expression after TCR engagement.

Materials and Methods

Mice

CT2 (36) and CT6 Tg (21) mice were generated as described (136) and bred to *Rag1*$^{-/-}$ [the Jackson Laboratory (JAX) #002216] and *FoxP3*$^{\text{IRES-GFP}}$ (JAX #006772) or *FoxP3*$^{\text{IRES-Thy1.1}}$. CT6 Tg mice were also bred to *FoxP3*$^{\text{CNS1-/-;GFP}}$, CD4-Cre *Eomes* $^{\text{fl/fl}}$ (123) mice, or CD4-Cre *IFNAR*$^{\text{fl/fl}}$ mice. *Eomes*$^{\text{fl/fl}}$ mice were a gift from W. Yokoyama (Washington University, St. Louis); *IFNAR*$^{\text{fl/fl}}$ mice were a gift from M. Diamond (Washington University, St. Louis); *FoxP3*$^{\text{CNS1-/-;GFP}}$ were a gift from A. Rudensky (Memorial Sloan Kettering Cancer Center). CD45.1 (JAX #006772) host mice used for adoptive transfer experiments were interbred in our colony to maintain their microbiota. Animal experiments were performed in a specific pathogen-free facility in accordance with the guidelines of the Institutional Animal Care and Use Committee at Washington University.

Adoptive transfer experiments

Naive ($CD4^{+}FoxP3^{-}CD25^{-}CD44^{lo}CD62L^{hi}$) T cells were FACS purified from the draining lymph nodes and spleens from CD45.2 Tg mice bred to *FoxP3*$^{\text{IRES-GFP}}$ *Rag1*$^{-/-}$ or *FoxP3*$^{\text{IRES-Thy1.1}}$ *Rag1*$^{-/-}$. When indicated, cells were labeled with Cell-Trace Violet (ThermoFisher) to assess proliferation and 10^5 cells were retro-orbitally injected into 3-4 weeks old wild-type CD45.1 *FoxP3*$^{\text{IRES-GFP}}$ hosts unless otherwise indicated. All experiments were conducted with littermate controls. For all transfer experiments, the distal mesenteric lymph node (dMLN), which drains the cecum, MLN, Spleen, and/or colon lamina propria were harvested at various time points after transfer and Tg cells ($CD45.2^{+}CD4^{+}V\alpha2^{+}$) were analyzed on a BD FACSAria IIu (BD

Biosciences). For cells harvested for gene-chip hybridization, $2x10^5$ naïve CT6 or CT6-*FoxP3*$^{CNS1-/-;GFP}$ cells were retro-orbitally transferred into 6-10 CD45.1 wild-type hosts. dMLN were harvested on d3 post transfer and DN, FoxP3$^-$CD25$^+$, FoxP3^{int}CD25$^-$, and FoxP3^{hi}CD25$^+$ cells were sort-purified into lysis buffer from RNAqueous Ambion Total RNA Isolation Kit (ThermoFisher; AM1219) with vortexing every 20 minutes throughout sort duration.

Gene chip hybridization

RNA was extracted from sort purified Tg cell population using the RNAqueous Ambion Total RNA Isolation Kit. cDNA was reverse transcribed and amplified using the Complete Whole Transcriptome Amplification Kit (Sigma-Aldrich). Degraded samples were removed before submission to the Washington University Genome Technology Access Center (GTAC) for hybridization on the Agilent 4x44k mouse genome array.

Retroviral overexpression and adoptive transfer experiments

Naïve CT6 Tg cells were sorted as described above and plated in α-CD3 (Bio X Cell #BE0001-1; 10 μg/ml) coated 24 well tissue culture plates at $1x10^6$ cells/well in 1ml. Additives to the culture included soluble α-CD28 (Bio X Cell #BE0015-1; 1 μg/ml), anti-cytokine antibodies [all Bio X Cell; α–transforming growth factor–β (20 μg/ml; #BE0057), α-IFNγ (5 μg/ml; #BE0054), α–IL-4 (5 μg/ml; #BE0045), and α–IL-12 (5 μg/ml; #BE0052)]. After 27 hours in culture, cell supernatant was aspirated and replaced with virus packaging overexpression constructs. Cells were spinfected for 2 hours at 37º. Immediately after spinfection, $3x10^5$ cells were retro-orbitally transferred into CD45.1 wild-type hosts. At 1 week after transfer, dMLN were harvested and

transduced or untransduced Tg cells ($CD45.2^+CD4^+V\alpha2^+$) were analyzed on a BD FACSAria IIu (BD Biosciences).

Lamina propria cell isolation

Colon lamina propria tissue was flushed with PBS to remove fecal content. To remove intraepithelial lymphocytes, lamina propria tissue was incubated in RPMI 1640 media containing 3% FBS, 20 mM HEPES, 1 mM DTT, and 50 mM EDTA for 20 min at 37˚C, and washed with RPMI 1640 plus 22.5 mM EDTA. Lymphocytes were isolated from remaining stromal tissue by mincing and digesting in 28.3 µg/ml Liberase TL (Roche) and 200 µg/ml RNase 1 (Roche) for 30 min at 37˚C. Suspended cells were filtered through a 40 µm filter prior to use.

Powrie transfer model

Polyclonal CD4-Cre^+ *Eomes* $^{fl/fl}$ *FoxP3*$^{IRES\text{-}GFP}$, CD4-Cre^- *Eomes* $^{fl/fl}$ *FoxP3*$^{IRES\text{-}GFP}$ naïve cells (CD45.2: $CD4^+$*FoxP3*$^{IRES\text{-}GFP\text{-}}CD44^{lo}CD62L^{hi}$) and Treg cells (CD45.1/2; $CD4^+$*FoxP3*$^{IRES\text{-}GFP+}$) were FACs purified using the BD FACSAria IIu (BD Biosciences). $2.5x10^5$ Eomes deficient or sufficient $CD4^+$ naïve cells were mixed with $0.5x10^5$ wild-type Treg cells and retro-orbitally transferred into CD45.1 *Rag*$^{-/-}$ hosts. Weight loss was evaluated up to 18 days post transfer. Cells were stimulated with PMA, Ionomycin, brefeldin (Biolegend), and monensin (Biolegend) for 3 hours. Cells were fixed with 1.5% PFA and membranes permeabilized with Permeabilization Buffer (eBioscience) for intracellular cytokine staining. Cells were analyzed on a BD FACSAria IIu (BD Biosciences).

Statistical analysis

GraphPad Prism v6 was used for statistical and graphical analysis. Statistical significance was calculated using the Student T test, *$*P<0.05, ** P<0.005, ***P≤0.001, **** P ≤0.0001$*; ns = not significant. Error bars = ± SEM. Quantile normalization of microarray data was performed with Arraystar. ANOVA and Student T tests were FDR adjusted using the Benjamini-Hochberg test using Arraystar, with *$p<0.05$* considered to be significant. Genesets for Gene Set Enrichment Analysis (GSEA) (163, 164) were downloaded from the GSEA database or curated from prior studies (2, 109, 113). GSEA analysis, statistical significance, and heat maps were generated with the GSEA Java Desktop Application. Plots were also generated with Microsoft Excel 2010.

‘

Results

Monoclonal FoxP3$^-$CD25$^+$ CT6 Tg cells cells exhibit a burst of transcriptional activity.

To understand the transcriptional activity that coordinates Treg development prior to FoxP3 expression, we examined the transcriptional profiles of a monoclonal population of CT6 transgenic (Tg) cells activated during homeostasis *in vivo*. Naive CT6 Tg cells, after transfer into wild-type hosts, preferentially differentiate into pTreg cells in response to *in vivo* derived signals in the cecum draining mesenteric lymph node (dMLN) (21, 36). We first defined populations of monoclonal TCR Tg cells by 4 discernable quadrants of FoxP3 and CD25 expression—FoxP3$^-$ CD25$^-$ (DN), FoxP3$^-$CD25$^+$, FoxP3^{int}CD25$^-$, and FoxP3^{hi}CD25$^+$ **(Fig. 3.1A).** As previously reported, CT6 Tg cells transferred into wild-type hosts first express CD25 24 hours and FoxP3 48 hours after transfer in the dMLN (36). As cells develop further, FoxP3^{hi}CD25$^+$ cells are enriched in the most proliferated fraction of Tg cells (36). Although it remains unclear if FoxP3^{hi}CD25$^+$ cells originate from the FoxP3$^-$CD25$^+$ fraction or the FoxP3^{int}CD25$^-$ populations of Tg cells, the detection of CD25 prior to FoxP3 supports that the DN and FoxP3$^-$CD25$^+$ populations represent the earliest developmental stages, and FoxP3^{int}CD25$^-$ and FoxP3^{hi}CD25$^+$ represent later developmental stages.

The DN population, which will include the earliest activated FoxP3$^-$CD25$^-$ cells, FoxP3$^-$ CD25$^+$, FoxP3^{int}CD25$^-$, and FoxP3^{hi}CD25$^+$ populations of monoclonal cells were sort purified from the dMLN on day 3 after transfer and submitted for gene-chip hybridization on the Agilent platform. We isolated Tg cells from the dMLN to capture cells from the anatomical site of antigen encounter and to minimize contamination by circulating naïve, non-activated cells. Gene expression of FoxP3^{hi}CD25$^+$, FoxP3$^-$CD25$^+$, and FoxP3^{int}CD25$^-$ cells were normalized to the DN

population and differentially expressed genes selected based on FDR-adjusted ANOVA p-values (<0.05) **(Fig. 3.1B).** The cell populations showed significant and distinct transcriptional differences. 153 genes were differentially expressed relative to the DN population by all 3 populations. Interestingly only 395 genes total were differentially expressed in the FoxP3^{int}CD25^{-} population. In contrast, F^{-}CD25^{+} cells differentially expressed the most at 2,831 genes and FoxP3^{hi}CD25^{+} cells differentially expressed 1201 genes. FoxP3^{hi}CD25^{+} cells, which represent the latest developmental stages in our analysis, shared a greater number of differentially expressed genes (excluding the 153 genes shared by all) with FoxP3^{-}CD25^{+} than with FoxP3^{int}CD25^{-} cells, with 854 and 46 shared, respectively. FoxP3^{-}CD25^{+} cells also differentially expressed the greatest number of uniquely differentially expressed genes, with 1705 genes uniquely altered out of 2,831 (49%) genes. FoxP3^{hi}CD25^{+} cells, in contrast, only uniquely differentially expressed 194 genes (16%) **(Fig. 3.1B).**

We evaluated the robustness of these observations by conducting pairwise comparisons of differentially expressed genes with Student T tests adjusted for false discovery with the Benjamini Hochberg test **(Fig. 3.1C).** FoxP3^{-}CD25^{+} cells still had the largest number of significantly differentially expressed genes (1,882 genes) relative to FoxP3^{int}CD25^{+} (0 genes, data ns) and FoxP3^{hi}CD25^{+} (29 genes) populations. This data shows that early and late developmental stages for *in vivo* derived pTreg cells exhibit significant transcriptional differences, with the most pronounced transcriptional activity occurring at the time of CD25 upregulation prior to FoxP3 expression. Interestingly, FoxP3 expression by itself did not elevate significant transcriptional activity, supporting proposals that FoxP3 largely facilitates Treg development through gene repression (111) or by amplifying gene expression triggered by non-FoxP3 signals like Tgfβ (109, 158) **(Fig. 3.1B).**

FoxP3$^+$ and FoxP3$^-$ Tg cells exhibit distinct functional pathways.

To gain insight on the functional differences of gene networks in these populations, we examined the relative enrichment of known functional pathways between the isolated FoxP3$^+$ and FoxP3$^-$ Tg cell populations. Gene set enrichment analysis (GSEA) (163, 164) was performed with 674 pathways from the Reactome database by doing pairwise comparisons between the 4 populations **(Fig. 3.1D, Fig. 3.8A).** FoxP3^{hi}CD25$^+$ and FoxP3$^-$CD25$^+$ cells were positively enriched (majority of genes in the gene set are upregulated) for DNA/RNA processing gene sets relative to the double negative population, consistent with their significant transcriptional activity **(Fig. 3.8A)** We further compared the two CD25$^+$ populations to each other to identify the top 15 enriched functions that may be IL-2 independent. The FoxP3$^-$CD25$^+$ cells were dominated by gene sets involved in nucleotide processing, which is also consistent with their higher levels of transcriptional activity, whereas the FoxP3^{hi}CD25$^+$ cells were relatively enriched for signaling pathways, including cytokine signaling in the immune system and type 1 interferon signaling **(Fig. 3.1D, Fig. 3.8B)** We evaluated the cell-intrinsic impact of IFNAR deficiency on the development of CT6 cells, and observed no impact on FoxP3 frequencies during homeostasis, or in mice treated with Poly:IC **(Fig. 3.8C data n.s.).** This suggests that genes in the type 1 interferon pathway may be differentially expressed in response to alternative receptors that signal through targets that intersect multiple pathways. Cumulatively, the data supports that FoxP3$^-$ CD25$^+$ cells are becoming equipped to rapidly initiate transcription, consistent with the notion of clonal expansion and proliferation, whereas FoxP3^{hi}CD25$^+$ cells are processing signals from the environment to fine-tune their phenotype.

Treg signature genes are expressed prior to FoxP3 upregulation.

Next, we assessed the expression of Treg signature genes (109) in the 4 Tg populations to determine when in development Treg cells begin to adopt Treg profiles. As expected, the $FoxP3^{hi}CD25^{+}$ cells were more enriched for Treg signature genes relative to $FoxP3^{-}CD25^{+}$ cells, but to our surprise, de-enriched when compared to DN cells **(Fig. 3.2A).** This indicated that DN cells express more Treg signature genes than the $FoxP3^{-}CD25^{+}$ cells. We confirmed this observation, finding 181 Treg signature genes that were positively enriched in the DN population **(Fig. 3.2A).** This demonstrates that a significant portion of genes characteristic to mature Treg cells are expressed predominantly in the DN population prior to FoxP3 upregulation.

We next investigated whether the DN cells may also express genes that are later amplified by, but not dependent on FoxP3. These genes, as expected, are more positively enriched in $FoxP3^{hi}CD25^{+}$ cells relative to DN cells and $FoxP3^{-}CD25^{+}$ cells **(Fig. 3.2B).** Consistent with the Treg signature GSEA results, DN cells are also relatively enriched for FoxP3-amplified genes (2), 60% of which are Treg signature genes, including *Tcf7, Ctla4, and Gpr15*. We further observed that activated CT6 CNS1 deficient cells, which have dramatically reduced FoxP3 frequencies (36), continue to express a number of Treg signature genes, including *Soc2*, despite the absence of FoxP3 expression **(Fig. 3.9D).** Thus, Treg signature genes, which can be amplified by FoxP3 and/or expressed independently of FoxP3, are expressed in early activated cells, but relatively de-enriched in $FoxP3^{-}$ cells expressing CD25.

Transcription factors are prevalently expressed in the DN population of CT6 Tg cells.

Given the enrichment of Treg signature and FoxP3-amplified genes in the DN population, we sought to identify transcription factors that may modulate the transcriptional

landscape of early activated cells. Similar numbers of transcription factors were enriched in FoxP3^{hi}CD25^{+} cells (46 genes) and DN cells (47 genes), including IL-10 regulators, *Ahr* and *Maf* (165, 166), and *Uhrf1*, a FoxP3 stabilizer (167) **(Figure 3.3A).** In DN cells, transcription factors belonging to the Nr4a family, which regulate FoxP3 expression in pTreg cells through interactions with the CNS1 enhancer and FoxP3 promoter (103, 104, 106), were enriched relative to FoxP3^{hi}CD25^{+} cells. Comparisons of FoxP3^{hi}CD25^{+} cells with FoxP3^{-}CD25^{+} determined that a greater number of transcription factors were enriched in FoxP3^{hi}CD25^{+} cells, with 92 genes relative to FoxP3^{-}CD25^{+} cells' 70 genes. Notably, neither PHD nor Musculin proteins, which antagonize Th1 and Th2 transcriptional programs respectively (107, 108), were amongst the most significantly differentially expressed. However, there were approximately twice as many transcription factors upregulated in DN relative to FoxP3^{-}CD25^{+} cells, with 208 upregulated in DN cells, but only 123 upregulated in FoxP3^{-}CD25^{+} cells. Of the 208 and 123 differentially expressed genes, 62 and 31 genes, respectively, reached FDR-adjusted statistical significance. Cumulatively, the significant number of transcription factors expressed in the DN population and expression of the Nr4a family of transcription factors demonstrate that 1) DN cells express a significant number of transcription factors that are downregulated in other populations, and 2) DN cells express transcription factors that are known to regulate FoxP3 transcription.

Eomes is expressed in FoxP3^{-}CD25^{lo} population of CT6 Tg cells.

Eomesodermin was the transcription factor that underwent the largest fold change, expressing a signal ~11x greater in DN and FoxP3^{-}CD25^{+} cells relative to FoxP3^{hi}CD25^{+} cells **(Figure 3.3A).** We verified the microarray results for Eomes *in vivo* via intracellular staining of CT6 Tg cells. Consistent with the microarray, Eomes expression was absent in the FoxP3^{+}

fraction of CT6 Tg cells **(Fig. 3.9A, Fig. 3.3B).** In CT6-*Nur77*^{GFP} mice, which express Nur77 signal in direct proportion to increasing strength of TCR stimulation (103, 168), we further observed that Eomes expression is limited to Nur77^{GFP+} cells that express low levels of CD25. Unexpectedly, high levels of Nur77^{GFP} did not correlate with high levels of CD25 expression, suggesting the possibility that CD25 expression either precedes TCR stimulation, or is downregulated when TCR engagement increases in strength. It is likely that that Eomes is detected in the DN fraction of the microarray due to the capture of a contaminating CD25^{lo} population. Thus, Eomes protein is highly expressed in a FoxP3^{-}CD25^{lo}Nur77^{GFP+} population of cells and absent in FoxP3^{+} Tg populations.

Eomes negatively regulates FoxP3 expression in developing CT6 Tg cells.

We next asked whether this potentially transient expression of Eomes has a functional impact on pTreg development by CT6 Tg cells. We verified that retroviral overexpression of Eomes in CD4^{+} T cells *in vitro* reduced FoxP3 upregulation, as previously reported, in the cells transduced with the overexpression construct (121) **(Fig. 3.9B).** FoxP3 expression was completely eliminated in cells expressing the highest levels of Eomes, but untransduced cells showed no FoxP3 defect, demonstrating that Eomes blockade of FoxP3 is cell-intrinsic. Eomes deficient cells activated in Th0 conditions also exhibited elevated levels of spontaneous FoxP3 expression in the absence of Tgfβ, given the inclusion of α-Tgfβ in the culture **(Fig. 3.9C).** This validates prior reports that Eomes restriction of FoxP3 is through cell-intrinsic mechanisms and not the result of extracellular signals in the culture (121).

Eomes restriction of Foxp3 has been reported i*n vitro* and in the context of monoclonal OT-II cells differentiating into pTreg cells in response to exogenously introduced oral antigens

(121). However, it remains unknown if Eomes serves a function in pTreg induction against antigen endogenous to the host. To evaluate the impact of Eomes for pTreg cells derived against homeostatically presented endogenous antigen, we retrovirally overexpressed Eomes-GFP or an empty Mig-GFP vector into CT6 Tg cells activated in Th0 conditions that preserves *in vivo* Treg differentiation **(Fig. 3.10A).** The cells were transferred 27 hours after retroviral spinfection into wild type hosts, and FoxP3 upregulation in transduced cells was assessed. Consistent with our *in vitro* results, cells overexpressed with Eomes exhibited a 2-fold reduction in FoxP3 percentages when analyzed one week post transfer **(Fig 3.4A).** We further overexpressed additional targets, with reported T cell functions, including BCL-6, NR4A1, and IRF8 into CT6 cells (102, 104, 169, 170). Cells overexpressed with BCL-6 exhibited no reduction in FoxP3 frequencies, showing that the reduction of FoxP3 in Eomes-overexpressed cells is not an artifact of transcription factor overexpression **(Fig 3.10C).** As expected, cells overexpressed with NR4A1 exhibited an increase in FoxP3, and IRF8 drove the expression of CXCR3, which traffics cells to sites of Th1 inflammation **(Fig. 3.10D, 3.10E).** Thus, this experimental approach recapitulates expected functions of transcription factors on Treg development, and verifies that FoxP3 reduction is function of Eomes.

To evaluate the effect of Eomes deficiency *in vivo*, CT6-CD4-Cre *Eomes*$^{fl/fl}$ mice were generated and naïve cells transferred into wild-type hosts. Eomes deficient cells exhibited a significant 1.5-fold increase in FoxP3 frequencies in the cecum draining lymph node and upward trended in the colon lamina propria 1 week after initial transfer **(Fig. 3.4B).** Increased FoxP3 percentages extended beyond the intestinal tissues, with a larger, 2-fold increase in FoxP3 percentages in cells isolated from the spleen **(Fig 3.11A).** Neither the FoxP3^{+} nor FoxP3^{-} fraction of cells exhibited increased Cell-Trace Violet dilution, CD25 upregulation, or cell numbers in

any of the examined tissues **(Fig. 3.4C, Fig. 3.11B).** Thus, increased frequencies of FoxP3 is unlikely the result of enhanced proliferation or activation. This data demonstrates that Eomes expression is not required for pTreg development *in vivo*, but reduces the efficiency of Treg maturation.

Eomes mediated FoxP3 restriction is not a universal property of Tbx transcription factors.

Considering that Tbet and Eomes share overlapping transcriptional targets (117) and the reported blockade of pTreg differentiation by Tbet (47, 143), we asked whether Eomes-mediated FoxP3 restriction is due to universal properties of the Tbx domain, or due to shared transcriptional targets specific to Tbet and Eomes. To address this question, we overexpressed Tbet proteins that cannot initiate transcription—a function predominantly conferred to the C-terminus region of the Tbet protein (146, 147). We use a dominant negative mutant with the carboxy terminus replaced with a drosophila engrailed domain (117), a mutant with a truncated C-terminus (146), and a mutant with a point mutation (Y182) in the Tbx domain (147). This mutation impairs the recruitment of epigenetic modifiers and therefore, transcription. The dominant negative mutant completely blocked FoxP3 upregulation, but the cells overexpressed with the Y182 point mutant expressed FoxP3 at similar percentages as those overexpressed with an empty vector **(Fig. 3.5A).** Interestingly, the Y182 mutant, contrary to prior reports (147), was able to drive the transcription and expression of CXCR3 **(Fig. 3.5A).** The retained transcriptional abilities point towards the possibility that FoxP3 blockade is the result of functions specific to the Tbx domain. However, the mutant with a truncated C-terminus did not reduce FoxP3 **(Fig. 3.5B)**. Furthermore, additional Tbx proteins, Tbx5, Tbx6, and Tbx10 failed to block FoxP3

upregulation **(Fig. 3.12A).** This data supports that FoxP3 blockade is not a universal property of Tbx proteins and is a function unique to share transcriptional targets of Tbet and Eomes.

Genes repressed by Eomes are enriched in FoxP3^{hi}CD25^{+} and FoxP3^{-}CD25^{+} cells

To determine if a transcriptional target shared by Tbet and Eomes is necessary for FoxP3 restriction, we activated Eomes deficient CD4^{+} T cells in Th1 polarizing conditions that induce Tbet. Interestingly, the Eomes deficient cells still exhibited enhanced spontaneous FoxP3 upregulation even in Th1 polarizing conditions **(Fig 3.5C).** Although it cannot be ruled out that shared transcriptional targets play a role in FoxP3 blockade, this data cumulatively suggests that there are non-overlapping targets of Tbet and Eomes that can restrict FoxP3. To gain insight on whether Eomes is mediating FoxP3 restriction through the activation or suppression of genes, we analyzed the expression patterns of genes regulated by Eomes during endoderm development (113), with the caveat being that endoderm cells may lack the expression of T cell genes regulated by Eomes. Targets downregulated in Eomes deficient cells, which would represent genes activated regulated by Eomes, did not exhibit substantial differential expression **(Fig. 3.12B).** In FoxP3^{hi}CD25^{+} cells and DN cells, equal numbers were differentially expressed, but only 1 gene reached statistical significance. When comparing FoxP3^{-}CD25^{+} to the DN population, there was a slight increase in the number of genes enriched in the DN population, with 52 enriched with a 2-fold difference in the DN population and 41 in FoxP3^{-}CD25^{+} cells. Of the 52 and 41 genes, 22 and 12 reach statistical significance, respectively **(Fig.3.12B).** Interestingly, genes that are up in Eomes deficient cells, representing genes repressed by Eomes, were enriched in the FoxP3^{hi}CD25^{+} population, with 52 genes up in FoxP3^{hi}CD25^{+} and 28 in DN cells **(Fig 3.5D).** 5 reached statistical significance in the FoxP3^{hi}CD25^{+} population, and 1 was

significantly enriched with a 2-fold difference in the DN population. This trend was consistent in comparisons of the FoxP3$^-$CD25$^+$ cells compared to DN cells, where there was a ~2-fold difference in genes enriched in DN vs. FoxP3$^-$CD25$^+$ cells **(Fig 3.5D).** This difference increased to 4-fold when analysis was restricted to statistically significant genes, with 12 enriched in FoxP3$^-$CD25$^+$, but 46 enriched in DN cells **(Fig 3.5D).** Although this gene set is unlikely comprehensive for T cell gene expression, this assessment suggests that Eomes in CT6 cells is predominantly executing gene repression.

Eomes deficiency enhances FoxP3 independent of effector T cell polarization.

We next sought to understand if Eomes regulates FoxP3 expression by promoting effector fates in CT6 Tg cells that ultimately fail to develop. We chose to address this question by examining differentiation of Eomes deficient polyclonal cells in an inflamed environment that favor effector cells. If Eomes modulates pTreg differentiation by driving alternative effector fates, we would expect to see increased effector cells corresponding with increased FoxP3 expression. Here, we did not use CT6 cells because Treg differentiation by CT6 monoclonal cells can differentiate into pTreg cells in multiple models of intestinal inflammation, suggesting they do not receive T effector specifying signals. Eomes deficient naïve cells were co-transferred with wild-type Treg cells into lymphopenic hosts to allow them to differentiate in a moderately inflamed environment. Like with our monoclonal observations, Eomes deficient naïve cells exhibited a 2-fold increase in Foxp3 frequencies relative to wild-type naïve cells **(Fig. 3.6A).** Despite reports that Eomes can promote IFNγ production in cooperation with Tbet, Eomes deficient cells did not exhibit reductions or elevations in IFNγ producing cells (117) **(Fig. 3.6B).** Furthermore, the mice with transferred Eomes deficient cells exhibited reduced weight loss

relative to mice transferred with Eomes wild-type cells **(Fig. 3.12A).** This data suggests firstly that Eomes deficiency can promote FoxP3 in a cell-intrinsic fashion in the context of inflammation, and secondly, the increase is not the result of a defect in effector T cell development.

Eomes regulates FoxP3 expression in early cell divisions.

One hypothesis is that Eomes expression temporarily suppresses FoxP3 until it can be downregulated by Tgfβ (121), slowing the rate of FoxP3 upregulation. To address this question, we evaluated FoxP3 expression in Eomes deficient and wild-type cells by each cell-division of TCR Tg cells stained with Cell-Trace-Violet prior to transfer into wild type hosts. Cells were analyzed 1 week post transfer for FoxP3 expression by GFP reporter from the dMLN. FoxP3 expression could be discerned in peak one (division 0), which contains undivided cells that are a mixture of activated and non-activated cells. The FoxP3 frequency increases with each division in wild-type cells. In Eomes deficient cells, the frequency of FoxP3 expression is elevated 2-fold in division 0 and 1 but not at later cell divisions **(Fig. 3.7A).** We further analyzed Eomes deficient cells at later timepoints during week 2 and 3 post transfer. The increase in FoxP3 frequencies by Eomes deficient cells was most pronounced at week 1 post transfer in intestinal tissues, with virtually no differences observed in the mesenteric lymph nodes by week 3 after initial naïve cell transfer **(Fig 3.7B, Fig. 3.14A).** The increase in FoxP3 percentages was maintained only in the spleen **(Fig. 7B, Fig. 3.14A).** Cells could not be recovered from the colon lamina propria, potentially due to cell death. This in contrast with observations of increased age positively correlating with increased FoxP3 frequencies (121). Interestingly, Eomes deficient cells displayed a mild decrease in CD25 expression, and no significant increase in CXCR3

expression **(Fig. 3.14A).** Thus, Eomes deficient FoxP3^{+} cells show a slight defect in maintaining their activation, but do not show signs of destabilizing to effector fates. Collectively, the reduced difference in FoxP3 frequencies at later time points and increase in FoxP3 percentages at early cell divisions clarifies that Eomes' function is limited to early stages of pTreg development. One possibility explaining the difference in polyclonal and our monoclonal observations is that Eomes is enhancing the constitutive generation of new pTreg cells developing in response to altered self-antigen or matured microbiota.

Discussion

Treg cells differ in their transcriptional profiles in a tissue specific fashion, indicating that developing and mature Treg cells are constitutively processing signals from their environment (171). Thus, the gene networks relevant to *in vivo* derived pTreg cells are likely to differ from *in vitro* derived Treg cells which are generated with the singular addition of Tgfβ. Given the difficulty of distinguishing early from late developing pTreg cells from polyclonal populations, information on the transcriptional maturation of *in vivo* developing pTreg cells has remained poorly characterized.

In this study, we captured the transcriptional profiles of a monoclonal population of colonic, pTreg cells. As expected, the profiles of early and late developing cells were highly distinct in terms of transcriptional targets and function. Early stages of $FoxP3^{-}CD25^{+}$ cells exhibited a burst of transcriptional activity, differentially expressing ~2.5x more genes than $FoxP3^{hi}CD25^{+}$ cells. However these later $FoxP3^{hi}CD25^{+}$ cells were more enriched for immune signaling processes, including type 1 interferon signaling. Deficiency in type 1 interferon signaling did not alter FoxP3 expression despite prior reports that type 1 interferon can enhance FoxP3 expression (56). These observations support that mature Treg cells process additional cytokine or co-stimulatory signals from their environment that are not necessary for FoxP3 induction. Another possibility explaining the discrepancy between prior reports and our assessment of IFNAR signaling in CT6 Tg cells is that pTreg development is process that may vary from tissue to tissue, or even T cell clone to clone.

We identified further discrepancies, having not observed differential expression of transcription factors that promote Treg development by suppressing effector lineages, including Msc2 and PHD proteins. This was surprising given that CNS1 deficient CT6 Tg cells do not

effectively divert to effector cell lineages, and actually generate a greater percentage of FoxP3^{+} cells over time (36). Thus, we hypothesized that CT6 cells would employ cell-intrinsic mechanisms preventing the adoption of effector fates in the form of these transcriptional regulators. Since this was not the case, it begs the question of whether the failure to adopt effector lineages by CT6 Tg cells, despite impaired Treg development, is due to the absence of effector polarizing signals, or a cell-intrinsic process that primes the cells to adopt a Treg fate prior to FoxP3 expression. It is interesting to consider that there are epigenetic mechanisms induced upon Tgfβ signaling, prior to FoxP3 induction, which prime the cells to develop into Treg cells without additional transcriptional regulators.

Eomes was the transcription factor whose expression levels were highest in FoxP3^{-} populations relative to FoxP3^{+} populations. Our study clarified that Eomes is upregulated upon TCR engagement, and restricts FoxP3 upregulation prior to extensive cell division. Its deficiency accelerates the rate of FoxP3 upregulation, with non-divided cells exhibiting increased FoxP3 frequencies relative non-divided Eomes sufficient cells. Furthermore, targets repressed by Eomes are upregulated in FoxP3^{hi}CD25^{+} cells that no longer express Eomes, supporting the possibility that Eomes' function in early developmental stages is largely repressive. One interpretation of this data is that Eomes upregulation transiently suppresses Treg development genes until it can be downregulated, potentially by Tgfβ. What remains unclear, however, is the evolutionary advantage of Eomes induction in developing pTreg cells as opposed to simply restricting its expression to effector T cells. We speculate that its upregulation in developing Treg cells is a vestigial process and that the primary role of Eomes is to regulate effector T cell development and function.

Given the recent advances of single-cell sequencing, it would be intriguing to further this study by investigating early developing pTreg cells at the single cell level by cell-division. Single cell analysis can further clarify relevant molecular networks and identify additional targets that may prime the epigenetic landscape of activated cells to favor Treg development. Furthermore, manipulation of transcription factors like NR4A1 and Eomes are sufficient to enhance Treg development *in vivo*, even in the context of inflammation. It is intriguing to consider the possibility of using gene-editing technology in conjunction with chimeric antigen receptor technology to design cell-based immunotherapies that can robustly maintain tolerogenic profiles in inflammatory contexts.

Figures

Figure 3.1

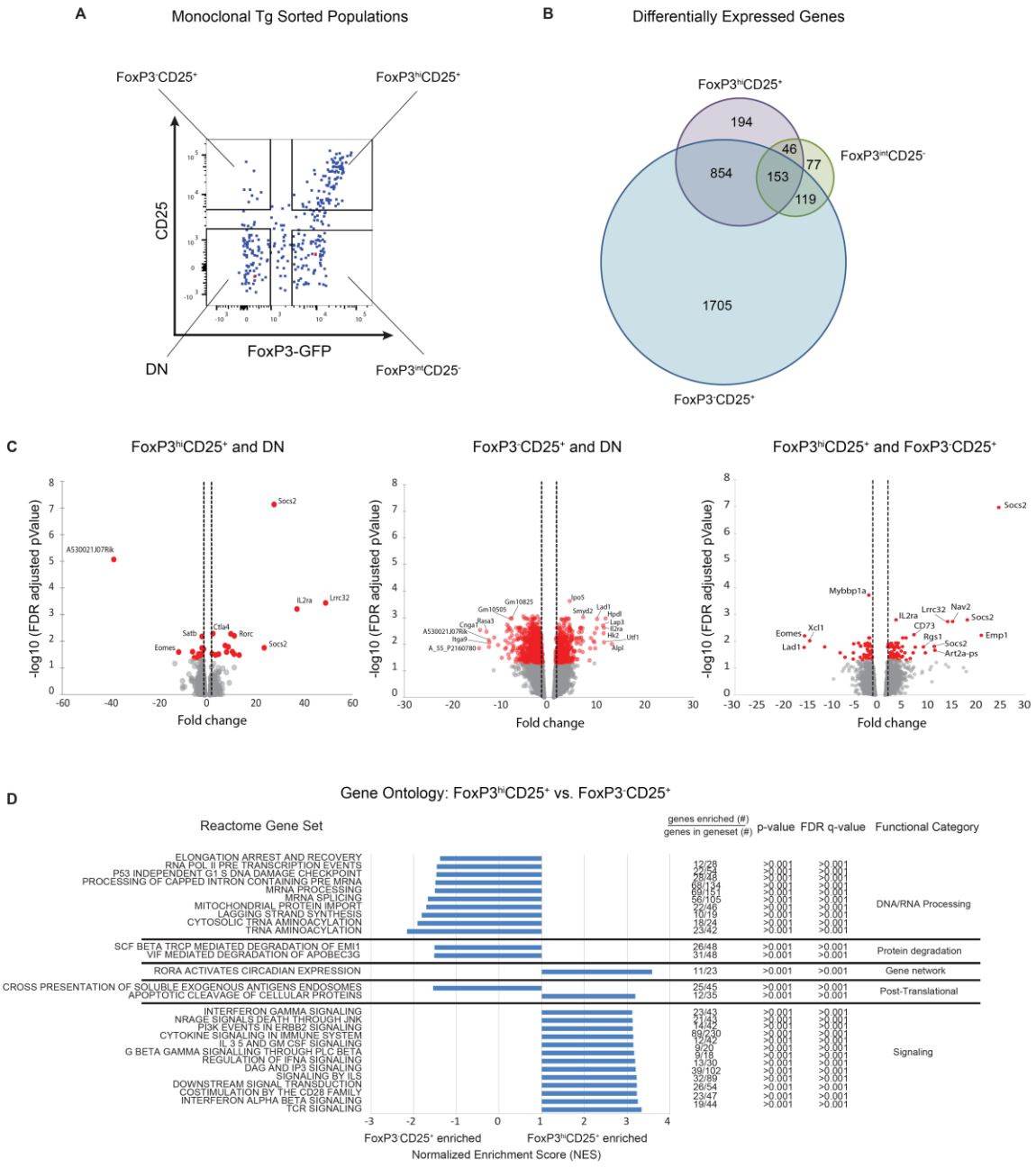

Figure 3.1: Transcriptional profiles of a monoclonal population of developing peripheral Treg cells. (A) 1.8 x 10^6 CT6 (CD45.2) naïve Tg cells ($CD44^{lo}CD62L^{hi}$) were sorted and transferred into 6-8 CD45.1 *FoxP3*$^{IRES\text{-}GFP}$ wild-type hosts colonized with *Helicobacter* antigen.

The dMLN, the initial site of CD25 upregulation by CT6 Tg cells, were harvested on day 3 post transfer and pooled from 6-10 hosts (replicates = 2, *n* = 3). 4 populations were defined by FoxP3 and CD25 expression: DN, $FoxP3^{-}CD25^{+}$, $FoxP3^{int}CD25^{-}$, and $FoxP3^{hi}CD25^{+}$. Monoclonal cells were sorted from pooled dMLN directly into lysis buffer and RNA/cDNA processed for gene chip hybridization. **(B**) 5,129 differentially expressed genes were selected by statistical significance (FDR adjusted p-value < 0.05). Duplicate probes with lower significance values were removed from analysis. Gene expression of $FoxP3^{-}CD25^{+}$, $FoxP3^{int}CD25^{-}$, and $FoxP3^{+}CD25^{+}$ cells were normalized to their gene expression values in DN populations. Genes with 1.5-fold change in gene expression were considered differentially expressed, and the numbers of differentially expressed genes and their overlap with each analyzed population was assessed. **(C)** Pairwise comparisons of differential gene expression for $FoxP3^{hi}CD25^{+}$, $FoxP3^{-}CD25^{-}$, and DN populations. Probes with expression values that fell below an arbitrary threshold were removed from analysis. Robustness of differential gene expression was evaluated with FDR adjusted Student T-test for pairwise comparisons. Genes differentially expressed by $FoxP3^{int}CD25^{-}$ cells did not reach statistical significance and are not shown here. Red denotes genes whose differential expression reached statistical significance (FDR adjusted $p<0.05$) and grey denotes genes that failed to reach statistical significance. Dotted lines mark 1.5 fold-change. **(D)** Gene Set Enrichment Analysis comparing $FoxP3^{hi}CD25^{+}$ cells with $FoxP3^{-}CD25^{+}$ cells. Analysis was done with 674 Reactome gene sets, with gene sets with less than 15 genes excluded from analysis. The Normalized Enrichment Score (NES) of the top 15 gene sets (ranked based on enrichment values) enriched in each population are displayed. Higher NES values signify greater enrichment.

Figure 3.2

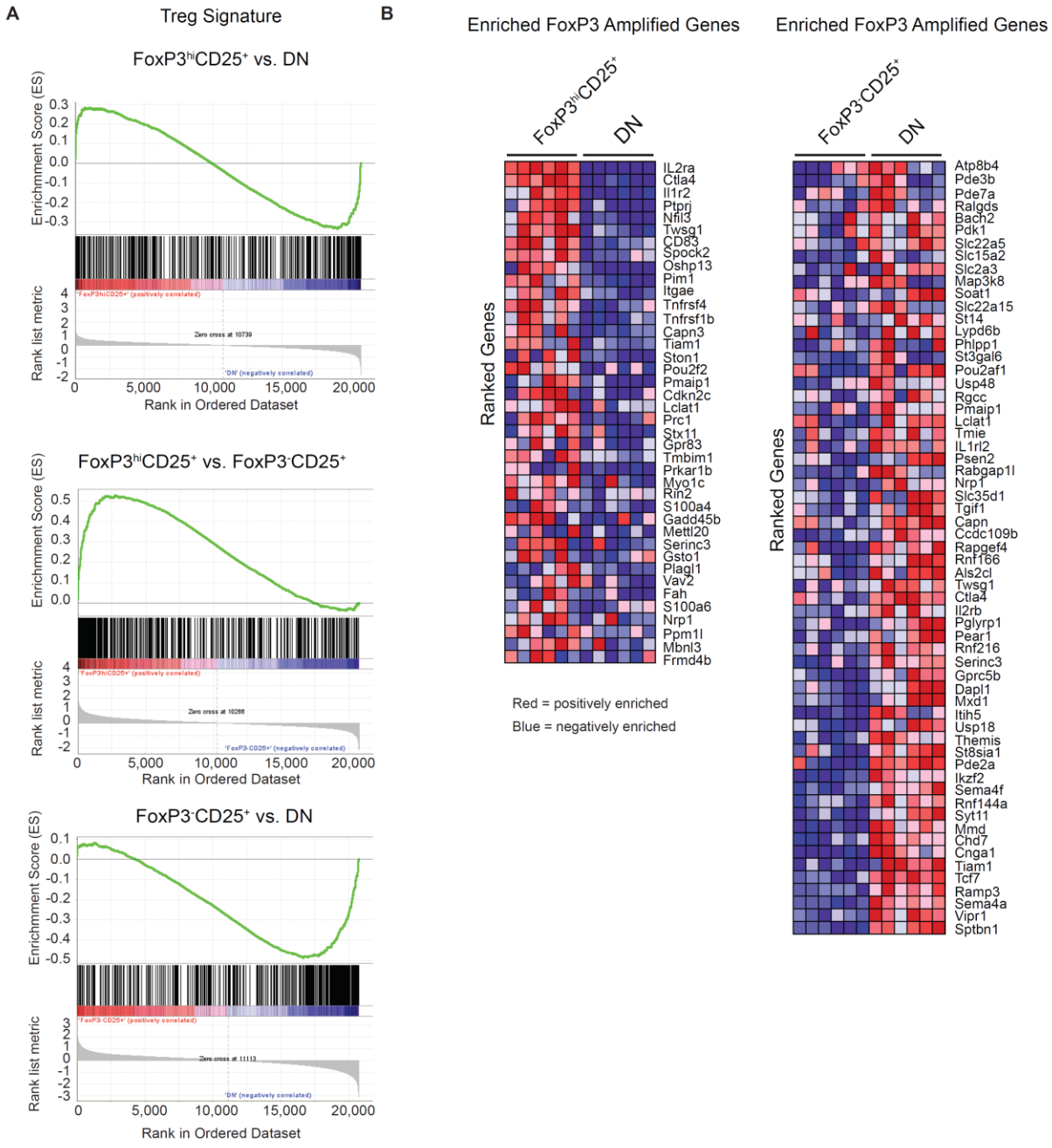

Figure 3.2: Treg signatures are expressed in early developing stages of in vivo generated peripheral Treg cells. (A) Gene Set Enrichment Analysis was performed with Treg signature gene set (640 probes). Genes in analyzed populations were ranked in accordance to the Broad

Institute's signal-to-noise metric and the enrichment for each gene assessed. The green line denotes the Enrichment Score for each gene, with values of 0 signifying no enrichment and positive enrichment scores signifying enrichment in the population listed first. The number of genes with positive or negative enrichment scores reflects the relative enrichment of the Treg signature gene set in each population. **(B)** Gene Set Enrichment Analysis was performed with a gene set consisting of FoxP3-amplified genes (233 probes). Significantly enriched genes displayed in heat maps, with red representing high expression and blue representing low expression.

Figure 3.3

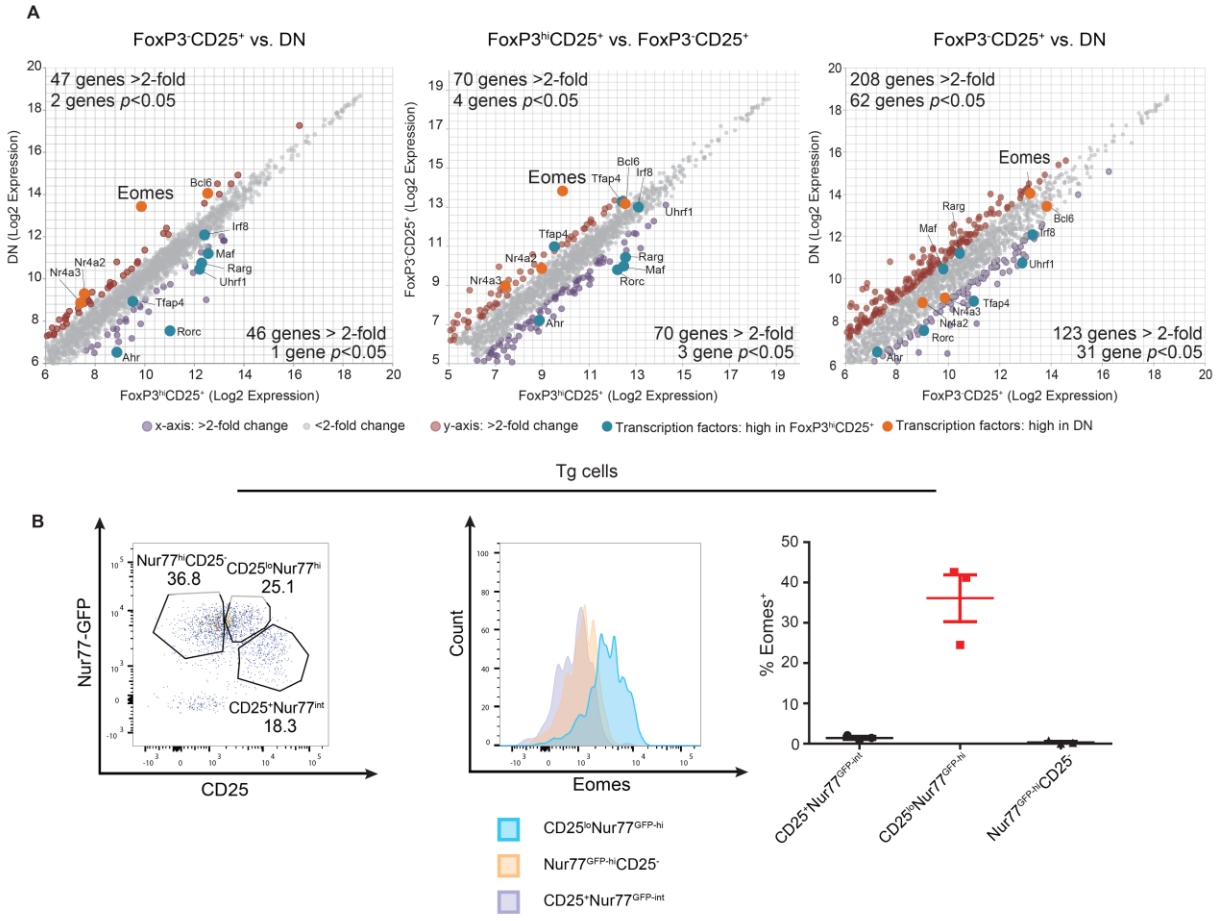

Figure 3.3: *Eomesodermin* expression is elevated in FoxP3^{-}CD25^{lo} cells but absent in FoxP3^{+} stages of peripheral Treg development. (A) Log2 expression values of known transcription factors. Transcription factors differentially expressed in FoxP3^{+} vs. FoxP3^{-} cells were highlighted, in addition to genes undergoing more than 2-fold change. Eomes is highlighted as the gene that undergoes differential fold change of the greatest magnitude. **(B)** CT6 Tg *Nur77*^{GFP} naïve (CD44^{lo}CD62L^{hi}) cells were sorted and transferred into CD45.1 *FoxP3*$^{IRES\text{-}GFP}$ WT hosts (replicates = 2, *n* = 1-2). dMLN was harvested and Tg cells stained intracellularly for Eomes expression. Eomes expression was quantified as a percentage of Tg cell populations, as

illustrated in representative FACs plots. Representative FACs plots are of Tg cells, distinguished by congenic markers, and gated on $CD4^{+}V\alpha2^{+}$.

Figure 3.4

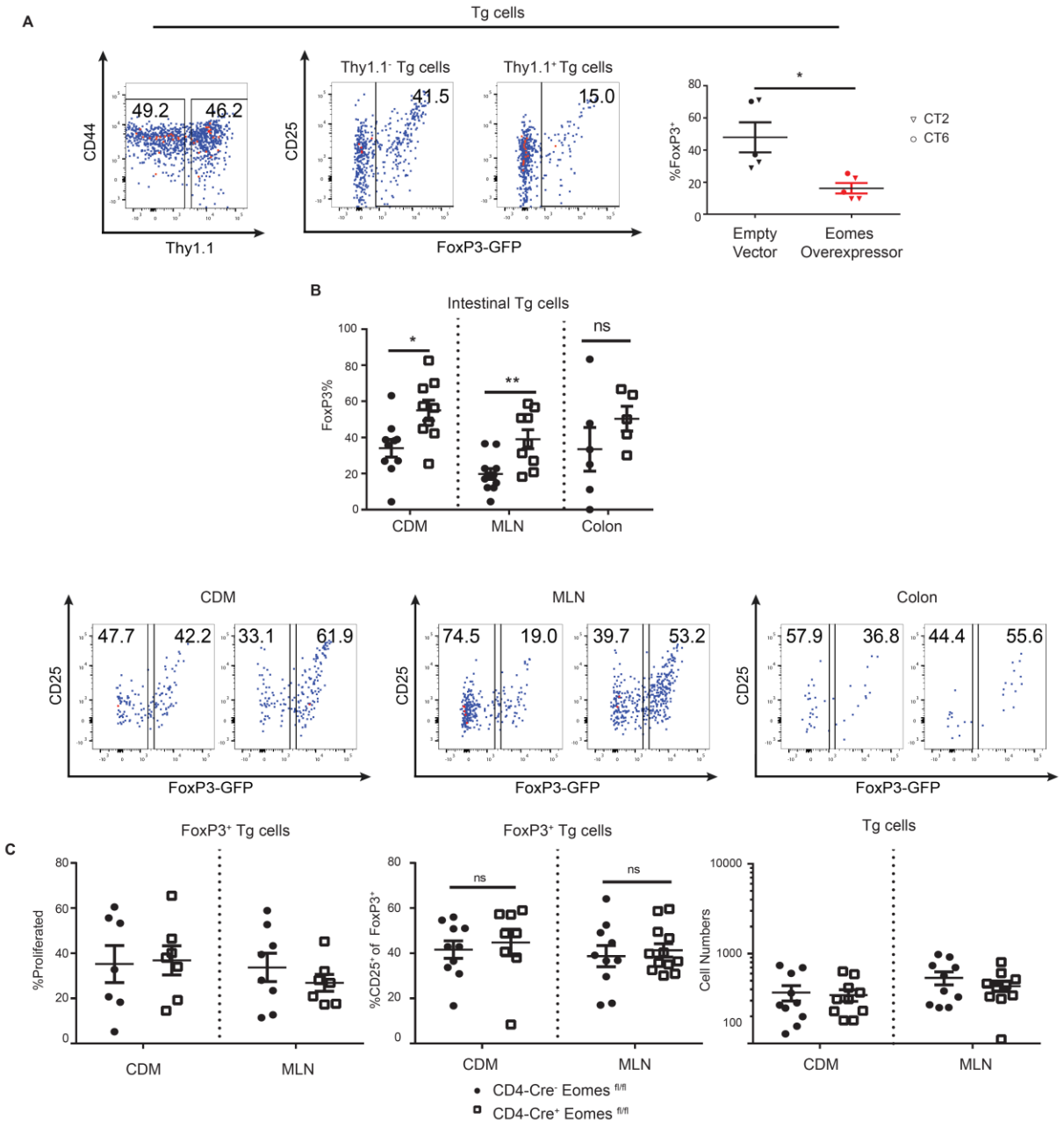

Figure 3.4: Eomes can restrain pTreg development against endogenously presented bacteria antigen. (A) CT6-*FoxP3*$^{\text{IRES-GFP}}$ or CT2-*FoxP3*$^{\text{IRES-GFP}}$ naïve Tg cells were sorted and activated in conditions that maintain Treg differentiation by Tg cells *in vivo* (see methods) for 27 hours before retroviral spinfection with an Eomes-Thy1.1 overexpression construct or an empty

Mig-Thy1.1 vector. Cells were retro-orbitally transferred ($3x10^5$ cells) into CD45.1 wild-type hosts immediately after spinfection Tg cells were analyzed via flow cytometry from the dMLN 1 week post transfer (replicates = 2, *n* = 2-3). Representative FACS plots of *FoxP3*$^{\text{IRES-GFP+}}$ percentages were gated on congenically marked $CD4^+V\alpha2^+Thy1.1^+$ cells. **(B)** CT6 CD4-Cre^+ *Eomes* $^{fl/fl}$ *FoxP3*$^{\text{IRES-GFP}}$ and CT6 CD4-Cre^- *Eomes* $^{fl/fl}$ *FoxP3*$^{\text{IRES-GFP}}$ naïve cells were sorted, labeled with Cell-Trace-Violet and transferred ($1x10^5$ cells) into wild-type hosts as described above (replicates = 2, *n* = 3-4). Shown are summary plots of *FoxP3*$^{\text{IRES-GFP}}$ expression, CD25 expression of Tg cells, and proliferated cells (2 or more cell divisions based on Cell-Trace Violet dilution) isolated from the dMLN node 1 week after transfer. Representative FACs plots are of *FoxP3*$^{\text{IRES-GFP}}$ expression. Cells were gated on congenically marked $CD4^+V\alpha2^+$ TCR Tg cells. Graphs are percentages of all Tg cells, *FoxP3*$^{\text{IRES-GFP+}}$ or *FoxP3*$^{\text{IRES-GFP-}}$ fractions of Tg cells. Statistical significance was calculated using Student T test, **P<0.05, ** P<0.005;* ns = not significant. Error bars = ±SEM.

Figure 3.5

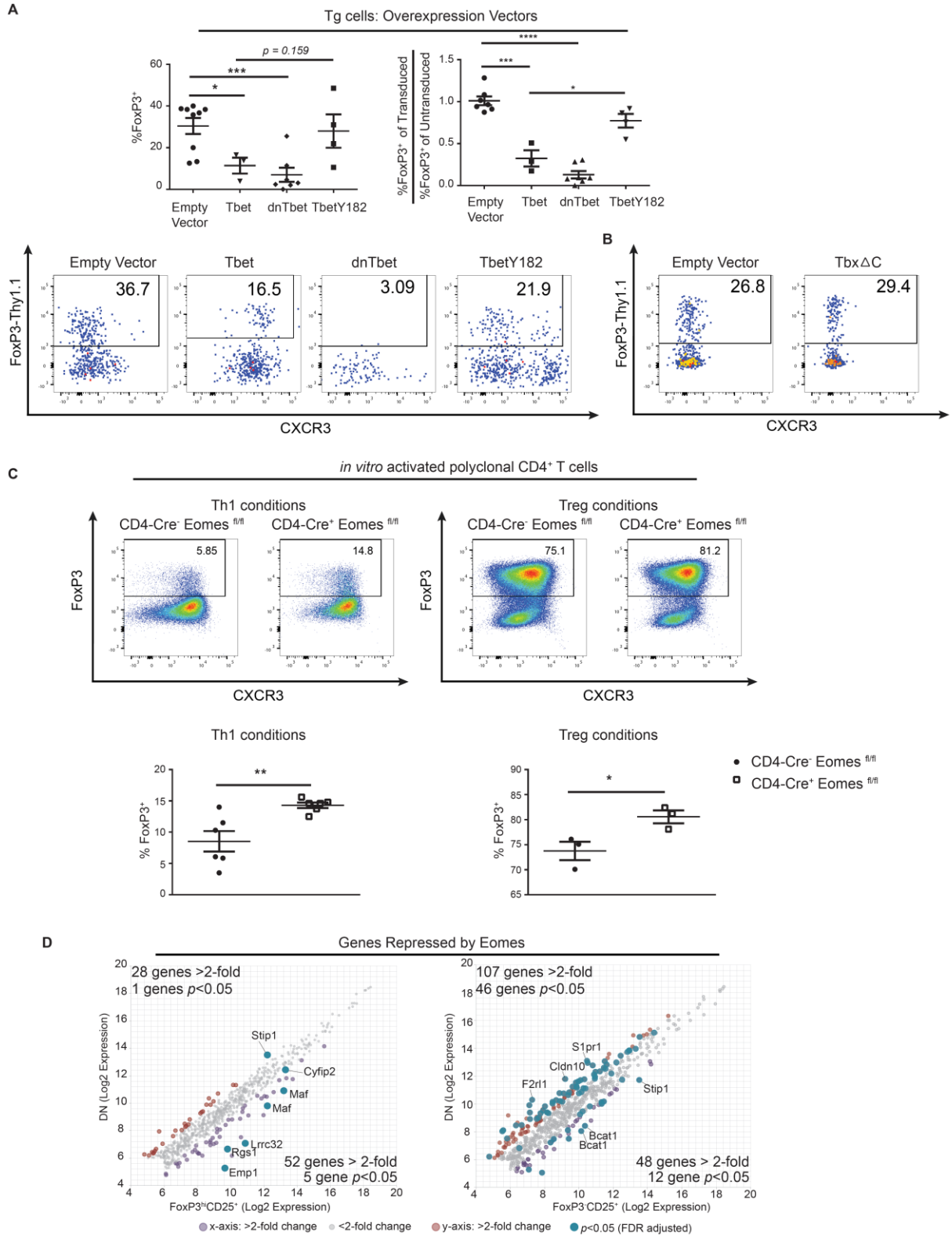
A
Tg cells: Overexpression Vectors
p = 0.159
%FoxP3+
Empty Vector
Tbet
dnTbet
TbetY182
%FoxP3+ of Transduced
%FoxP3+ of Untransduced
B
Empty Vector
Tbet
dnTbet
TbetY182
36.7
16.5
3.09
21.9
FoxP3-Thy1.1
CXCR3
Empty Vector
TbxΔC
26.8
29.4
C
in vitro activated polyclonal CD4+ T cells
Th1 conditions
Treg conditions
CD4-Cre- Eomes fl/fl
CD4-Cre+ Eomes fl/fl
5.85
14.8
75.1
81.2
FoxP3
CXCR3
% FoxP3+
D
Genes Repressed by Eomes
28 genes >2-fold
1 genes p<0.05
52 genes > 2-fold
5 gene p<0.05
107 genes >2-fold
46 genes p<0.05
48 genes > 2-fold
12 gene p<0.05
DN (Log2 Expression)
FoxP3hiCD25+ (Log2 Expression)
FoxP3-CD25+ (Log2 Expression)
Stip1
Cyfip2
Maf
Lrrc32
Rgs1
Emp1
S1pr1
Cldn10
F2rl1
Bcat1
x-axis: >2-fold change
<2-fold change
y-axis: >2-fold change
p<0.05 (FDR adjusted)

Figure 3.5: Eomes represses gene transcription through unique targets independently of Tbet. **(A-B)** CT6-*FoxP3*$^{\text{IRES-Thy1.1}}$ naïve Tg cells were sorted, *in vitro* activated, and retrovirally transduced with overexpression constructs on the Mig-GFP backbone as described in Figure 3.4 (replicates = 2-3, *n* = 2-3). Summary plots and representative FACs plots are of Tg cells isolated from the dMLN 1 week after transfer. *FoxP3*$^{\text{IRES-Thy1.1+}}$ percentages were gated on CD4^{+}Vα2^{+}GFP^{+} cells. The FoxP3 percentages used to determine the ratio of FoxP3 percentages in transduced and untransduced cells were derived from CD4^{+}Vα2^{+}GFP^{+} (transduced) or CD4^{+}Vα2^{+}GFP^{-} (untransduced) gates. A value of 1 indicates little difference in FoxP3% between the untransduced and transduced cell populations. **(C)** Polyclonal CD4-Cre^{+} *Eomes* $^{\text{fl/fl}}$ *FoxP3*$^{\text{IRES-GFP}}$ and CD4-Cre^{-} *Eomes* $^{\text{fl/fl}}$ *FoxP3*$^{\text{IRES-GFP}}$ naïve cells were sorted and activated in polarizing conditions (see methods). Cells were analyzed for *FoxP3*$^{\text{IRES-GFP}}$ expression after 3 days in culture. Summary plots and representative FACs plots are gated on CD4^{+} cells. Statistical significance was calculated using Student T test, **P<0.05, ** P<0.005, *** P ≤0.001, **** P≤0.0001*; Error bars = ±SEM. **(D)** Log2 expression values of transcription factors that are repressed by Eomes in FoxP3$^{\text{hi}}$CD25^{+} and FoxP3^{-}CD25^{+} cells relative to DN cells. Gene expression data generated as described in Figure 1. Blue dots indicate transcription factors whose expression are 2-fold or greater and reach statistical significance by FDR-adjusted student T test ($p<0.05$)

Figure 3.6

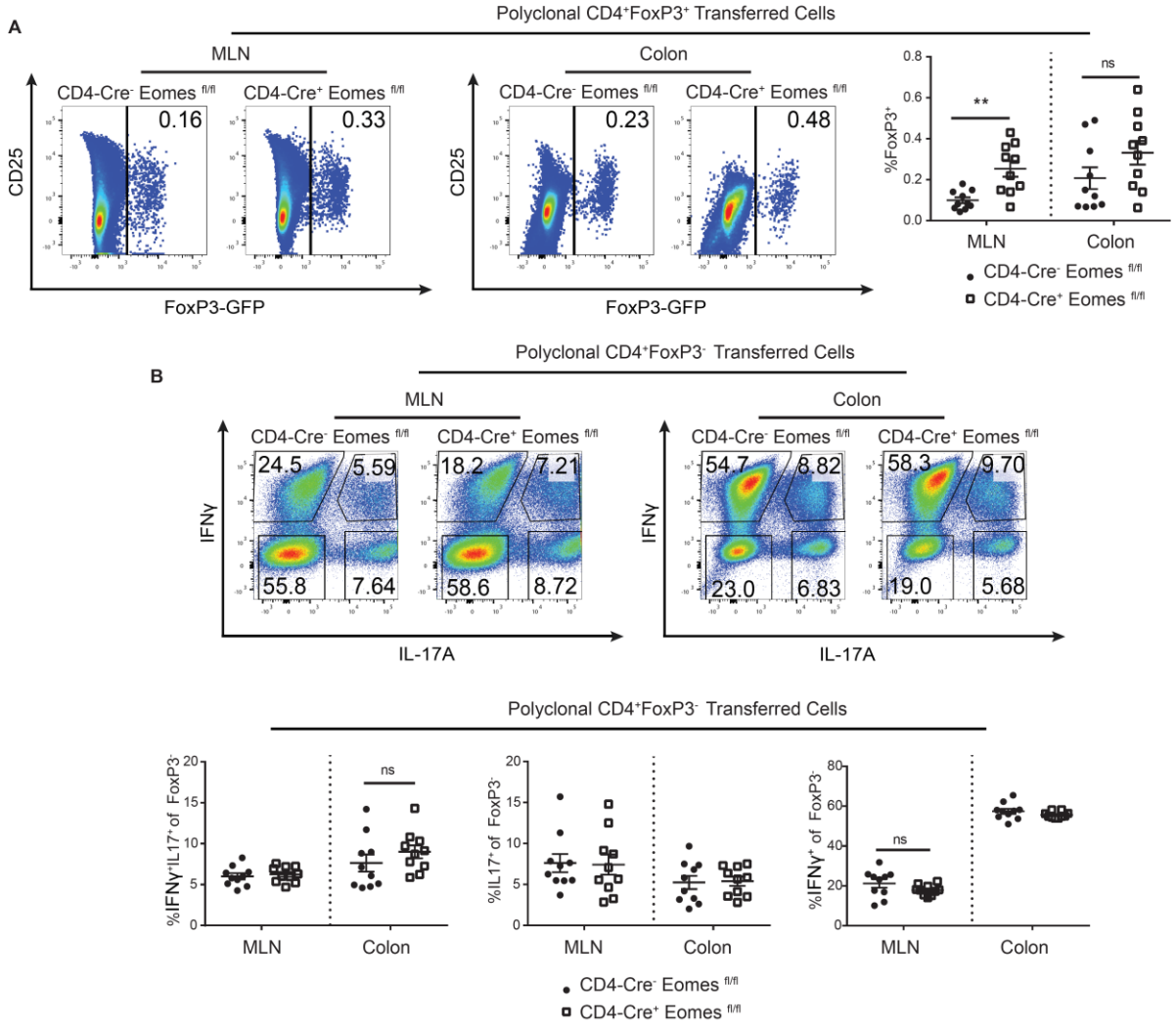

Figure 3.6: Eomes deficient cells sustain enhanced Treg differentiation in inflammatory contexts. (A-B) Polyclonal CD4-Cre^{+} *Eomes* $^{fl/fl}$ *FoxP3*$^{IRES\text{-}GFP}$ and CD4-Cre^{-} *Eomes* $^{fl/fl}$ *FoxP3*$^{IRES\text{-}GFP}$ naïve cells (CD45.2: CD4^{+}FoxP3^{-}CD44^{lo}CD62L^{hi}) and wild-type congenically marked Treg cells (CD45.1/2: CD4^{+}*FoxP3*$^{IRES\text{-}GFP+}$) were sorted. Either 2.5x10^{5} CD4-Cre^{+} *Eomes* $^{fl/fl}$ *FoxP3*$^{IRES\text{-}GFP}$ CD4-Cre^{-} *Eomes* $^{fl/fl}$ *FoxP3*$^{IRES\text{-}GFP}$ were mixed with 0.5x10^{5} Treg cells

and retro-orbitally transferred into $Rag^{-/-}$ hosts (replicates = 2, n = 5). MLN and colon were harvested at 18 days after transfer when mice lost 30% of their weight. $5x10^6$ cells were cultured with PMA, Ionomycin, brefeldin, and monensin for 3 hours before intracellular cytokine staining. Summary plots and representative FACs plots are gated on $CD4^+CD3^+CD45.2^+$ (sorted naïve cells) for *FoxP3*$^{IRES\text{-}GFP}$ analysis or $CD4^+CD3^+CD45.2^+$*FoxP3*$^{IRES\text{-}GFP\text{-}}$ for evaluation of IFNγ and IL-17A production. Statistical significance was calculated using Student T test, ** *P<0.005*, ns = not significant; Error bars = ±SEM.

Figure 3.7

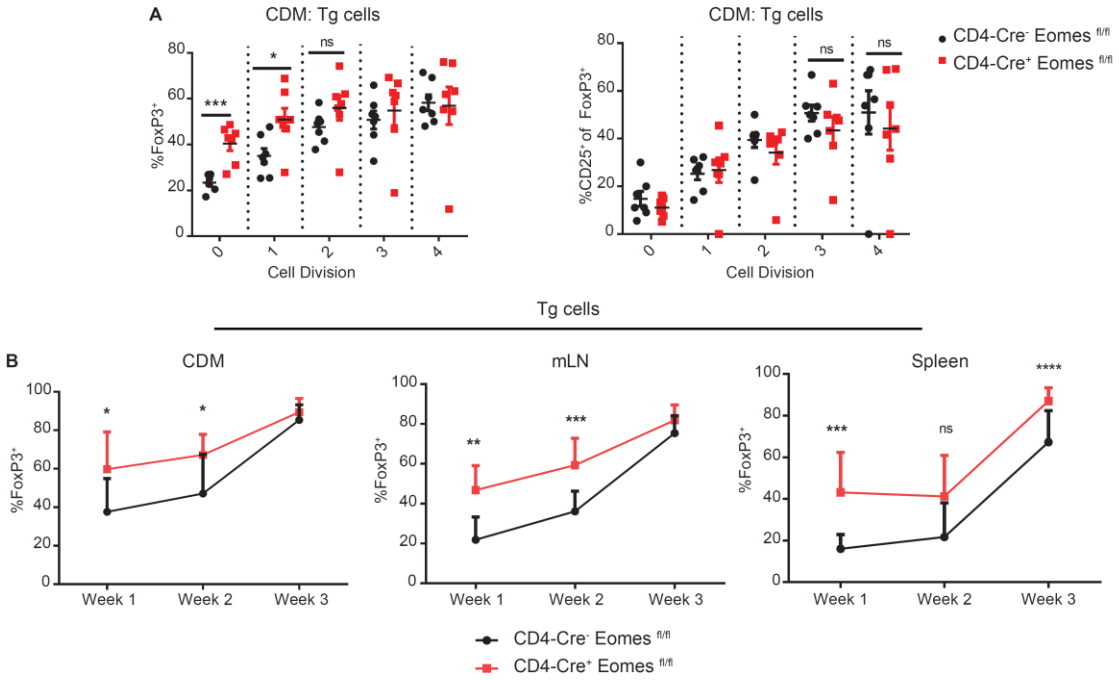

Figure 3.7: Eomes restrains peripheral Treg development by slowing the rate of FoxP3 expression. (A) CT6 CD4-Cre^{+} *Eomes* $^{fl/fl}$ *FoxP3*$^{IRES\text{-}GFP}$ and CT6 CD4-Cre^{-} *Eomes* $^{fl/fl}$ *FoxP3*$^{IRES\text{-}GFP}$ naïve cells were sorted, labeled with Cell-Trace-Violet and transferred (1x10^{5} cells) into wild-type hosts as described in Figure 4 (replicates = 2, *n* = 3-4). dMLN was harvested and Tg cells analyzed 1 week after transfer. Cells undergoing 0 divisions or 1-4 divisions were distinguished based on peaks of Cell-Trace-Violet dilution, with the first peak indicating cells that have not yet divided. *FoxP3*$^{IRES\text{-}GFP}$ and CD25^{+} percentages are based on congenically marked CD4^{+}Va2^{+} or CD4^{+}Va2^{+} *FoxP3*$^{IRES\text{-}GFP+}$ cells in populations of cells distinguished by their number of divisions. **(B)** CT6 CD4-Cre^{+} *Eomes* $^{fl/fl}$ *FoxP3*$^{IRES\text{-}GFP}$ and CT6 CD4-Cre^{-} *Eomes* $^{fl/fl}$ *FoxP3*$^{IRES\text{-}GFP}$ naïve cells were sorted and retro-orbitally transferred into wild-type hosts as

described above, with Tg cells analyzed from the dMLN, MLN, and Spleen (replicates = 3, *n* = 3-4). Representative control and experimental groups from littermate controls were analyzed at 1, 2, or 3 weeks post transfer. Statistical significance was calculated using Student T test, *$P<0.05$, ** $P<0.005$, *** $P \leq 0.001$, **** $P \leq 0.0001$, ns = not significant; Error bars = ±SEM.

Figure 3.8

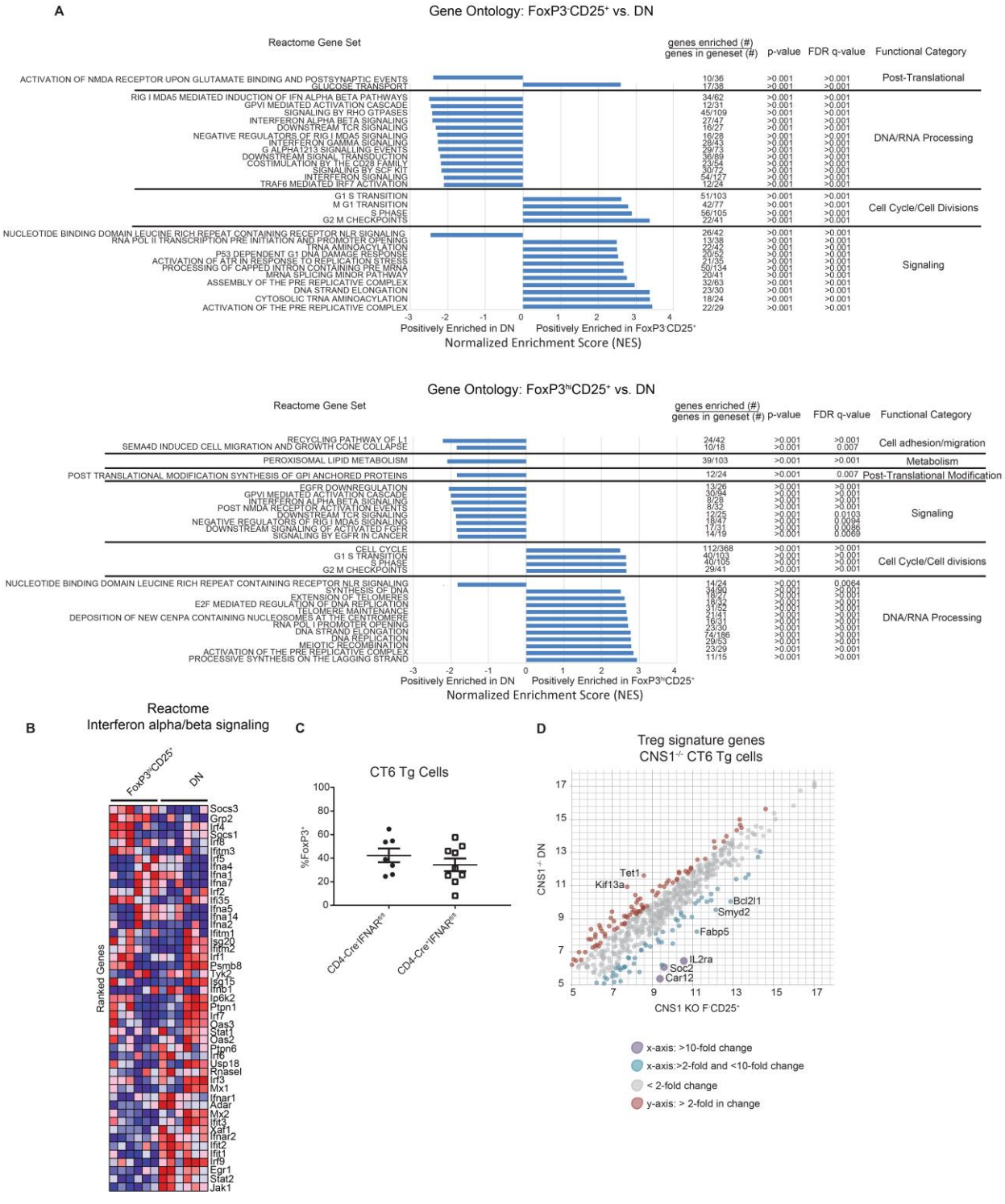
A
Gene Ontology: FoxP3⁻CD25⁺ vs. DN
Reactome Gene Set
genes enriched (#) genes in geneset (#)
p-value
FDR q-value
Functional Category
ACTIVATION OF NMDA RECEPTOR UPON GLUTAMATE BINDING AND POSTSYNAPTIC EVENTS 10/36 >0.001 >0.001 Post-Translational
GLUCOSE TRANSPORT 17/38 >0.001 >0.001
RIG I MDA5 MEDIATED INDUCTION OF IFN ALPHA BETA PATHWAYS 34/62 >0.001 >0.001
GPVI MEDIATED ACTIVATION CASCADE 12/31 >0.001 >0.001
SIGNALING BY RHO GTPASES 45/109 >0.001 >0.001
INTERFERON ALPHA BETA SIGNALING 27/47 >0.001 >0.001
DOWNSTREAM TCR SIGNALING 16/27 >0.001 >0.001
NEGATIVE REGULATORS OF RIG I MDA5 SIGNALING 18/28 >0.001 >0.001 DNA/RNA Processing
INTERFERON GAMMA SIGNALING 28/43 >0.001 >0.001
G ALPHA(12/13) SIGNALLING EVENTS 29/73 >0.001 >0.001
DOWNSTREAM SIGNAL TRANSDUCTION 36/89 >0.001 >0.001
COSTIMULATION BY THE CD28 FAMILY 23/64 >0.001 >0.001
SIGNALING BY SCF KIT 30/72 >0.001 >0.001
INTERFERON SIGNALING 54/127 >0.001 >0.001
TRAF6 MEDIATED IRF7 ACTIVATION 12/24 >0.001 >0.001
G1 S TRANSITION 51/103 >0.001 >0.001
M G1 TRANSITION 42/77 >0.001 >0.001 Cell Cycle/Cell Divisions
S PHASE 56/105 >0.001 >0.001
G2 M CHECKPOINTS 22/41 >0.001 >0.001
NUCLEOTIDE BINDING DOMAIN LEUCINE RICH REPEAT CONTAINING RECEPTOR NLR SIGNALING 26/42 >0.001 >0.001
RNA POL II TRANSCRIPTION PRE INITIATION AND PROMOTER OPENING 13/38 >0.001 >0.001
TRNA AMINOACYLATION 22/42 >0.001 >0.001
P53 DEPENDENT G1 DNA DAMAGE RESPONSE 20/52 >0.001 >0.001
ACTIVATION OF ATR IN RESPONSE TO REPLICATION STRESS 21/35 >0.001 >0.001 Signaling
PROCESSING OF CAPPED INTRON CONTAINING PRE MRNA 50/134 >0.001 >0.001
MRNA SPLICING MINOR PATHWAY 20/41 >0.001 >0.001
ASSEMBLY OF THE PRE REPLICATIVE COMPLEX 32/63 >0.001 >0.001
DNA STRAND ELONGATION 23/30 >0.001 >0.001
CYTOSOLIC TRNA AMINOACYLATION 18/24 >0.001 >0.001
ACTIVATION OF THE PRE REPLICATIVE COMPLEX 22/29 >0.001 >0.001
-3 -2 -1 0 1 2 3 4
Positively Enriched in DN
Positively Enriched in FoxP3⁻CD25⁺
Normalized Enrichment Score (NES)
Gene Ontology: FoxP3ʰⁱCD25⁺ vs. DN
Reactome Gene Set
genes enriched (#) genes in geneset (#)
p-value
FDR q-value
Functional Category
RECYCLING PATHWAY OF L1 24/42 >0.001 >0.001 Cell adhesion/migration
SEMA4D INDUCED CELL MIGRATION AND GROWTH CONE COLLAPSE 10/18 >0.001 0.007
PEROXISOMAL LIPID METABOLISM 39/103 >0.001 >0.001 Metabolism
POST TRANSLATIONAL MODIFICATION SYNTHESIS OF GPI ANCHORED PROTEINS 12/24 >0.001 0.007 Post-Translational Modification
EGFR DOWNREGULATION 13/26 >0.001 >0.001
GPVI MEDIATED ACTIVATION CASCADE 30/94 >0.001 >0.001
INTERFERON ALPHA BETA SIGNALING 8/28 >0.001 >0.001
POST NMDA RECEPTOR ACTIVATION EVENTS 8/32 >0.001 >0.001 Signaling
DOWNSTREAM TCR SIGNALING 12/25 >0.001 0.0103
NEGATIVE REGULATORS OF RIG I MDA5 SIGNALING 18/47 >0.001 0.0094
DOWNSTREAM SIGNALING OF ACTIVATED FGFR 17/31 >0.001 0.0086
SIGNALING BY EGFR IN CANCER 14/19 >0.001 0.0069
CELL CYCLE 112/368 >0.001 >0.001
G1 S TRANSITION 40/103 >0.001 >0.001 Cell Cycle/Cell divisions
S PHASE 40/105 >0.001 >0.001
G2 M CHECKPOINTS 29/41 >0.001 >0.001
NUCLEOTIDE BINDING DOMAIN LEUCINE RICH REPEAT CONTAINING RECEPTOR NLR SIGNALING 14/24 >0.001 0.0064
SYNTHESIS OF DNA 34/99 >0.001 >0.001
EXTENSION OF TELOMERES 18/41 >0.001 >0.001
E2F MEDIATED REGULATION OF DNA REPLICATION 19/32 >0.001 >0.001
TELOMERE MAINTENANCE 31/52 >0.001 >0.001
DEPOSITION OF NEW CENPA CONTAINING NUCLEOSOMES AT THE CENTROMERE 21/41 >0.001 >0.001 DNA/RNA Processing
RNA POL I PROMOTER OPENING 16/31 >0.001 >0.001
DNA STRAND ELONGATION 23/30 >0.001 >0.001
DNA REPLICATION 74/186 >0.001 >0.001
MEIOTIC RECOMBINATION 29/53 >0.001 >0.001
ACTIVATION OF THE PRE REPLICATIVE COMPLEX 23/29 >0.001 >0.001
PROCESSIVE SYNTHESIS ON THE LAGGING STRAND 11/15 >0.001 >0.001
-3 -2 -1 0 1 2 3 4
Positively Enriched in DN
Positively Enriched in FoxP3ʰⁱCD25⁺
Normalized Enrichment Score (NES)
B
Reactome
Interferon alpha/beta signaling
FoxP3ʰⁱCD25⁺
DN
Ranked Genes
Socs3
Grp2
Irf4
Socs1
Irf8
Ifitm3
Irf5
Ifna4
Ifna1
Ifna7
Irf2
Ifi35
Ifna5
Ifna14
Ifna2
Ifitm1
Isg20
Ifitm2
Irf1
Psmb8
Tyk2
Isg15
Jak2
Ifnb1
Ip6k2
Ptpn1
Irf7
Oas3
Stat1
Oas2
Ptpn6
Irf9
Usp18
Rnasel
Irf3
Mx1
Ifnar1
Adar
Mx2
Ifit3
Xaf1
Ifnar2
Ifit2
Ifit1
Irf9
Egr1
Stat2
Jak1
C
CT6 Tg Cells
%FoxP3⁺
100
80
60
40
20
0
CD4-Cre⁺IFNAR¹ᶠˡ/ᶠˡ
CD4-Cre⁺IFNAR¹ᶠˡ/ᶠˡ
D
Treg signature genes
CNS1⁻/⁻ CT6 Tg cells
CNS1⁻/⁻ DN
CNS1 KO F⁻CD25⁺
17
15
13
11
9
7
5
Tet1
Kif13a
Bcl2l1
Smyd2
Fabp5
IL2ra
Soc2
Car12
x-axis: >10-fold change
x-axis:>2-fold and <10-fold change
< 2-fold change
y-axis: > 2-fold in change

Figure 3.8: Gene set enrichment analysis of developing populations of monoclonal Tg cells. **(A-B)** GSEA analysis was performed on FoxP3^{-}CD25^{+}, DN, and FoxP3^{hi}CD25^{+} populations as described in Figure 3.2. **(B)** Heat map illustrates expression patterns of genes from Reactome's Interferon alpha/beta signaling dataset ranked by GSEA's default signal-to-noise metric. **(C)** CD45.2 CT6 CD4-Cre^{+}*IFNAR* $^{fl/fl}$ *FoxP3*$^{IRES\text{-}GFP}$ and CT6 CD4-Cre^{-} *IFNAR* $^{fl/fl}$ *FoxP3*$^{IRES\text{-}GFP}$ naïve cells were sorted and 1.5x10^{5} naïve cells (CD44^{lo}CD62L^{hi}) retro-orbitally injected into CD45.1 wild-type hosts. Tg cells were analyzed from dMLN 1 week after transfer. Summary plot of FoxP3 percentages gated on congenically marked CD4^{+}Va2^{+} cells. **(D)** CT6 *FoxP3*$^{IRES\text{-}GFP}$ CNS1$^{-/-}$ naïve Tg cells were sorted and transferred into 6-10 CD45.1 wild-type hosts. DN and FoxP3^{-}CD25^{+} fractions, as depicted in figure 1, were sorted and submitted for gene-chip hybridization as described in Figure 1 (replicate = 1, *n* = 3). Log2 fold values of Treg signature genes in the dataset are depicted. Purple dots signify genes that exhibited a 10-fold or more enrichment in the FoxP3^{-}CD25^{+} fraction of CNS1$^{-/-}$ Tg cells.

Figure 3.9

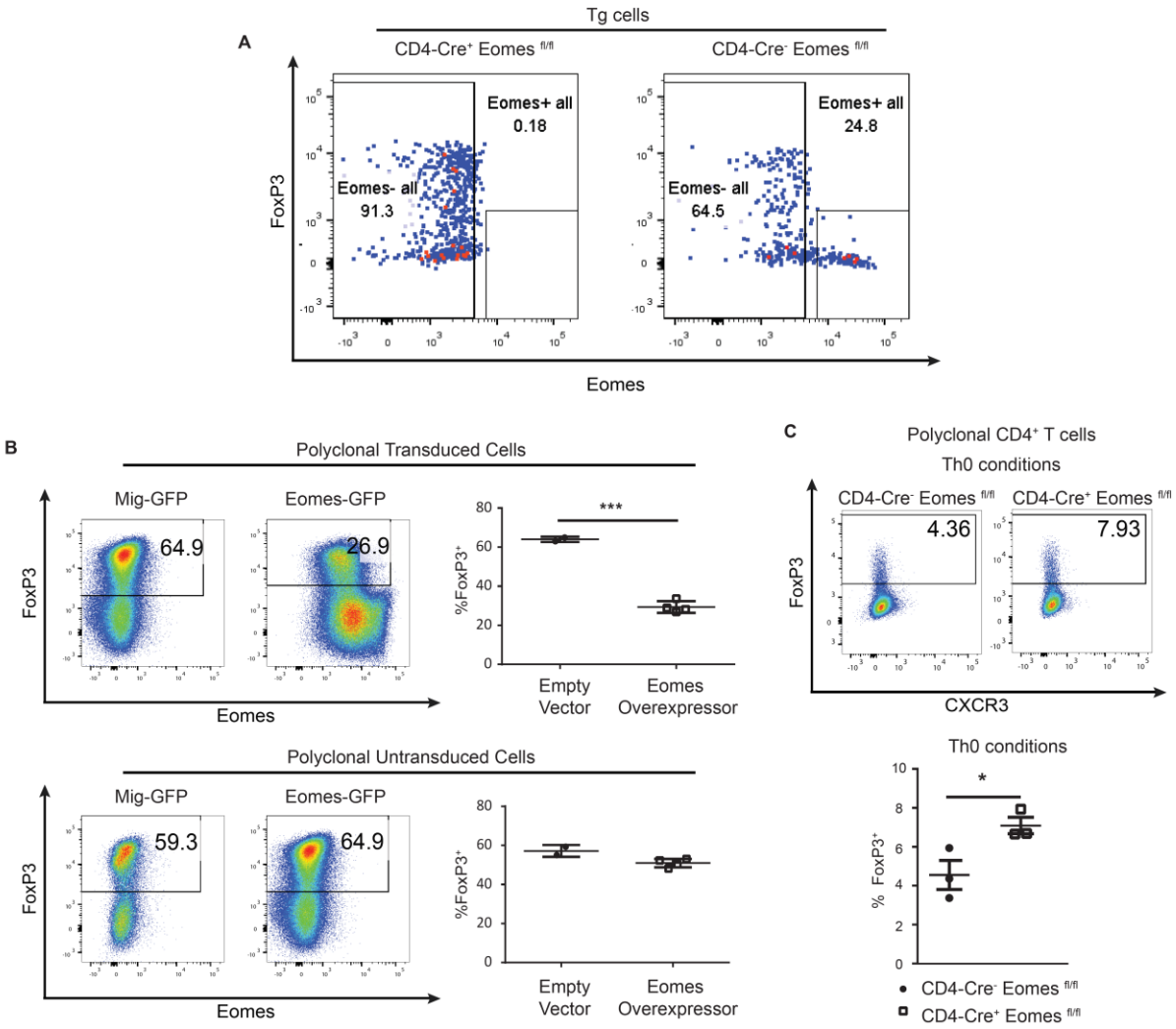

Figure 3.9: Eomes inhibition of FoxP3 is cell-intrinsic. (A) CT6 CD4-Cre^{+} *Eomes* $^{fl/fl}$ *FoxP3*$^{IRES\text{-}GFP}$ and CT6 CD4-Cre^{-} *Eomes* $^{fl/fl}$ *FoxP3*$^{IRES\text{-}GFP}$ naïve cells were sorted and transferred into congenically marked wild-type hosts. dMLNs were harvested 1 week after transferred and intra-cellularly stained for Eomes expression. **(B)** Polyclonal wild-type naïve cells (CD4^{+}FoxP3^{-} CD44^{lo}CD62L^{hi}) were sorted and activated in Th0 conditions (see methods). Cells were retrovirally spinfected with an Eomes-GFP overexpression construct or empty Mig-GFP construct, cultured for 3 days, and intracellularly stained for Eomes and FoxP3 (replicates = 2, *n*

= 1-2). Representative FACs plots and summary plots of FoxP3 percentages of the transduced and untransduced cells were either gated on $CD4^{+}GFP^{+}$ or $CD4^{+}GFP^{-}$ cells. **(C)** Polyclonal CD4-Cre^{+} *Eomes* $^{fl/fl}$ $FoxP3^{IRES\text{-}GFP}$ and CD4-Cre^{-} *Eomes* $^{fl/fl}$ $FoxP3^{IRES\text{-}GFP}$ naïve cells were sorted and activated in Th0 conditions (see method) and cultured for 3 days (replicates = 2, *n* = 1-2). $FoxP3^{IRES\text{-}GFP}$ percentages of summary and representative FACs plots were gated on $CD4^{+}$ cells. Statistical significance was calculated using Student T test, *$P<0.05$, ** $P<0.005$; Error bars = ±SEM.

Figure 3.10

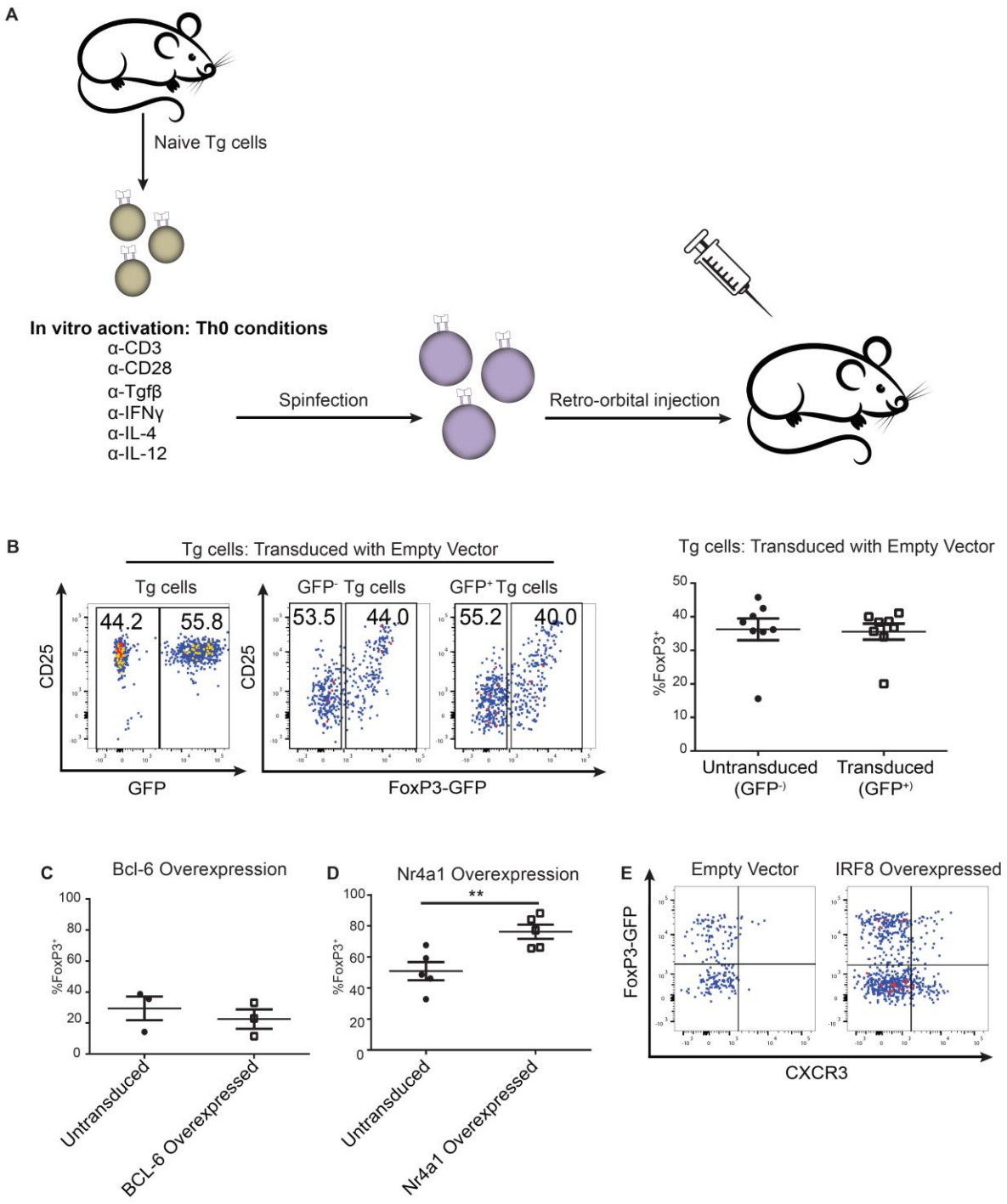
A
Naive Tg cells
In vitro activation: Th0 conditions
α-CD3
α-CD28
α-Tgfβ
α-IFNγ
α-IL-4
α-IL-12
Spinfection
Retro-orbital injection
B
Tg cells: Transduced with Empty Vector
Tg cells
GFP- Tg cells
GFP+ Tg cells
44.2
55.8
53.5
44.0
55.2
40.0
CD25
GFP
FoxP3-GFP
Tg cells: Transduced with Empty Vector
%FoxP3+
Untransduced (GFP-)
Transduced (GFP+)
C
Bcl-6 Overexpression
%FoxP3+
Untransduced
BCL-6 Overexpressed
D
Nr4a1 Overexpression
**
%FoxP3+
Untransduced
Nr4a1 Overexpressed
E
Empty Vector
IRF8 Overexpressed
FoxP3-GFP
CXCR3

Figure 3.10: Transcription factor overexpression in CT6 cells induces biologically relevant phenotypes. **(A)** Schematic of retroviral transduction protocol for analysis of overexpression constructs. **(A-E)** CT6-*FoxP3*$^{\text{IRES-Thy1.1}}$ naïve Tg cells were sorted, *in vitro* activated, and retrovirally transduced with overexpression constructs on the Mig-GFP backbone as described in Figure 4 (replicates = 2, *n* = 1-2). Summary plots and representative FACs plots are of Tg cells isolated from the dMLN 1 week after transfer. *FoxP3*$^{\text{IRES-Thy1.1+}}$ percentages were gated on $CD4^+V\alpha2^+GFP^+$ or $CD4^+V\alpha2^+GFP^-$ cells. Statistical significance was calculated using Student T test, ** *P<0.005;* Error bars = ±SEM. **(C)** FACs plot illustrating CXCR3 expression in Tg cells transduced with an IRF8 overexpression vector or an empty Mig-GFP vector (replicates = 1, *n* = 3). Cells were gated on $CD4^+V\alpha2^+GFP^+$.

Figure 3.11

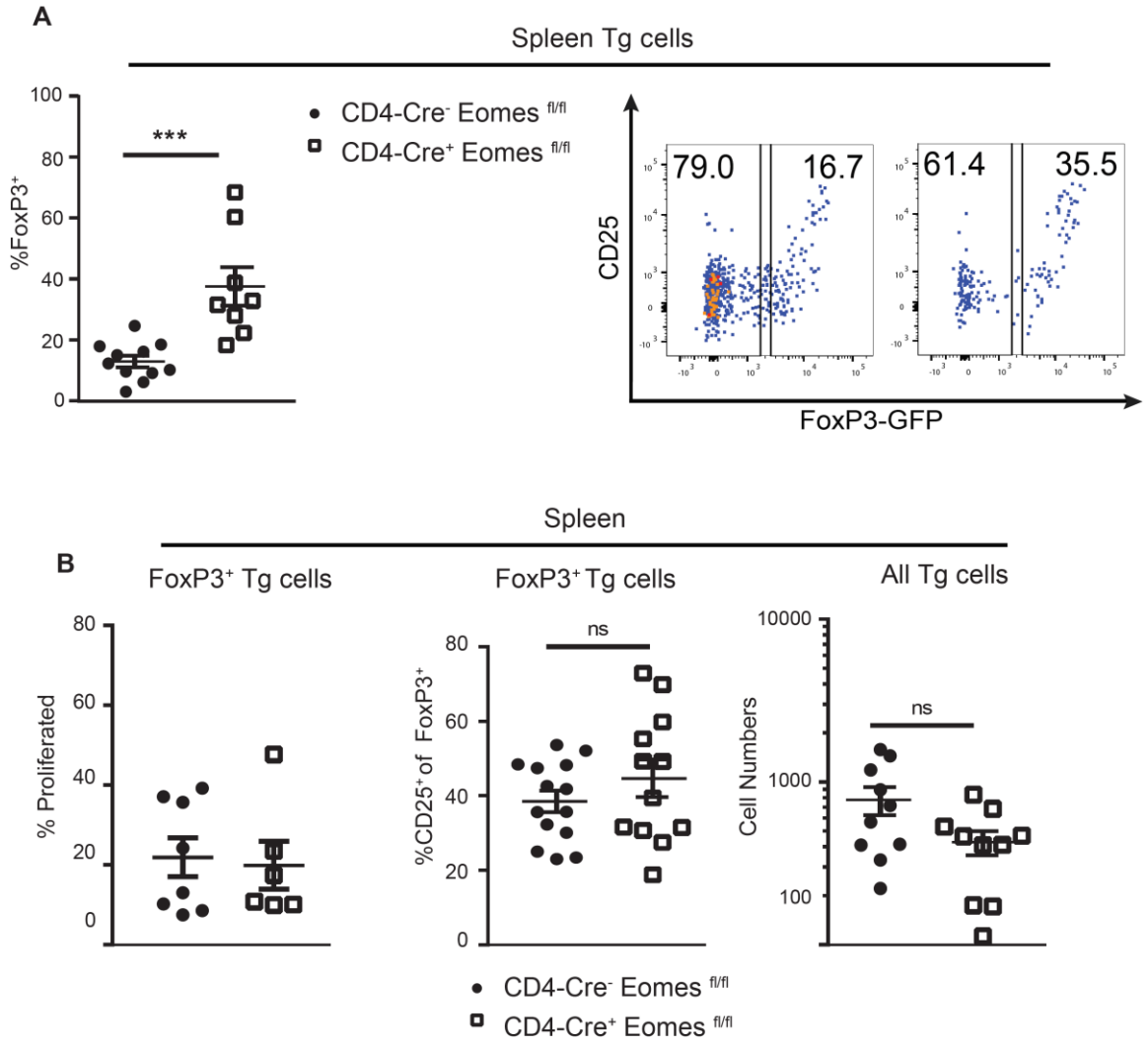

Figure 3.11: Eomes restraint of FoxP3 in CT6 cells extends to non-intestinal sites. (A-B) Spleen data are from experiments described in Figure 3.4. Shown are summary plots of *FoxP3*$^{\text{IRES-GFP}}$ expression, CD25 expression of Tg cells, and proliferated cells (2 or more cell divisions based on Cell-Trace Violet dilution) isolated from the spleen 1 week after transfer.

Representative FACs plots are of *FoxP3*$^{\text{IRES-GFP}}$ expression. Cells were gated on congenically marked CD4^{+}Vα2^{+} TCR Tg cells. Graphs are percentages of all Tg cells, *FoxP3*$^{\text{IRES-GFP+}}$ or *FoxP3*$^{\text{IRES-GFP-}}$ fractions of Tg cells. Statistical significance was calculated using Student T test *** $P \leq 0.001$, ns = not significant; Error bars = ±SEM.

Figure 3.12

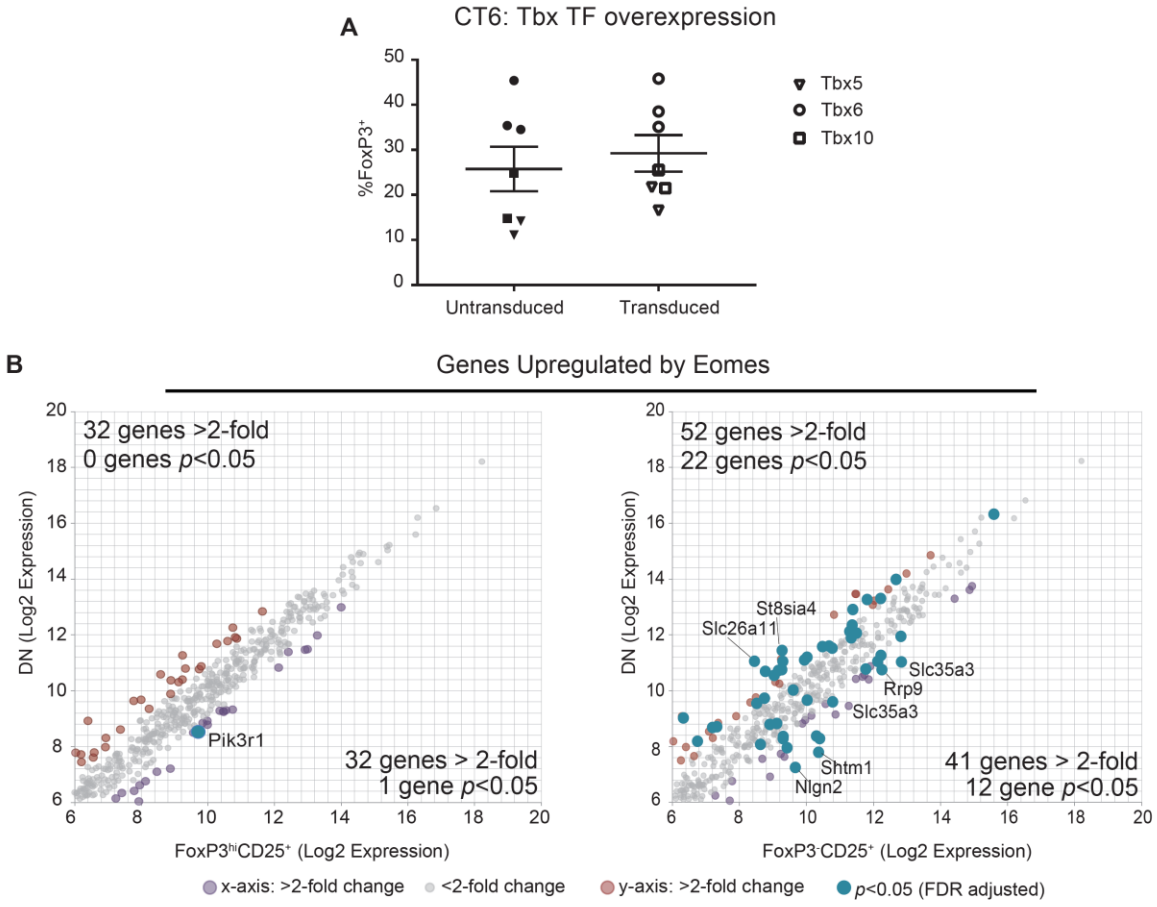

Figure 3.12: FoxP3 restraint by Eomes is not due to universal properties of the Tbx domain. (A) CT6-*FoxP3*$^{\text{IRES-GFP}}$ naïve Tg cells were sorted and Tbx constructs overexpressed as described in Figure 3.4 and Supplemental Figure 3 (replicates = 3, n = 2). Summary plots and representative FACs plots are of Tg cells isolated from the dMLN 1 week after transfer. *FoxP3*$^{\text{IRES-Thy1.1+}}$ percentages were gated on CD4^{+}Vα2^{+}GFP^{+} or CD4^{+}Vα2^{+}GFP^{-} cells. **(B)** Log2 fold change values in FoxP3^{-}CD25^{+}, FoxP3^{hi}CD25^{+}, and DN CT6 Tg cells of transcription factors activated by Eomes. Green dots denote genes that reached statistical significance based on Student T test (FDR adjusted P<0.05).

Figure 3.13

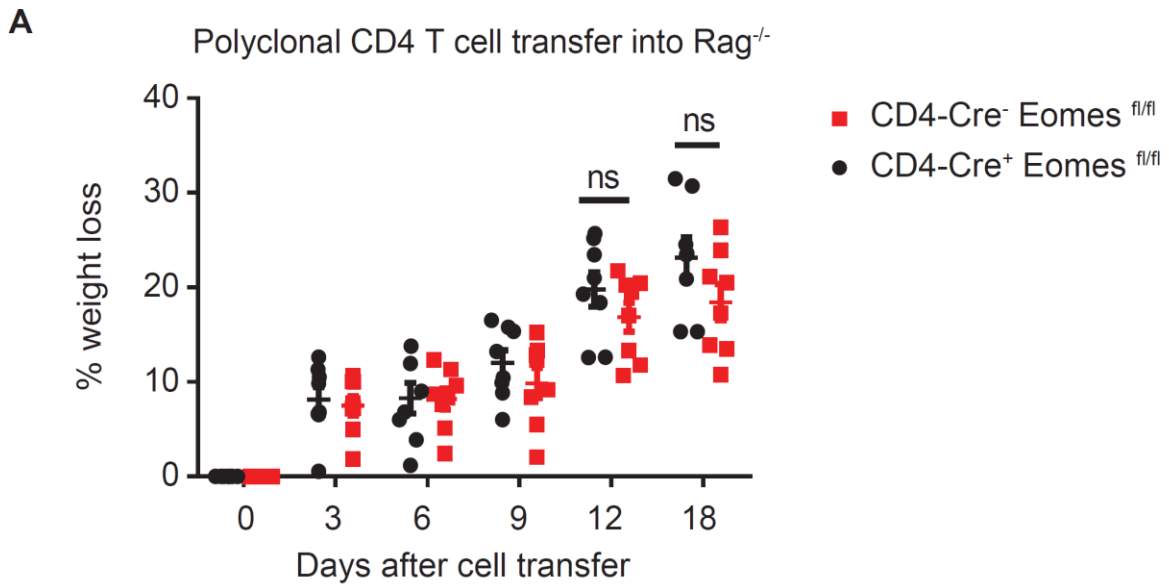

Figure 3.13: Eomes deficient polyclonal CD4$^+$ T cells induce disease less effectively than wild-type polyclonal T cells. (A) Weight loss of hosts for experiment depicted in Figure 3.6.

Figure 3.14

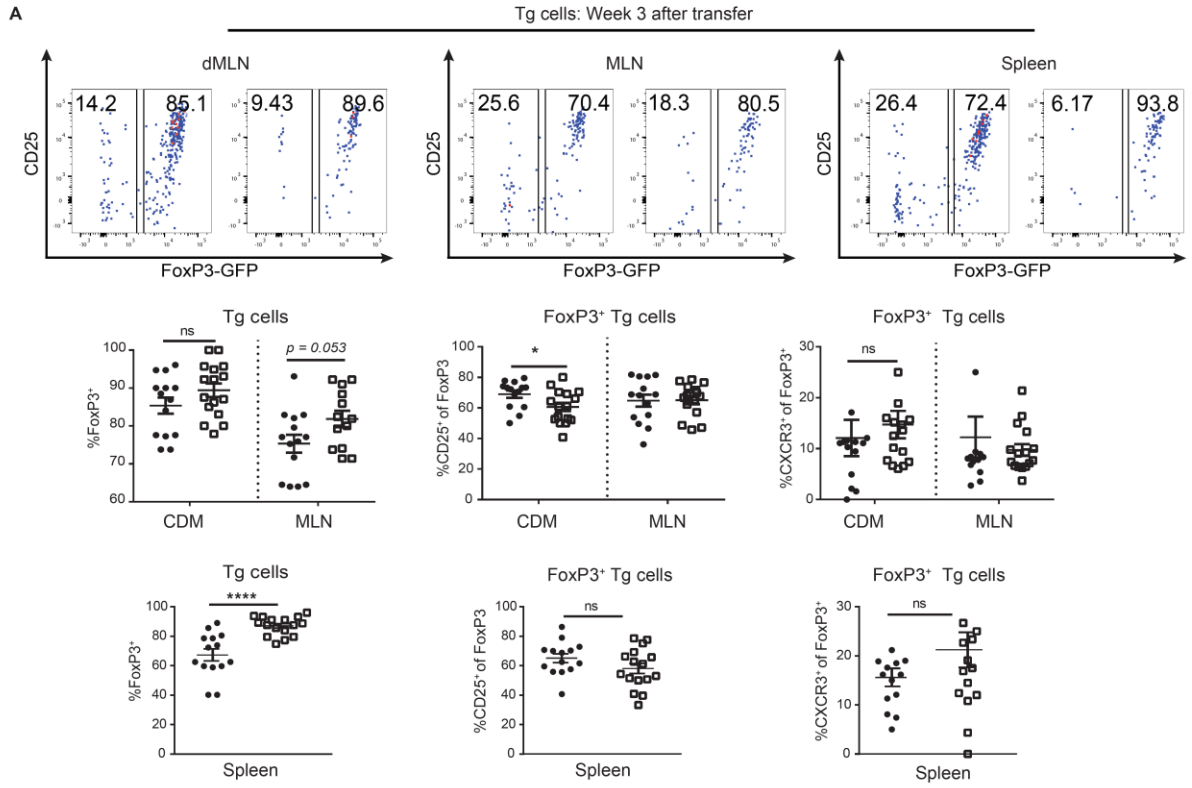

Figure 3.14: Eomes deficient monoclonal cells at later timepoints. (A) Representative summary and FACs plots of experiment performed in Figure 3.7B. Shown are summary plots of *FoxP3*$^{\text{IRES-GFP}}$ expression, CD25 expression of Tg cells, and CXCR3 expression isolated from the dMLN node 3 weeks after transfer. Representative FACs plots are of *FoxP3*$^{\text{IRES-GFP}}$ expression. Cells were gated on congenically marked CD4^{+}Vα2^{+} TCR Tg cells. Graphs are percentages of all Tg cells or *FoxP3*$^{\text{IRES-GFP+}}$ fractions of Tg cells. Statistical significance was calculated using Student T test, *$P<0.05$, ** $P<0.005$, *** $P \leq 0.001$, **** $P \leq 0.0001$; ns = not significant. Error bars = ±SEM.

Chapter 4: Conclusions and Future Directions

Part 1: pTreg development during intestinal inflammation

Environmental sources of inflammation have been correlated with increased incidence of intestinal diseases (172–174). A plausible hypothesis for this correlation is that intestinal insults impair tolerogenic responses that maintain gut homeostasis in the face of consistent insult by commensal, food, and self-antigen. Over time, sub-optimal tolerance mechanisms may no longer restrain heightened effector responses, resulting in aberrant immune responses to commensal antigens and the manifestation of intestinal diseases. It has been demonstrated that effector T cell responses can be generated against commensal bacteria during inflammation caused by *Toxoplasma gondii* and DSS mediated colitis, which generate Th1 and Th17 cells, respectively (133). However, the impact of inflammation on pTreg cells has remained relatively uninvestigated.

Treg cells are well-accepted to be critical for tolerance to self-antigens, and pTreg cells are emerging to serve a unique function for maintaining tolerance to commensal antigens along mucosal surfaces (13, 22, 175). Commensal bacteria actively induce the generation of pTreg cells, potentially as a mechanism to prevent effector responses, which would result in damage both to the host and the bacteria (13, 14, 18). Work in our laboratory demonstrated a proof of principle--developing pTreg cells, utilizing TCR Tg cells specific to *Helicobacter* antigen, can aberrantly differentiate into Th17 cells during extreme insult in the form of DSS and α-IL10R treatment (18). Thus, it is possible that inflammation, which elevates effector T cell responses in the gut, concurrently drives disease by diverting the commensal-specific pTreg cells into pro-inflammatory effector cells.

My thesis work evaluated whether this observation is universal or relevant in select contexts by evaluating multiple commonly used models of colitis and infections. Surprisingly, pTreg development against *Helicobacter* was largely resilient to a spectrum of intestinal inflammation, which included models driven by elevated innate immune responses and/or effector adaptive responses. Given that Th1, Th2, and Th17 cytokines can block FoxP3 expression *in vitro*, a digestible notion is that effector polarizing cytokines heightened in inflamed environments would overwhelm Treg signals and divert them to effector fates. Although the ability of effector cytokines to antagonize FoxP3 is not a point of debate, the observations from this study brings into question the *in vivo*, physiological relevance of these *in vitro* derived conclusions. Rather, the maintenance of pTreg generation against *Helicobacter* antigen during multiple different forms of inflammation suggests that pTreg development is largely sequestered from inflammatory cytokines elevated in gut tissue. Rather than being diverted to effector fates, the TCR Tg cells exhibited signs of impaired activation. Therefore, the environmental changes caused by intestinal infections may largely impair the strength and efficiency of pTreg development by modulating the levels of antigen presentation.

It is important to note that prior interrogation of effector cytokines' influence on *in vivo* pTreg development were done in polyclonal contexts or with OT-II transgenic cells that require the administration of exogenous OVA antigen (132). Polyclonal studies have provided insight on how Treg populations are affected by intestinal inflammation, including the expansion of Treg cells in experimental models of colitis (176), or the expression of genes that enhance their suppressive function during insult caused by Treg depletion (54, 55). However, these studies were unable to distinguish the effects of inflammation on pre-existing, mature Treg cells from the effects on developing, immature Treg cells. Additionally, studying pTreg cells generated by

OT-II cells encountering OVA antigen does not accurately address the question of how pTreg cells generated against homeostatically accessible antigen is affected by inflammation. This is a critical distinction to make, given that failure to develop tolerance to antigens that are readily accessible can lead to sustained immune responses and long-term damage. In contrast, exogenously introduced antigens are eventually cleared from the host and are likely to induce only a short-term immune response. Our lab's monoclonal approach against *Helicobacter* antigen circumvented these limitations and clarified that pTreg development against homeostatically accessible commensal antigen can persist during intestinal inflammation.

Given the comprehensive nature of this study, we were able to identify one model of intestinal inflammation that impaired pTreg development and identified key characteristics that distinguishes it from other models. In DSS and HFD, naïve CT2 and CT6 Tg cells responded differently, with CT2 Tg cells maintaining their Treg differentiation capabilities and CT6 Tg cells exhibiting reduced frequencies of FoxP3 expression. The phenotypes of CT2 and CT6 Tg cells were observed in the polyclonal Treg population based on TCR repertoire analysis, showing that the inflammatory environment caused by DSS and HFD does not globally inhibit pTreg development. It further supports our monoclonal observations— inflammation may impair pTreg selection by altering the delivery or presentation of antigens of different subsets of T cell clones. Both the mucosal and lumen bacterial communities in DSS and HFD treated mice contained a bloom of *Enterobacter* species and were generally more similar in bacteria composition than the mucosal and lumen in healthy mice. This was unique to DSS and HFD, suggesting that models that induce dramatic antigenic changes can render pTreg development vulnerable to disruption.

Future directions

Why certain pTreg TCR subsets, and not others, are affected by DSS and HFD remains a question that is not fully addressed. In this study, we present the possibility that differences are in part influenced by 1) T cell intrinsic factors, and 2) antigen-intrinsic factors. Specifically, 1) the degree of cross-reactivity of a TCR and 2) the availability of antigens for presentation to cross-reactive TCRs. TCR cross-reactivity is a double-edged sword, facilitating effective clearance of invading pathogens and tolerance, but may also lead to autoimmune responses and breaches in tolerance (177, 178). TCR cross reactivity in effector T cell populations ensures effective immune responses against invading pathogens by maximizing the chance for reactivity and preventing the pathogen from escaping through mutations (178). In the context of autoimmune diseases, effector TCRs are weakly reactive to many autoantigens, and can launch weak responses against antigens they cross-react with when Treg mediated suppression is impaired (178, 179). Lastly, viral infections with epitopes that are molecularly similar to self-antigen are thought to generate memory effector T cell responses that later react to self-antigen (177).

Although cross-reactivity of Treg TCRs has been less explored, Treg TCRs exhibit increased TCR diversity and display a broad range of affinities to antigen (35, 37, 180). These features support the notion that Treg TCR repertoires are broad and highly sensitive to self-antigens to maximize the effector responses they can suppress. Philosophically, it would be logical that cross-reactivity can heighten Treg TCR responses to self-antigen and promote tolerance against both self and bacteria antigen. CT6 Tg cells react to *Clostridium* antigen (21), and were more recently found to react robustly against *Helicobacte*r antigen (18), presumably due to higher affinity. We further found that CT6 Tg cells weakly react to *Enterobacter* antigen, opening up the possibility that CT6 Tg cells are reacting to *Enterobacter* antigen in non-Treg inducing environments. Notably, CT2 has not demonstrated any reactivity to other tested bacteria

antigen. *Enterobacter* antigen, but not *Helicobacter typhlonius* antigen, can compete with *Helicobacter apodemus* for TCR stimulation. This supports the theory that antigens can divert CT6 cells away from *Helicobacter apodemus* antigens and stimulate them in a non-Treg inducing environment. This parallels studies evaluating the relationship between viral and self-antigen—new antigens introduced during disease pathogenesis may drive aberrant T cell responses against homeostatically available self or non-self-antigens. Thus, TCR specificity may determine the outcome of pTreg development in part, due to the TCR's level of cross-reactivity to antigens introduced by the inflammatory model. However, studies validating TCR reactivity to multiple commensal bacteria needs to be established *in vivo* using peptides isolated from multiple bacteria species. It would also be interesting to investigate the properties of these peptides to determine if there are molecular features, common to certain antigens expressed by multiple species of bacteria, which promote their stimulation of adaptive immune responses.

CT2 and CT6 Tg cells are unique examples of T cell clones that adopt a single fate *in vivo*. Transduction of the CT2 and CT6 TCR into T cells transgenic for a TCR that does not recognize any endogenous mouse epitopes, is sufficient to direct the cells to develop into pTreg cells. However, the extent to which CT2 and CT6 Tg cells are representative of a polyclonal Treg population has not been thoroughly investigated. TCR repertoire analysis shows that Treg TCR populations have TCRs uniquely found in Treg repertoires, but also contain TCRs that overlap in effector TCR repertoires. Furthermore, libraries of Treg TCRs have not been thoroughly tested to understand if a majority of Treg TCRs can direct cells into Treg fates, or if their occurrence in the Treg population is in response to variables that are independent of the TCR. Determining the proportion of TCRs that direct predominantly Treg fates would be

valuable for elucidating why certain TCRs direct Treg fates, others TCRs multiple fates, and why some TCRs are more susceptible to the volatility caused by intestinal insult.

Lastly, the cumulative observations of CT2 and CT6 Tg cell differentiation in multiple inflammatory models demonstrates that there is focused sequestration of Treg and Teffector inducing signals in the environment of TCR:pMHC engagement. pTreg differentiation is largely preserved in inflamed tissues. In the case of a defect, the defect was limited to one TCR Tg clone. This suggests that firstly, there are remarkable protective mechanisms in place that cannot be perturbed even by severe intestinal insult and secondly, that there undefined mechanisms that ensure the separation of these signals. This is consistent with our findings that showed strong separation of effector and Treg TCR repertoires. In particular, Th1 and Treg repertoires were most distinct, which is consistent with the robust blockade of FoxP3 by Th1 cytokines. The evidence is suggestive that inflammatory cytokine signals caused by environmental insults alone is likely not sufficient to abrogate Treg mediated suppression. Thus, failures of Treg responses during inflammation are unlikely to be a factor that drives autoimmune disease, but may play a more nuanced role in modulating disease severity. The cellular and molecular mechanisms preserving the sequestration of effector and regulatory T cells would be interesting to clarify in order to 1) further our understanding of *in vivo* regulators of $CD4^+$ T cell differentiation and 2) how these processes are endangered by risk factors for autoimmune diseases.

Part 2: Transcriptional profiles early and late developing *in vivo* pTreg cells

Treg development is driven by a highly orchestrated process of inducing and suppressing the appropriate gene networks to drive the development of a tolerogenic phenotype. Transcriptional regulation of FoxP3 in particular, has been an intensely studied area. Epigenetic regions and numerous transcription factors facilitate Treg development by inducing FoxP3, antagonizing effector fates, or stabilizing FoxP3 expression (12, 103, 107, 108). Additionally, effector transcription factor expression can antagonize FoxP3 (47, 48, 143), although the precise mechanisms of blockade remain unknown. One of the challenges of investigating transcriptional networks is that transcription factors are pleiotropically expressed in multiple cell types. Thus, their interrogation is restricted to *in vitro* studies or *in vivo* studies using mouse models with conditional deletions.

In vitro studies have proven invaluable for deciphering molecular mechanisms, but are limited due to the exclusion of additional signals *in vivo* that may influence gene transcription. This is particularly relevant for Treg differentiation studies, given that the transcriptional profiles of Treg cells vary from tissue to tissue (159), supporting that Treg cells *in vivo* process signals other than Tgfβ. Conditional knockouts limit gene deficiencies to T cells or Treg cells. However, it remains difficult to exclude cell-extrinsic effects, given that deficiencies in the T cells themselves can have an impact on the environment which feeds back into transcriptional changes in the T cells themselves. Thus, assessing the transcriptional profiles of *in vivo* developing Treg cells is valuable for efforts to understand the *in vivo* relevance of identified transcriptional regulators and identify additional networks or factors that may modulate Treg differentiation.

My thesis work profiles the transcriptional landscape of monoclonal Tg cells that develop into pTreg cells in homeostatic conditions. Other monoclonal models of pTreg induction direct

cells to become both effector and Treg cells, including the OVA: OTII model of oral tolerance (132). CT6 Tg cells in contrast, become predominantly FoxP3$^+$ with percentages increasing over time of development (36). FoxP3$^-$ CT6 Tg cells do not exhibit signs of effector cytokine production in homeostatic conditions (36). Thus, the feasibility of isolating monoclonal populations of CT6 Tg cells provided a unique opportunity to capture pure, transcriptional snapshots of cells that are being activated in *in vivo* Treg differentiation conditions.

Monoclonal CT6 Tg cells underwent a burst of transcriptional activity prior to FoxP3 expression, consistent with the fact that T cells undergo significant morphological and metabolic changes as they are activated and clonally expand. Genes enriched in the early activated populations of Tg cells were positively enriched for Treg signature genes that can be amplified by FoxP3. This has been suggested by previous work, which found significant overlap between Treg signature genes and the activation profiles of both *in vivo* and *in vitro* activated CD4$^+$ T cells (109). These differentially expressed genes however, were significantly distinct from the Treg signature genes enriched in FoxP3$^+$ fractions of monoclonal cells. Therefore, a majority of the differentially expressed genes do not sustain their differential expression by FoxP3 upregulation. Speculatively, this could mean that that a majority of the genes are generalized to T cell activation and not Treg differentiation. Alternatively, it can also mean that a significant number of genes need to be repressed in order to allow for Treg differentiation to continue, consistent with studies that found FoxP3 to operate mainly as a gene repressor (111).

In our analysis, we did not observe the differential expression of genes reported to promote Treg development by suppressing effector fates. This brings into question the extent to which the function of these transcription factors are cell-intrinsic, and/or the relevance of their function for colon Treg cells *in vivo*. However, Nr4a family of transcription factors were

upregulated in early activated cells, but downregulated in FoxP3$^+$ cells. This supports published findings that Nr4a family of transcription factors are regulating the expression of FoxP3 by modulating transcriptional activity within the FoxP3 locus.

In early activated Tg cells, Eomes was the transcription factor whose expression levels was most notably enriched. Eomes can restrict FoxP3 in a cell-intrinsic fashion and serve clear effector function in CD8$^+$ T cells and NK cells by regulating IFNγ production. However, its role in CD4$^+$ cells has remained murky. It can negatively regulate effector cells by controlling IL-5 production by Th2 cells (181), and negatively regulates Th17 development (91), but can also enhance effector functions by cooperating with Tbet to amplify IFNγ production (126, 127). Thus, it is unclear what determines whether Eomes exerts both tolerance and effector promoting functions in CD4$^+$ T cells. In our study, Eomes was the transcription factor most highly enriched in early activated cells relative to FoxP3$^+$ Tg cells. We further validated that Eomes can impair the efficiency of FoxP3 upregulation by CT6 Tg cells, but is never co-expressed with FoxP3. Thus, we show that Eomes-mediated mechanisms for regulating FoxP3 are restricted to cells during early, and not late, developmental stages upon TCR engagement.

Interestingly, Eomes can be downregulated by Smad-independent Tgfβ signaling in CD4$^+$ T cells (91), promoting Th17 differentiation and development. Thus, it is possible that Eomes is universally upregulated in activated T cells upon TCR engagement, and differentiation signals modulate either its sustained expression or loss of expression. In the case of Treg cells, it is likely that Eomes is downregulated when Tgfβ signaling is initiated, ensuring the suppression of its FoxP3-repressive profile.

Future directions

Cumulatively, these findings clarify the *in vivo* relevance of transcriptional regulators FoxP3, including Eomes. The absence of transcription factors that antagonize effector T cell fates brings to light the possibility that these transcriptional regulators may need to be triggered, and are thus, absent in homeostatic conditions. Thus, it is interesting to question whether the early activated cells undergoing significant transcriptional changes have already committed to becoming FoxP3^{+} cells, or are adopting the proposed "Th0" state that remains pluripotent. If transcriptional regulators that antagonize alternative fates are indeed upregulated by effector signals to promote Treg differentiation, it could suggest that these early activated cells are primed to adopt Treg fates prior to FoxP3 induction. Epigenetic profiling of early activated cells would be valuable to assess the accessibility of Treg vs. effector genes in these FoxP3^{-} activated cells. Interrogating these questions would complement the observations in part 1 of this thesis, which observed resilience of Treg cells against inflammatory signals. It would be interesting to understand if cell-intrinsic mechanisms that preserve Treg differentiation during inflammation are contributing to the preservation of CT2, but not CT6 Tg differentiation during DSS and HFD.

References

1. Fontenot, J. D., M. A. Gavin, and A. Y. Rudensky. 2003. Foxp3 programs the development and function of CD4+CD25+ regulatory T cells. *Nat. Immunol.* 4: 330–336.

2. Gavin, M. A., J. P. Rasmussen, J. D. Fontenot, V. Vasta, V. C. Manganiello, J. A. Beavo, and A. Y. Rudensky. 2007. Foxp3-dependent programme of regulatory T-cell differentiation. *Nature* 445: 771–775.

3. Fontenot, J. D., J. P. Rasmussen, L. M. Williams, J. L. Dooley, A. G. Farr, and A. Y. Rudensky. 2005. Regulatory T Cell Lineage Specification by the Forkhead Transcription Factor Foxp3. *Immunity* 22: 329–341.

4. Lin, W., D. Haribhai, L. M. Relland, N. Truong, M. R. Carlson, C. B. Williams, and T. A. Chatila. 2007. Regulatory T cell development in the absence of functional Foxp3. *Nat. Immunol.* 8: 359–368.

5. Ramsdell, F., and S. F. Ziegler. 2014. FOXP3 and scurfy: how it all began. *Nat. Rev. Immunol.* 14: 343–349.

6. Zheng, Y., and A. Y. Rudensky. 2007. Foxp3 in control of the regulatory T cell lineage. *Nat. Immunol.* 8: 457–462.

7. RUSSELL, W. L. 1951. X-ray-induced mutations in mice. *Cold Spring Harb. Symp. Quant. Biol.* 16: 327–36.

8. Brunkow, M. E., E. W. Jeffery, K. A. Hjerrild, B. Paeper, L. B. Clark, S.-A. Yasayko, J. E. Wilkinson, D. Galas, S. F. Ziegler, and F. Ramsdell. 2001. Disruption of a new forkhead/winged-helix protein, scurfin, results in the fatal lymphoproliferative disorder of the scurfy mouse. *Nat. Genet.* 27: 68–73.

9. Ochs, H. D., C. L. Bennett, J. Christie, F. Ramsdell, M. E. Brunkow, P. J. Ferguson, L. Whitesell, T. E. Kelly, F. T. Saulsbury, and P. F. Chance. 2001. The immune dysregulation, polyendocrinopathy, enteropathy, X-linked syndrome (IPEX) is caused by mutations of *FOXP3*. *Nat. Genet.* 27: 20–21.

10. Powell, B. R., N. R. M. Buist, C. . F.R.C.P., and P. Stenzel. 1982. An X-linked syndrome of diarrhea, polyendocrinopathy, and fatal infection in infancy. *J. Pediatr.* 100: 731–737.

11. Kim, J. M., J. P. Rasmussen, and A. Y. Rudensky. 2007. Regulatory T cells prevent catastrophic autoimmunity throughout the lifespan of mice. *Nat. Immunol.* 8: 191–197.

12. Zheng, Y., S. Josefowicz, A. Chaudhry, X. P. Peng, K. Forbush, and A. Y. Rudensky. 2010. Role of conserved non-coding DNA elements in the Foxp3 gene in regulatory T-cell fate. *Nature* 463: 808–12.

13. Atarashi, K., T. Tanoue, T. Shima, A. Imaoka, T. Kuwahara, Y. Momose, G. Cheng, S. Yamasaki, T. Saito, Y. Ohba, T. Taniguchi, K. Takeda, S. Hori, I. I. Ivanov, Y. Umesaki, K. Itoh, and K. Honda. 2011. Induction of colonic regulatory T cells by indigenous Clostridium species. *Science* 331: 337–41.

14. Atarashi, K., T. Tanoue, K. Oshima, W. Suda, Y. Nagano, H. Nishikawa, S. Fukuda, T. Saito, S. Narushima, K. Hase, S. Kim, J. V Fritz, P. Wilmes, S. Ueha, K. Matsushima, H. Ohno, B. Olle, S. Sakaguchi, T. Taniguchi, H. Morita, M. Hattori, and K. Honda. 2013. Treg induction by a rationally selected mixture of Clostridia strains from the human microbiota. *Nature* 500: 232–6.

15. Smith, P. M., M. R. Howitt, N. Panikov, M. Michaud, C. A. Gallini, M. Bohlooly-Y, J. N. Glickman, and W. S. Garrett. 2013. The microbial metabolites, short-chain fatty acids, regulate colonic Treg cell homeostasis. *Science* 341: 569–73.

16. Arpaia, N., C. Campbell, X. Fan, S. Dikiy, J. van der Veeken, P. deRoos, H. Liu, J. R. Cross, K. Pfeffer, P. J. Coffer, and A. Y. Rudensky. 2013. Metabolites produced by commensal bacteria promote peripheral regulatory T-cell generation. *Nature* 504: 451–5.

17. Furusawa, Y., Y. Obata, S. Fukuda, T. a Endo, G. Nakato, D. Takahashi, Y. Nakanishi, C. Uetake, K. Kato, T. Kato, M. Takahashi, N. N. Fukuda, S. Murakami, E. Miyauchi, S. Hino, K. Atarashi, S. Onawa, Y. Fujimura, T. Lockett, J. M. Clarke, D. L. Topping, M. Tomita, S. Hori, O. Ohara, T. Morita, H. Koseki, J. Kikuchi, K. Honda, K. Hase, and H. Ohno. 2013. Commensal microbe-derived butyrate induces the differentiation of colonic regulatory T cells. *Nature* 504: 446–50.

18. Chai, J. N., Y. Peng, S. Rengarajan, B. D. Solomon, T. L. Ai, Z. Shen, J. S. A. Perry, K. A. Knoop, T. Tanoue, S. Narushima, K. Honda, C. O. Elson, R. D. Newberry, T. S. Stappenbeck, A. L. Kau, D. A. Peterson, J. G. Fox, and C.-S. Hsieh. 2017. Helicobacter species are potent drivers of colonic T cell responses in homeostasis and inflammation. *Sci. Immunol.* 2: eaal5068.

19. Round, J. L., S. M. Lee, J. Li, G. Tran, B. Jabri, T. a Chatila, and S. K. Mazmanian. 2011. The Toll-like receptor 2 pathway establishes colonization by a commensal of the human microbiota. *Science* 332: 974–7.

20. Round, J. L., and S. K. Mazmanian. 2010. Inducible Foxp3 + regulatory T-cell development by a commensal bacterium of the intestinal microbiota. 2010.

21. Lathrop, S. K., S. M. Bloom, S. M. Rao, K. Nutsch, C.-W. Lio, N. Santacruz, D. a Peterson, T. S. Stappenbeck, and C.-S. Hsieh. 2011. Peripheral education of the immune system by colonic commensal microbiota. *Nature* 478: 250–4.

22. Josefowicz, S. Z., R. E. Niec, H. Y. Kim, P. Treuting, T. Chinen, Y. Zheng, D. T. Umetsu, and A. Y. Rudensky. 2012. Extrathymically generated regulatory T cells control mucosal TH2 inflammation. *Nature* 482: 395–399.

23. Frank, D. N., and N. R. Pace. 2008. Gastrointestinal microbiology enters the metagenomics era. *Curr. Opin. Gastroenterol.* 24: 4–10.

24. Ley, R. E., M. Hamady, C. Lozupone, P. J. Turnbaugh, R. R. Ramey, J. S. Bircher, M. L. Schlegel, T. A. Tucker, M. D. Schrenzel, R. Knight, and J. I. Gordon. 2008. Evolution of Mammals and Their Gut Microbes. *Science (80-.).* 320: 1647–1651.

25. Round, J. L., and S. K. Mazmanian. 2009. The gut microbiota shapes intestinal immune responses during health and disease. *Nat. Rev. Immunol.* 9: 313–23.

26. Macpherson, A. J., and N. L. Harris. 2004. Opinion: Interactions between commensal

intestinal bacteria and the immune system. *Nat. Rev. Immunol.* 4: 478–485.

27. Ivanov, I. I., R. D. L. Frutos, N. Manel, K. Yoshinaga, D. B. Rifkin, R. B. Sartor, B. B. Finlay, and D. R. Littman. 2008. Specific microbiota direct the differentiation of IL-17-producing T-helper cells in the mucosa of the small intestine. *Cell Host Microbe* 4: 337–49.

28. Ivanov, I. I., K. Atarashi, N. Manel, E. L. Brodie, T. Shima, U. Karaoz, D. Wei, K. C. Goldfarb, C. a Santee, S. V Lynch, T. Tanoue, A. Imaoka, K. Itoh, K. Takeda, Y. Umesaki, K. Honda, and D. R. Littman. Induction of intestinal Th17 cells by segmented filamentous bacteria. *Cell* 139: 485–98.

29. Atarashi, K., T. Tanoue, M. Ando, N. Kamada, Y. Nagano, S. Narushima, W. Suda, A. Imaoka, H. Setoyama, T. Nagamori, E. Ishikawa, T. Shima, T. Hara, S. Kado, T. Jinnohara, H. Ohno, T. Kondo, K. Toyooka, E. Watanabe, S. Yokoyama, S. Tokoro, H. Mori, Y. Noguchi, H. Morita, I. I. Ivanov, T. Sugiyama, G. Nuñez, J. G. Camp, M. Hattori, Y. Umesaki, and K. Honda. 2015. Th17 Cell Induction by Adhesion of Microbes to Intestinal Epithelial Cells. *Cell* 163: 367–380.

30. Weaver, C. T., R. D. Hatton, P. R. Mangan, and L. E. Harrington. 2007. IL-17 Family Cytokines and the Expanding Diversity of Effector T Cell Lineages. *Annu. Rev. Immunol.* 25: 821–852.

31. Yang, Y., M. B. Torchinsky, M. Gobert, H. Xiong, M. Xu, J. L. Linehan, F. Alonzo, C. Ng, A. Chen, X. Lin, A. Sczesnak, J.-J. Liao, V. J. Torres, M. K. Jenkins, J. J. Lafaille, and D. R. Littman. 2014. Focused specificity of intestinal TH17 cells towards commensal bacterial antigens. *Nature* 510: 152–6.

32. Atarashi, K., W. Suda, C. Luo, T. Kawaguchi, I. Motoo, S. Narushima, Y. Kiguchi, K. Yasuma, E. Watanabe, T. Tanoue, C. A. Thaiss, M. Sato, K. Toyooka, H. S. Said, H. Yamagami, S. A. Rice, D. Gevers, R. C. Johnson, J. A. Segre, K. Chen, J. K. Kolls, E. Elinav, H. Morita, R. J. Xavier, M. Hattori, and K. Honda. 2017. Ectopic colonization of oral bacteria in the intestine drives TH1 cell induction and inflammation. *Science* 358: 359–365.

33. Cebula, A., M. Seweryn, G. A. Rempala, S. Pabla, R. A, McIndoe, T. L. Denning, L. Bry, P. Kraj, P. Kisielow, and L. Ignatowicz. 2013. Thymus-derived regulatory T cells contribute to tolerance to commensal microbiota. *Nature* 497: 258–262.

34. Kullberg, M. C., D. Jankovic, P. L. Gorelick, P. Caspar, J. J. Letterio, A. W. Cheever, and A. Sher. 2002. Bacteria-triggered CD4(+) T regulatory cells suppress Helicobacter hepaticus-induced colitis. *J. Exp. Med.* 196: 505–15.

35. Lathrop, S. K., N. A. Santacruz, D. Pham, J. Luo, and C.-S. Hsieh. 2008. Antigen-specific peripheral shaping of the natural regulatory T cell population. *J Exp Med.* 205: 3105–3117.

36. Nutsch, K., J. N. Chai, T. L. Ai, R.-G. Emilie, T. Feehley, C. R. Nagler, and C.-S. Hsieh. 2016. Rapid and Efficient Generation of Regulatory T Cells to Commensal Antigens in the Periphery. *Cell Rep.* 17: 206–220.

37. Solomon, B. D., and C.-S. Hsieh. 2016. Antigen-Specific Development of Mucosal Foxp3+RORγt+ T Cells from Regulatory T Cell Precursors. *J. Immunol.* 197: 3512–3519.

38. Honda, K., and D. R. Littman. 2016. The microbiota in adaptive immune homeostasis and

disease. 535: 75–84.

39. Round, J. L., S. M. Lee, J. Li, G. Tran, B. Jabri, T. A. Chatila, and S. K. Mazmanian. 2011. The Toll-like receptor 2 pathway establishes colonization by a commensal of the human microbiota. *Science* 332: 974–7.

40. Nikolich-Žugich, J., M. K. Slifka, and I. Messaoudi. 2004. The many important facets of T-cell repertoire diversity. *Nat. Rev. Immunol.* 4: 123–132.

41. Koh, W.-P., E. Chan, K. Scott, G. McCaughan, M. France, and B. Fazekas de St. Groth. 1999. TCR-Mediated Involvement of CD4+ Transgenic T cells in Spontaneous Inflammatory Bowel Disease in Lymphopenic Mice. *J Immunol* 162: 7208–7216.

42. Mizoguchi, A., E. Mizoguchi, L. J. Saubermann, K. Higaki, R. S. Blumberg, and A. K. Bhan. 2000. Limited CD4 T-cell diversity associated with colitis in T-cell receptor α mutant mice requires a T helper 2 environment. *Gastroenterology* 119: 983–995.

43. Föhse, L., J. Suffner, K. Suhre, B. Wahl, C. Lindner, C.-W. Lee, S. Schmitz, J. D. Haas, S. Lamprecht, C. Koenecke, A. Bleich, G. J. Hämmerling, B. Malissen, S. Suerbaum, R. Förster, and I. Prinz. 2011. High TCR diversity ensures optimal function andhomeostasis of Foxp3 $^{+}$ regulatory Tcells. *Eur. J. Immunol.* 41: 3101–3113.

44. Milner, J. D., J. M. Ward, A. Keane-Myers, and W. E. Paul. 2007. Lymphopenic mice reconstituted with limited repertoire T cells develop severe, multiorgan, Th2-associated inflammatory disease. *Proc. Natl. Acad. Sci. U. S. A.* 104: 576–81.

45. Samy, E. T., L. A. Parker, C. P. Sharp, and K. S. K. Tung. 2005. Continuous control of autoimmune disease by antigen-dependent polyclonal CD4+CD25+ regulatory T cells in the regional lymph node. *J. Exp. Med.* 202: 771–81.

46. Bonertz, A., J. Weitz, D. - Ho Kim Pietsch, and N. N. Rahbari. 2009. Antigen - specific Tregs control T cell responses against a limited repertoire of tumor antigens in patients with colorectal carcinoma. *J. Clin. Invest.* 119: 3311–3321.

47. Wei, J., O. Duramad, O. a Perng, S. L. Reiner, Y.-J. Liu, and F. X.-F. Qin. 2007. Antagonistic nature of T helper 1/2 developmental programs in opposing peripheral induction of Foxp3+ regulatory T cells. *Proc. Natl. Acad. Sci. U. S. A.* 104: 18169–18174.

48. Hadjur, S., L. Bruno, A. Hertweck, B. S. Cobb, B. Taylor, A. G. Fisher, and M. Merkenschlager. 2009. IL4 blockade of inducible regulatory T cell differentiation: The role of Th2 cells, Gata3 and PU.1. *Immunol. Lett.* 122: 37–43.

49. Ulloa, L., J. Doody, and J. Massagué. 1999. Inhibition of transforming growth factor-β/SMAD signalling by the interferon-γ/STAT pathway. *Nature* 397: 710–713.

50. Caretto, D., S. D. Katzman, A. V Villarino, E. Gallo, and A. K. Abbas. 2010. Cutting edge: the Th1 response inhibits the generation of peripheral regulatory T cells. *J. Immunol. {(Baltimore,} Md. 1950)* 184: 30–4.

51. Zhou, L., I. I. Ivanov, R. Spolski, R. Min, K. Shenderov, T. Egawa, D. E. Levy, W. J. Leonard, and D. R. Littman. 2007. IL-6 programs T H -17 cell differentiation by promoting sequential engagement of the IL-21 and IL-23 pathways. *Nat. Immunol.* 8.

52. Bailey-Bucktrout, S. L., M. Martinez-Llordella, X. Zhou, B. Anthony, W. Rosenthal, H. Luche, H. J. Fehling, and J. a Bluestone. 2013. Self-antigen-driven activation induces instability of regulatory T cells during an inflammatory autoimmune response. *Immunity* 39: 949–62.

53. Zhou, X., S. L, Bailey-Bucktrout, L. T. Jeker, C. Penaranda, M.-L. Marc, M. Ashby, M. Nakayama, W. Rosenthal, and J. a Bluestone. Instability of the transcription factor Foxp3 leads to the generation of pathogenic memory T cells in vivo. *Nat. Immunol.* 10: 1000–1007.

54. van der Veeken, J., A. J. Gonzalez, H. Cho, A. Arvey, S. Hemmers, C. S. Leslie, and A. Y. Rudensky. 2016. Memory of Inflammation in Regulatory T Cells. *Cell* 166: 977–990.

55. Arvey, A., J. van der Veeken, R. M. Samstein, Y. Feng, J. A. Stamatoyannopoulos, and A. Y. Rudensky. 2014. Inflammation-induced repression of chromatin bound by the transcription factor Foxp3 in regulatory T cells. *Nat. Immunol.* 15: 580–587.

56. Thompson, L. J., J.-F. Lai, A. C. Valladao, T. D. Thelen, Z. L. Urry, and S. F. Ziegler. 2016. Conditioning of naive CD4(+) T cells for enhanced peripheral Foxp3 induction by nonspecific bystander inflammation. *Nat. Immunol.* 17: 297–303.

57. Geem, D., V. Ngo, A. Harusato, B. Chassaing, A. T. Gewirtz, R. D. Newberry, and T. L. Denning. 2016. Contribution of Mesenteric Lymph Nodes and {GALT} to the Intestinal Foxp3+ Regulatory {T-Cell} Compartment. 2: 274–280.e3.

58. Crepin, V. F., J. W. Collins, M. Habibzay, and G. Frankel. 2016. Citrobacter rodentium mouse model of bacterial infection. *Nat. Protoc.* 11: 1851–1876.

59. Zheng, Y., P. A. Valdez, D. M. Danilenko, Y. Hu, S. M. Sa, Q. Gong, A. R. Abbas, Z. Modrusan, N. Ghilardi, F. J. de Sauvage, and W. Ouyang. 2008. Interleukin-22 mediates early host defense against attaching and effacing bacterial pathogens. *Nat. Med.* 14: 282–289.

60. Shiomi, H., A. Masuda, S. Nishiumi, M. Nishida, T. Takagawa, Y. Shiomi, H. Kutsumi, R. S. Blumberg, T. Azuma, and M. Yoshida. 2010. Gamma interferon produced by antigen-specific CD4+ T cells regulates the mucosal immune responses to Citrobacter rodentium infection. *Infect. Immun.* 78: 2653–66.

61. Collins, J. W., K. M. Keeney, V. F. Crepin, V. a K. Rathinam, K. a Fitzgerald, B. B. Finlay, and G. Frankel. 2014. Citrobacter rodentium: infection, inflammation and the microbiota. *Nat. Rev. Microbiol.* 12: 612–623.

62. Zheng, Y., P. A. Valdez, D. M. Danilenko, Y. Hu, S. M. Sa, Q. Gong, A. R. Abbas, Z. Modrusan, N. Ghilardi, F. J. de Sauvage, and W. Ouyang. 2008. Interleukin-22 mediates early host defense against attaching and effacing bacterial pathogens. 14: 282–289.

63. Bry, L., M. Brigl, and M. B. Brenner. 2006. CD4+-T-cell effector functions and costimulatory requirements essential for surviving mucosal infection with Citrobacter rodentium. *Infect. Immun.* 74: 673–81.

64. Grashoff, C., B. D. Hoffman, M. D. Brenner, R. Zhou, M. Parsons, M. T. Yang, M. a McLean, S. G. Sligar, C. S. Chen, T. Ha, and M. a Schwartz. 2010. Measuring mechanical tension across vinculin reveals regulation of focal adhesion dynamics. *Nature* 466: 263–6.

65. Bry, L., and M. B. Brenner. 2004. Critical Role of T Cell-Dependent Serum Critical Role of

T Cell-Dependent Serum Antibody, but Not the Gut-Associated Lymphoid Tissue, for Surviving Acute Mucosal Infection with Citrobacter rodentium, an Attaching and Effacing Pathogen. *J Immunol J. Immunol-ogy* 172: 433–441.

66. Denkers, E. Y., and R. T. Gazzinelli. 1998. Regulation and function of T-cell-mediated immunity during Toxoplasma gondii infection. *Clin. Microbiol. Rev.* 11: 569–88.

67. Mordue, D. G., F. Monroy, M. La Regina, C. A. Dinarello, and L. D. Sibley. 2001. Acute Toxoplasmosis Leads to Lethal Overproduction of Th1 Cytokines. *J. Immunol.* 167: 4574–4584.

68. Gazzinelli, R. T., M. Wysocka, S. Hieny, T. Scharton-Kersten, A. Cheever, R. Kühn, W. Müller, G. Trinchieri, and A. Sher. 1996. In the absence of endogenous IL-10, mice acutely infected with Toxoplasma gondii succumb to a lethal immune response dependent on CD4+ T cells and accompanied by overproduction of IL-12, IFN-gamma and TNF-alpha. *J. Immunol.* 157: 798–805.

69. Yap, G., M. Pesin, and A. Sher. 2000. Toxoplasma gondii Intracellular Pathogen, Mediating Chronic Resistance to the Production in T Cells γ Maintenance of IFN- Cutting Edge: IL-12 Is Required for the Cutting Edge: IL-12 Is Required for the Maintenance of IFN- Production in T Cells Mediating Chronic Resistance to the Intracellular Pathogen, Toxoplasma gondii. *J Immunol* 165: 628–631.

70. Solomon, L., S. Mansor, P. Mallon, E. Donnelly, M. Hoper, M. Loughrey, S. Kirk, and K. Gardiner. 2010. The dextran sulphate sodium (DSS) model of colitis: an overview. *Comp. Clin. Path.* 19: 235–239.

71. Araki, Y., K. Mukaisyo, H. Sugihara, Y. Fujiyama, and T. Hattorie. 2010. Increased apoptosis and decreased proliferation of colonic epithelium in dextran sulfate sodium-induced colitis in mice YOSHIO. *Oncol. Rep.* 24: 869–874.

72. Wirtz, S., C. Neufert, B. Weigmann, and M. F. Neurath. 2007. Chemically induced mouse models of intestinal inflammation. *Nat. Protoc.* 2: 541–546.

73. Dieleman, Palmen, Akol, Bloemena, PENA, Meuwissen, and Van Rees. 1998. Chronic experimental colitis induced by dextran sulphate sodium (DSS) is characterized by Th1 and Th2 cytokines. *Clin. Exp. Immunol.* 114: 385–391.

74. Kim, K.-A., W. Gu, I.-A. Lee, E.-H. Joh, and D.-H. Kim. 2012. High Fat Diet-Induced Gut Microbiota Exacerbates Inflammation and Obesity in Mice via the TLR4 Signaling Pathway. *PLoS One* 7: e47713.

75. Ding, S., M. M. Chi, B. P. Scull, R. Rigby, N. M. J. Schwerbrock, S. Magness, C. Jobin, and P. K. Lund. 2010. High-Fat Diet: Bacteria Interactions Promote Intestinal Inflammation Which Precedes and Correlates with Obesity and Insulin Resistance in Mouse. *PLoS One* 5: e12191.

76. Park, E. J., J. H. Lee, G.-Y. Yu, G. He, S. R. Ali, R. G. Holzer, C. H. Österreicher, H. Takahashi, and M. Karin. 2010. Dietary and Genetic Obesity Promote Liver Inflammation and Tumorigenesis by Enhancing IL-6 and TNF Expression. *Cell* 140: 197–208.

77. Moreira, A. P. B., T. F. S. Texeira, A. B. Ferreira, M. do Carmo Gouveia Peluzio, and R. de Cássia Gonçalves Alfenas. 2012. Influence of a high-fat diet on gut microbiota, intestinal permeability and metabolic endotoxaemia. *Br. J. Nutr.* 108: 801–809.

78. Miele, L., V. Valenza, G. La Torre, M. Montalto, G. Cammarota, R. Ricci, R. Mascianà, A. Forgione, M. L. Gabrieli, G. Perotti, F. M. Vecchio, G. Rapaccini, G. Gasbarrini, C. P. Day, and A. Grieco. 2009. Increased intestinal permeability and tight junction alterations in nonalcoholic fatty liver disease. *Hepatology* 49: 1877–1887.

79. Schulz, M. D., Ç. Atay, J. Heringer, F. K. Romrig, S. Schwitalla, B. Aydin, P. K. Ziegler, J. Varga, W. Reindl, C. Pommerenke, G. Salinas-Riester, A. Böck, C. Alpert, M. Blaut, S. C. Polson, L. Brandl, T. Kirchner, F. R. Greten, S. W. Polson, and M. C. Arkan. 2014. High-fat-diet-mediated dysbiosis promotes intestinal carcinogenesis independently of obesity. *Nature* 514: 508–512.

80. Godfrey, V. L., J. E. Wilkinson, E. M. Rinchik, and L. B. Russell. 1991. Fatal lymphoreticular disease in the scurfy (sf) mouse requires T cells that mature in a sf thymic environment: potential model for thymic education. *Proc. Natl. Acad. Sci. U. S. A.* 88: 5528–32.

81. Hori, S., T. Nomura, and S. Sakaguchi. 2003. Control of Regulatory T cell Development by the Transcription Factor FoxP3. *Science* 299: 1057–1061.

82. Wan, Y. Y., and R. A. Flavell. 2005. Identifying Foxp3-expressing suppressor T cells with a bicistronic reporter. *Proc. Natl. Acad. Sci. U. S. A.* 102: 5126–31.

83. Kuczma, M., R. Podolsky, N. Garge, D. Daniely, R. Pacholczyk, L. Ignatowicz, and P. Kraj. 2009. Foxp3-deficient regulatory T cells do not revert into conventional effector CD4+ T cells but constitute a unique cell subset. *J. Immunol.* 183: 3731–41.

84. Zhang, Y. E. 2009. Non-Smad pathways in TGF-β signaling. *Cell Res.* 19: 128–139.

85. Chen, W., W. Jin, N. Hardegen, K.-J. Lei, L. Li, N. Marinos, G. McGrady, and S. M. Wahl. 2003. Conversion of peripheral CD4+CD25- naive T cells to CD4+CD25+ regulatory T cells by TGF-beta induction of transcription factor Foxp3. *J. Exp. Med.* 198: 1875–86.

86. Gu, A.-D., Y. Wang, L. Lin, S. S. Zhang, and Y. Y. Wan. 2012. Requirements of transcription factor Smad-dependent and -independent TGF-β signaling to control discrete T-cell functions. *Proc. Natl. Acad. Sci. U. S. A.* 109: 905–10.

87. Lu, L.-F., M. P. Boldin, A. Chaudhry, L.-L. Lin, K. D. Taganov, T. Hanada, A. Yoshimura, D. Baltimore, and A. Y. Rudensky. Function of {miR-146a} in controlling Treg cell-mediated regulation of Th1 responses. *Cell* 142: 914–29.

88. Delisle, J.-S., M. Giroux, G. Boucher, J.-R. Landry, M.-P. Hardy, S. Lemieux, R. G. Jones, B. T. Wilhelm, and C. Perreault. 2013. The TGF-β-Smad3 pathway inhibits CD28-dependent cell growth and proliferation of CD4 T cells. *Genes Immun.* 14: 115–126.

89. Takimoto, T., Y. Wakabayashi, T. Sekiya, N. Inoue, R. Morita, K. Ichiyama, R. Takahashi, M. Asakawa, G. Muto, T. Mori, E. Hasegawa, S. Saika, S. Shizuya, T. Hara, M. Nomura, and A. Yoshimura. 2010. Smad2 and Smad3 are redundantly essential for the TGF-beta-mediated regulation of regulatory T plasticity and Th1 development. *J. Immunol.* 185: 842–55.

90. Lu, L., J. Wang, F. Zhang, Y. Chai, D. Brand, X. Wang, D. a Horwitz, W. Shi, and S. G. Zheng. 2010. Role of SMAD and non-SMAD signals in the development of Th17 and regulatory T cells. *J. Immunol.* 184: 4295–306.

91. Ichiyama, K., T. Sekiya, N. Inoue, T. Tamiya, I. Kashiwagi, A. Kimura, R. Morita, G. Muto, T. Shichita, R. Takahashi, and A. Yoshimura. 2011. Transcription factor Smad-independent T helper 17 cell induction by transforming-growth factor-β is mediated by suppression of eomesodermin. *Immunity* 34: 741–54.

92. Hill, J. A., J. A. Hall, C.-M. Sun, Q. Cai, N. Ghyselinck, P. Chambon, Y. Belkaid, D. Mathis, and C. Benoist. 2008. Retinoic acid enhances Foxp3 induction indirectly by relieving inhibition from CD4+CD44hi Cells. *Immunity* 29: 758–70.

93. Coombes, J. L., K. R. R. Siddiqui, C. V Arancibia-Cárcamo, J. Hall, C.-M. Sun, Y. Belkaid, and F. Powrie. 2007. A functionally specialized population of mucosal CD103+ DCs induces Foxp3+ regulatory T cells via a TGF-beta and retinoic acid-dependent mechanism. *J. Exp. Med.* 204: 1757–64.

94. Elias, K. M., A. Laurence, T. S. Davidson, G. Stephens, Y. Kanno, E. M. Shevach, and J. J. O'Shea. 2008. Retinoic acid inhibits Th17 polarization and enhances FoxP3 expression through a Stat-3/Stat-5 independent signaling pathway. *Blood* 111: 1013–20.

95. Mucida, D., Y. Park, G. Kim, O. Turovskaya, I. Scott, M. Kronenberg, and H. Cheroutre. 2007. Reciprocal TH17 and regulatory T cell differentiation mediated by retinoic acid. *Science* 317: 256–60.

96. Xiao, S., H. Jin, T. Korn, S. M. Liu, M. Oukka, B. Lim, and V. K. Kuchroo. 2008. Retinoic acid increases Foxp3+ regulatory T cells and inhibits development of Th17 cells by enhancing TGF-beta-driven Smad3 signaling and inhibiting IL-6 and IL-23 receptor expression. *J. Immunol.* 181: 2277–84.

97. Quintana, F. J., A. S. Basso, A. H. Iglesias, T. Korn, M. F. Farez, E. Bettelli, M. Caccamo, M. Oukka, and H. L. Weiner. 2008. Control of Treg and TH17 cell differentiation by the aryl hydrocarbon receptor. *Nature* 453: 65–71.

98. Mezrich, J. D., J. H. Fechner, X. Zhang, B. P. Johnson, W. J. Burlingham, and C. A. Bradfield. 2010. An interaction between kynurenine and the aryl hydrocarbon receptor can generate regulatory T cells. *J. Immunol.* 185: 3190–8.

99. Murphy, K. A., C. M. Villano, R. Dorn, and L. A. White. 2004. Interaction between the aryl hydrocarbon receptor and retinoic acid pathways increases matrix metalloproteinase-1 expression in keratinocytes. *J. Biol. Chem.* 279: 25284–93.

100. Arpaia, N., C. Campbell, X. Fan, S. Dikiy, J. van der Veeken, P. deRoos, H. Liu, J. R. Cross, K. Pfeffer, P. J. Coffer, and A. Y. Rudensky. 2013. Metabolites produced by commensal bacteria promote peripheral regulatory T-cell generation. *Nature* 504: 451–455.

101. Waldecker, M., T. Kautenburger, H. Daumann, C. Busch, and D. Schrenk. 2008. Inhibition of histone-deacetylase activity by short-chain fatty acids and some polyphenol metabolites formed in the colon. *J. Nutr. Biochem.* 19: 587–593.

102. Sekiya, T., I. Kashiwagi, N. Inoue, R. Morita, S. Hori, H. Waldmann, A. Y. Rudensky, H. Ichinose, D. Metzger, P. Chambon, and A. Yoshimura. 2011. The nuclear orphan receptor Nr4a2 induces Foxp3 and regulates differentiation of {CD4+} T cells. 2: 269.

103. Bandukwala, H. S., and A. Rao. 2013. "Nurr"ishing Treg cells: Nr4a transcription factors

control Foxp3 expression. *Nat. Immunol.* 14: 201–203.

104. Sekiya, T., I. Kashiwagi, R. Yoshida, T. Fukaya, R. Morita, A. Kimura, H. Ichinose, D. Metzger, P. Chambon, and A. Yoshimura. 2013. Nr4a receptors are essential for thymic regulatory T cell development and immune homeostasis. *Nat. Immunol.* 14: 230–237.

105. Fassett, M. S., W. Jiang, A. M. D'Alise, D. Mathis, and C. Benoist. 2012. Nuclear receptor Nr4a1 modulates both regulatory T-cell (Treg) differentiation and clonal deletion. *Proc. Natl. Acad. Sci. U. S. A.* 109: 3891–6.

106. Sekiya, T., I. Kashiwagi, N. Inoue, R. Morita, S. Hori, H. Waldmann, A. Y. Rudensky, H. Ichinose, D. Metzger, P. Chambon, and A. Yoshimura. 2011. The nuclear orphan receptor Nr4a2 induces Foxp3 and regulates differentiation of CD4+ T cells. *Nat. Commun.* 2: 269.

107. Wu, C., Z. Chen, V. Dardalhon, S. Xiao, T. Thalhamer, M. Liao, A. Madi, R. F. Franca, T. Han, M. Oukka, and V. Kuchroo. 2017. The transcription factor musculin promotes the unidirectional development of peripheral Treg cells by suppressing the TH2 transcriptional program. *Nat. Immunol.* 18: 344–353.

108. Clever, D., R. Roychoudhuri, M. G. Constantinides, M. H. Askenase, M. Sukumar, C. A. Klebanoff, R. L. Eil, H. D. Hickman, Z. Yu, J. H. Pan, D. C. Palmer, A. T. Phan, J. Goulding, L. Gattinoni, A. W. Goldrath, Y. Belkaid, and N. P. Restifo. 2016. Oxygen Sensing by T Cells Establishes an Immunologically Tolerant Metastatic Niche. *Cell* 166: 1117–1131.e14.

109. Hill, J. A., M. Feuerer, K. Tash, S. Haxhinasto, J. Perez, R. Melamed, D. Mathis, and C. Benoist. 2007. Foxp3 Transcription-Factor-Dependent and -Independent Regulation of the Regulatory T Cell Transcriptional Signature. *Immunity* 27: 786–800.

110. Oh, S. A., M. Liu, B. G. Nixon, D. Kang, A. Toure, M. Bivona, and M. O. Li. 2017. Foxp3-independent mechanism by which TGF-β controls peripheral T cell tolerance. *Proc. Natl. Acad. Sci. U. S. A.* 114: E7536–E7544.

111. Zheng, Y., S. Z. Josefowicz, A. Kas, T.-T. Chu, M. A. Gavin, and A. Y. Rudensky. 2007. Genome-wide analysis of Foxp3 target genes in developing and mature regulatory T cells. *Nature* 445: 936–940.

112. Probst, S., and S. J. Arnold. 2017. Eomesodermin—At Dawn of Cell Fate Decisions During Early Embryogenesis. *Curr. Top. Dev. Biol.* 122: 93–115.

113. Teo, A. K. K., S. J. Arnold, M. W. B. Trotter, S. Brown, L. T. Ang, Z. Chng, E. J. Robertson, N. R. Dunn, and L. Vallier. 2011. Pluripotency factors regulate definitive endoderm specification through eomesodermin. *Genes Dev.* 25: 238–50.

114. Kidder, B. L., and S. Palmer. 2010. Examination of transcriptional networks reveals an important role for TCFAP2C, SMARCA4, and EOMES in trophoblast stem cell maintenance. *Genome Res.* 20: 458–72.

115. Szabo, S. J., S. T. Kim, G. L. Costa, X. Zhang, C. G. Fathman, and L. H. Glimcher. 2000. A Novel Transcription Factor, T-bet, Directs Th1 Lineage Commitment. *Cell* 100: 655–669.

116. Daussy, C., F. Faure, K. Mayol, S. Viel, G. Gasteiger, E. Charrier, J. Bienvenu, T. Henry, E. Debien, U. a Hasan, J. Marvel, K. Yoh, S. Takahashi, I. Prinz, S. de Bernard, L. Buffat, and T.

Walzer. 2014. T-bet and Eomes instruct the development of two distinct natural killer cell lineages in the liver and in the bone marrow. *J. Exp. Med.* 211: 563–77.

117. Pearce, E. L. 2003. Control of Effector CD8+ T Cell Function by the Transcription Factor Eomesodermin. *Science (80-.).* 302: 1041–1043.

118. Ichiyama, K., T. Sekiya, N. Inoue, T. Tamiya, I. Kashiwagi, A. Kimura, R. Morita, G. Muto, T. Shichita, R. Takahashi, and A. Yoshimura. Transcription factor Smad-independent T helper 17 cell induction by transforming-growth factor-β is mediated by suppression of eomesodermin. *Immunity* 34: 741–54.

119. Bettelli, E., Y. Carrier, W. Gao, T. Korn, T. B. Strom, M. Oukka, H. L. Weiner, and V. K. Kuchroo. Reciprocal developmental pathways for the generation of pathogenic effector {TH17} and regulatory T cells. *Nature* 441: 235–8.

120. Endo, Y., C. Iwamura, M. Kuwahara, A. Suzuki, K. Sugaya, D. J. Tumes, K. Tokoyoda, H. Hosokawa, M. Yamashita, and T. Nakayama. 2011. Eomesodermin controls interleukin-5 production in memory T helper 2 cells through inhibition of activity of the transcription factor GATA3. *Immunity* 35: 733–45.

121. Lupar, E., M. Brack, L. Garnier, S. Laffont, K. S. Rauch, K. Schachtrup, S. J. Arnold, J.-C. Guéry, and A. Izcue. 2015. Eomesodermin Expression in CD4+ T Cells Restricts Peripheral Foxp3 Induction. *J. Immunol.* 195: 4742–52.

122. Zhang, P., J. S. Lee, K. H. Gartlan, I. S. Schuster, I. Comerford, A. Varelias, M. A. Ullah, S. Vuckovic, M. Koyama, R. D. Kuns, K. R. Locke, K. J. Beckett, S. D. Olver, L. D. Samson, M. Montes de Oca, F. de Labastida Rivera, A. D. Clouston, G. T. Belz, B. R. Blazar, K. P. MacDonald, S. R. McColl, R. Thomas, C. R. Engwerda, M. A. Degli-Esposti, A. Kallies, S.-K. Tey, and G. R. Hill. 2017. Eomesodermin promotes the development of type 1 regulatory T (TR1) cells. *Sci. Immunol.* 2: eaah7152.

123. Intlekofer, A. M., A. Banerjee, N. Takemoto, S. M. Gordon, C. S. Dejong, H. Shin, C. A. Hunter, E. J. Wherry, T. Lindsten, and S. L. Reiner. 2008. Anomalous type 17 response to viral infection by CD8+ T cells lacking T-bet and eomesodermin. *Science* 321: 408–11.

124. Aranami, T., and T. Yamamura. 2008. Th17 Cells and Autoimmune Encephalomyelitis (EAE/MS). *Allergol. Int.* 57: 115–120.

125. Bommiasamy, H., M. West, B. Stockinger, J. M. Coghill, and J. S. Serody. 2014. Plasticity of Th17 Cells and Conversion to Th1 Cells during Acute GvHD. *Blood* 124.

126. Yang, Y., J. Xu, Y. Niu, J. S. Bromberg, and Y. Ding. 2008. T-bet and eomesodermin play critical roles in directing T cell differentiation to Th1 versus Th17. *J. Immunol.* 181: 8700–10.

127. Suto, A., A. L. Wurster, S. L. Reiner, and M. J. Grusby. 2006. IL-21 inhibits IFN-gamma production in developing Th1 cells through the repression of Eomesodermin expression. *J. Immunol.* 177: 3721–7.

128. Edwards, E. S., C. Smith, and R. Khanna. 2014. Phenotypic and transcriptional profile correlates with functional plasticity of antigen-specific CD4+ T cells. *Immunol. Cell Biol.* 92: 181–190.

129. Maynard, C. L., L. E. Harrington, K. M. Janowski, J. R. Oliver, C. L. Zindl, A. Y. Rudensky, and C. T. Weaver. 2007. Regulatory T cells expressing interleukin 10 develop from Foxp3+ and Foxp3- precursor cells in the absence of interleukin 10. *Nat. Immunol.* 8: 931–41.

130. Schiering, C., T. Krausgruber, A. Chomka, A. Fröhlich, K. Adelmann, E. Wohlfert, J. Pott, T. Griseri, J. Bollrath, A. N. Hegazy, O. J. Harrison, B. M. J. Owens, M. Löhning, Y. Belkaid, P. G. Fallon, and F. Powrie. The alarmin IL-33 promotes regulatory T-cell function in the intestine. *Nature* .

131. Hadis, U., B. Wahl, O. Schulz, H.-W. Matthias, A. Schippers, N. Wagner, W. Müller, T. Sparwasser, R. Förster, and O. Pabst. 2011. Intestinal Tolerance Requires Gut Homing and Expansion of FoxP3+ Regulatory T Cells in the Lamina Propria. 34: 237–246.

132. Worbs, T., U. Bode, S. Yan, M. W. Hoffmann, G. Hintzen, G. Bernhardt, R. Förster, and O. Pabst. 2006. Oral tolerance originates in the intestinal immune system and relies on antigen carriage by dendritic cells. 203: 519–527.

133. Hand, T. W., L. M. Santos, N. Bouladoux, M. J. Molloy, A. J. Pagán, M. Pepper, C. L. Maynard, C. O. Elson, and Y. Belkaid. 2012. Acute Gastrointestinal Infection Induces Long-Lived Microbiota-Specific T Cell Responses. 337: 1553–1556.

134. Hayashi, A., T. Sato, N. Kamada, Y. Mikami, K. Matsuoka, T. Hisamatsu, T. Hibi, A. Roers, H. Yagita, T. Ohteki, A. Yoshimura, and T. Kanai. 2013. A Single Strain of Clostridium butyricum Induces Intestinal IL-10-Producing Macrophages to Suppress Acute Experimental Colitis in Mice. 13: 711–722.

135. Wurzelmann, J. I., C. M. Lyles, and R. S. Sandler. Childhood infections and the risk of inflammatory bowel disease. *Dig Dis Sci* 39: 555–560.

136. Bautista, J. L., C.-W. J. Lio, S. K. Lathrop, K. Forbush, Y. Liang, J. Luo, A. Y. Rudensky, and C.-S. Hsieh. 2009. Intraclonal competition limits the fate determination of regulatory T cells in the thymus. *Nat. Immunol.* 10: 610–617.

137. Liston, A., K. M. Nutsch, A. G. Farr, J. M. Lund, J. P. Rasmussen, P. A. Koni, and A. Y. Rudensky. 2008. Differentiation of regulatory Foxp3+ T cells in the thymic cortex. *Proc. Natl. Acad. Sci. U. S. A.* 105: 11903–8.

138. Reinhardt, R. L., H.-E. Liang, and R. M. Locksley. 2009. Cytokine-secreting follicular T cells shape the antibody repertoire. *Nat. Immunol.* 10: 385–393.

139. Hsieh, C.-S., Y. Zheng, Y. Liang, J. D. Fontenot, and A. Y. Rudensky. 2006. An intersection between the self-reactive regulatory and nonregulatory T cell receptor repertoires. *Nat. Immunol.* 7: 401–410.

140. Devkota, S., Y. Wang, M. W. Musch, V. Leone, F.-P. Hannah, A. Nadimpalli, D. A. Antonopoulos, B. Jabri, and E. B. Chang. 2012. Dietary-fat-induced taurocholic acid promotes pathobiont expansion and colitis in Il10-/- mice. *Nature* 487: 104–108.

141. Ise, W., M. Kohyama, K. M. Nutsch, H. M. Lee, A. Suri, E. R. Unanue, T. L. Murphy, and K. M. Murphy. 2010. CTLA-4 suppresses the pathogenicity of self antigen–specific T cells by cell-intrinsic and cell-extrinsic mechanisms. *Nat. Immunol.* 11: 129–135.

142. Hall, A., D. P. Beiting, C. Tato, B. John, G. Oldenhove, C. Lombana, G. Pritchard, J. S. Silver, N. Bouladoux, J. S. Stumhofer, T. H. Harris, J. Grainger, E. D. Wojno, S. Wagage, D. S. Roos, P. Scott, L. A. Turka, S. Cherry, S. L. Reiner, D. Cua, Y. Belkaid, M. M. Elloso, and C. A. Hunter. 2012. The cytokines interleukin 27 and interferon-γ promote distinct Treg cell populations required to limit infection-induced pathology. 37: 511–523.

143. Caretto, D., S. D. Katzman, A. V Villarino, E. Gallo, and A. K. Abbas. 2010. Cutting edge: the Th1 response inhibits the generation of peripheral regulatory T cells. *J. Immunol.* 184: 30–4.

144. Mantel, P. Y., H. Kuipers, O. Boyman, C. Rhyner, N. Ouaked, B. Rückert, C. Karagiannidis, B. N. Lambrecht, R. W. Hendriks, R. Crameri, C. A. Akdis, K. Blaser, and C. B. Schmidt-Weber. 2007. GATA3-driven Th2 responses inhibit TGF-β1-induced FOXP3 expression and the formation of regulatory T cells. *PLoS Biol.* 5: 2847–2861.

145. Boehm, F., M. Martin, R. Kesselring, G. Schiechl, E. K. Geissler, H.-J. Schlitt, and F.-F. Stefan. 2012. Deletion of Foxp3+ regulatory T cells in genetically targeted mice supports development of intestinal inflammation. 12: 1–11.

146. Lewis, M. D., S. a Miller, M. M. Miazgowicz, K. M. Beima, and A. S. Weinmann. 2007. T-bet's ability to regulate individual target genes requires the conserved T-box domain to recruit histone methyltransferase activity and a separate family member-specific transactivation domain. *Mol. Cell. Biol.* 27: 8510–21.

147. Miller, S. a, A. C. Huang, M. M. Miazgowicz, M. M. Brassil, and A. S. Weinmann. 2008. Coordinated but physically separable interaction with H3K27-demethylase and H3K4-methyltransferase activities are required for T-box protein-mediated activation of developmental gene expression. *Genes Dev.* 22: 2980–93.

148. Lin, S., T. C. Thomas, L. H. Storlien, and X. F. Huang. 2000. Development of high fat diet-induced obesity and leptin resistance in C57Bl/6J mice. *Int. J. Obes.* 24: 639–646.

149. Ivanov, I. I., B. S. McKenzie, L. Zhou, C. E. Tadokoro, A. Lepelley, J. J. Lafaille, D. J. Cua, and D. R. Littman. 2006. The orphan nuclear receptor RORgammat directs the differentiation program of proinflammatory IL-17+ T helper cells. *Cell* 126: 1121–33.

150. Ma, X., M. Torbenson, A. R. A. Hamad, M. J. Soloski, and Z. Li. 2007. High-fat diet modulates non-CD1d-restricted natural killer T cells and regulatory T cells in mouse colon and exacerbates experimental colitis. *Clin. Exp. Immunol.* 151: 130–138.

151. Gruber, L., S. Kisling, P. Lichti, F.-P. Martin, S. May, M. Klingenspor, M. Lichtenegger, M. Rychlik, and D. Haller. 2013. High Fat Diet Accelerates Pathogenesis of Murine Crohn's Disease-Like Ileitis Independently of Obesity. *PLoS One* 8: e71661.

152. Gottschalk, R. A., E. Corse, and J. P. Allison. 2010. TCR ligand density and affinity determine peripheral induction of Foxp3 in vivo. *J. Exp. Med.* 207: 1701–11.

153. Winter, S. E., M. G. Winter, M. N. Xavier, P. Thiennimitr, V. Poon, M. A. Keestra, R. C. Laughlin, G. Gomez, J. Wu, S. D. Lawhon, I. Popova, S. J. Parikh, G. L. Adams, R. M. Tsolis, V. J. Stewart, and A. J. Bäumler. 2013. Host-derived nitrate boosts growth of E. coli in the inflamed gut. *Sci New York N Y* 339: 708.

154. Houston, S. A., V. Cerovic, C. Thomson, J. Brewer, A. M. Mowat, and S. Milling. 2015.

The lymph nodes draining the small intestine and colon are anatomically separate and immunologically distinct. *Mucosal Immunol* 9: 468–478.

155. Abbas, A. K., K. M. Murphy, and A. Sher. 1996. Functional diversity of helper T lymphocytes. *Nature* 383: 787–793.

156. Ho, I.-C., and L. H. Glimcher. 2002. Transcription: Tantalizing Times for T Cells. *Cell* 109: S109–S120.

157. Sakaguchi, S., T. Yamaguchi, T. Nomura, and M. Ono. 2008. Regulatory T Cells and Immune Tolerance. *Cell* 133: 775–787.

158. Fontenot, J. D., J. P. Rasmussen, M. A. Gavin, and A. Y. Rudensky. 2005. A function for interleukin 2 in Foxp3-expressing regulatory T cells. *Nat. Immunol.* 6: 1142–1151.

159. Feuerer, M., J. A. Hill, D. Mathis, and C. Benoist. 2009. Foxp3+ regulatory T cells: differentiation, specification, subphenotypes. *Nat. Immunol.* 10: 689–695.

160. Burzyn, D., W. Kuswanto, D. Kolodin, J. L. Shadrach, M. Cerletti, Y. Jang, E. Sefik, T. G. Tan, A. J. Wagers, C. Benoist, and D. Mathis. 2013. A Special Population of regulatory T Cells Potentiates muscle repair. *Cell* 155.

161. Burzyn, D., C. Benoist, and D. Mathis. 2013. Regulatory T cells in nonlymphoid tissues. *Nat. Immunol.* 14: 1007–1013.

162. Kalekar, L. A., S. E. Schmiel, S. L. Nandiwada, W. Y. Lam, L. O. Barsness, N. Zhang, G. L. Stritesky, D. Malhotra, K. E. Pauken, J. L. Linehan, M. G. O'Sullivan, B. T. Fife, K. A. Hogquist, M. K. Jenkins, and D. L. Mueller. 2016. CD4+ T cell anergy prevents autoimmunity and generates regulatory T cell precursors. *Nat. Immunol.* 17: 304–314.

163. Subramanian, A., P. Tamayo, V. K. Mootha, S. Mukherjee, B. L. Ebert, M. A. Gillette, A. Paulovich, S. L. Pomeroy, T. R. Golub, E. S. Lander, and J. P. Mesirov. 2005. Gene set enrichment analysis: a knowledge-based approach for interpreting genome-wide expression profiles. *Proc. Natl. Acad. Sci. U. S. A.* 102: 15545–50.

164. Mootha, V. K., C. M. Lindgren, K.-F. Eriksson, A. Subramanian, S. Sihag, J. Lehar, P. Puigserver, E. Carlsson, M. Ridderstråle, E. Laurila, N. Houstis, M. J. Daly, N. Patterson, J. P. Mesirov, T. R. Golub, P. Tamayo, B. Spiegelman, E. S. Lander, J. N. Hirschhorn, D. Altshuler, and L. C. Groop. 2003. PGC-1α-responsive genes involved in oxidative phosphorylation are coordinately downregulated in human diabetes. *Nat. Genet.* 34: 267–273.

165. Pot, C., L. Apetoh, and V. K. Kuchroo. 2011. Type 1 regulatory T cells (Tr1) in autoimmunity. *Semin. Immunol.* 23: 202–8.

166. Mascanfroni, I. D., M. C. Takenaka, A. Yeste, B. Patel, Y. Wu, J. E. Kenison, S. Siddiqui, A. S. Basso, L. E. Otterbein, D. M. Pardoll, F. Pan, A. Priel, C. B. Clish, S. C. Robson, and F. J. Quintana. 2015. Metabolic control of type 1 regulatory T cell differentiation by AHR and HIF1-α. *Nat. Med.* 21: 638–646.

167. Obata, Y., Y. Furusawa, T. A. Endo, J. Sharif, D. Takahashi, K. Atarashi, M. Nakayama, S. Onawa, Y. Fujimura, M. Takahashi, T. Ikawa, T. Otsubo, Y. I. Kawamura, T. Dohi, S. Tajima, H. Masumoto, O. Ohara, K. Honda, S. Hori, H. Ohno, H. Koseki, and K. Hase. 2014. The

epigenetic regulator Uhrf1 facilitates the proliferation and maturation of colonic regulatory T cells. *Nat. Immunol.* 15: 571–579.

168. Moran, A. E., K. L. Holzapfel, Y. Xing, N. R. Cunningham, J. S. Maltzman, J. Punt, and K. A. Hogquist. 2011. T cell receptor signal strength in Treg and iNKT cell development demonstrated by a novel fluorescent reporter mouse. *J. Exp. Med.* 208: 1279–89.

169. Choi, Y. S., R. Kageyama, D. Eto, T. C. Escobar, R. J. Johnston, L. Monticelli, C. Lao, and S. Crotty. 2011. ICOS Receptor Instructs T Follicular Helper Cell versus Effector Cell Differentiation via Induction of the Transcriptional Repressor Bcl6. *Immunity* 34: 932–946.

170. Lee, W., H. S. Kim, S. Y. Baek, and G. R. Lee. 2016. Transcription factor IRF8 controls Th1-like regulatory T-cell function. *Cell. Mol. Immunol.* 13: 785–794.

171. Feuerer, M., J. A. Hill, D. Mathis, and C. Benoist. 2009. Foxp3+ regulatory T cells: differentiation, specification, subphenotypes. *Nat. Immunol.* 10: 689–695.

172. Maslowski, K. M., and C. R. Mackay. 2011. Diet, gut microbiota and immune responses. *Nat. Immunol.* 12: 5–9.

173. Molodecky, N. A., I. S. Soon, D. M. Rabi, W. A. Ghali, M. Ferris, G. Chernoff, E. I. Benchimol, R. Panaccione, S. Ghosh, H. W. Barkema, and G. G. Kaplan. 2012. Increasing Incidence and Prevalence of the Inflammatory Bowel Diseases With Time, Based on Systematic Review. *Gastroenterology* 142: 46–54.e42.

174. Walter, J., and R. Ley. 2011. The Human Gut Microbiome: Ecology and Recent Evolutionary Changes. *Annu. Rev. Microbiol.* 65: 411–429.

175. Ivanov, I. I., K. Atarashi, N. Manel, E. L. Brodie, T. Shima, U. Karaoz, D. Wei, K. C. Goldfarb, C. a Santee, S. V Lynch, T. Tanoue, A. Imaoka, K. Itoh, K. Takeda, Y. Umesaki, K. Honda, and D. R. Littman. 2009. Induction of intestinal Th17 cells by segmented filamentous bacteria. *Cell* 139: 485–98.

176. Yamada, A., R. Arakaki, M. Saito, T. Tsunematsu, Y. Kudo, and N. Ishimaru. 2016. Role of regulatory T cell in the pathogenesis of inflammatory bowel disease. *World J. Gastroenterol.* 22: 2195–205.

177. Kamradt, T., and R. Volkmer-Engert. 2004. Cross-reactivity of T lymphocytes in infection and autoimmunity. *Mol. Divers.* 8: 271–280.

178. Anderson, A. C., H. Waldner, V. Turchin, C. Jabs, M. Prabhu Das, V. K. Kuchroo, and L. B. Nicholson. 2000. Autoantigen-Responsive T Cell Clones Demonstrate Unfocused TCR Cross-Reactivity toward Multiple Related Ligands: Implications for Autoimmunity. *Cell. Immunol.* 202: 88–96.

179. Stephens, L. A., D. Gray, and S. M. Anderton. 2005. CD4+CD25+ regulatory T cells limit the risk of autoimmune disease arising from T cell receptor crossreactivity. *Proc. Natl. Acad. Sci. U. S. A.* 102: 17418–23.

180. Lee, H.-M., J. L. Bautista, J. Scott-Browne, J. F. Mohan, and C.-S. Hsieh. 2012. A Broad Range of Self-Reactivity Drives Thymic Regulatory T Cell Selection to Limit Responses to Self. *Immunity* 37: 475–486.

181. Endo, Y., C. Iwamura, M. Kuwahara, A. Suzuki, K. Sugaya, D. J. Tumes, K. Tokoyoda, H. Hosokawa, M. Yamashita, and T. Nakayama. Eomesodermin controls interleukin-5 production in memory T helper 2 cells through inhibition of activity of the transcription factor {GATA3.}. *Immunity* 35: 733–45.